ANTI-OBESITY PROPERTIES OF DEEP SEA WATER ON ADIPOCYTES CELL

SAMIHAH ZURA BINTI MOHD NANI

UNIVERSITI TEKNOLOGI MALAYSIA

EFFECTS OF DEEP SEA WATER ON ANTI-OBESITY PROPERTIES ON ADIPOCYTES CELL

SAMIHAH ZURA BINTI MOHD NANI

UNIVERSITI TEKNOLOGI MALAYSIA

"I hereby declare that I have read this thesis and in my opinion this thesis is sufficient in terms of scope and quality for the award of the degree of Master of Philosophy"

Signature	:……
Name of supervisor	: Prof. Dato' Ir. Dr. A. Bakar bin Jaafar
Date	:

ANTI-OBESITY PROPERTIES OF DEEP SEA WATER ON ADIPOCYTES CELL

SAMIHAH ZURA BINTI MOHD NANI

A thesis submitted in fulfillment of the
requirements for the award of the degree
Master of Philosophy

Malaysia-Japan International Institute of Technology
UniversitiTeknologi Malaysia

AUGUST 2017

DECLARATION

I declare that this thesis entitled "*Anti-Obesity Properties of Deep Sea Water on Adipocytes Cell*" is the result of my own research except cited in references. The thesis has not been accepted for any degree and is not concurrently submitted in candidature of any degree.

Signature :… ……

Name : Samihah Zura Binti Mohd Nani

Date : 17th August 2017

DEDICATION

Specially dedicated to my beloved parents

ACKNOWLEDGEMENT

First and foremost, Alhamdulillah. All praises and thanks to Allah, the most gracious and the most merciful, for the strengths and His blessing in completing this thesis. I would like to express my heartfelt gratitude towards my mom, dad, all my siblings and other family members who always support and motivate me in pursuing my master degree.

My utmost appreciation to my supervisor, Prof. Dato' Ir. Dr. A. Bakar bin Jaafar, and my co-supervisor, Dr. Akbariah bt. Mahdzir, for their unlimited support and constructive guidance of this work. I would like to extend my special appreciation to my co-supervisor, Prof. Dr. Fadzilah Adibah binti Abdul Majid for her constant support, professional guidance, and meticulous revision of this work. Deepest thanks to her for gave access to the laboratory and research facilities at Tissue Culture Engineering Research Group (TCERG), Faculty of Chemical Engineering, Universiti Teknologi Malaysia (UTM). I would like to extend my appreciation to all members of TCERG for unlimited guidance, support and friendship. My special and genuine thanks to Prof. Dr. Toshinari Takamura for giving me opportunity to learn, do research, and join the impressive research team in the Department of Endocrinology and Metabolism, Kanazawa University, Japan. Sincere appreciation goes to all members of this department for their supports, kindness, friendship and all wonderful memories. Sincere gratitude to Prof. Emeritus Dr. Md Nor bin Musa and all members of UTM Ocean Thermal Energy Center for generous support and teamwork. I also would like to express deepest gratitude to Malaysia-Japan International Institute of Technology for the facilities and scholarship. I would like to thanks the provided grant used for this research entitled as 'Grant Universiti Penyelidikan', Vot (A.J091600.5500.07529). Last but not least, sincere thanks to my friends and others those support me.

ABSTRACT

Deep sea water (DSW) has been recognized as having a beneficial potential to promote health and a preventive potential against life style diseases including obesity, diabetes, and cardiovascular diseases. Previous clinical studies indicated that it reduces white adipose tissue (WAT). These findings inspired to test the effect of DSW on brown adipogenesis. Induction of adipose tissue browning represents one of important approach that could regulate deleteriously lipid-overloaded WAT into metabolically active and healthy adipocytes. 3T3-L1 preadipocytes were obtained from clonal mouse embryo, and stromal vascular fraction (SVF) cells were isolated from mice adipose tissue. 3T3-L1 preadipocytes were differentiated into adipocytes, while isolated SVF cells were differentiated into beige adipocytes. DSW-treated 3T3-L1 adipocytes and beige adipocytes were harvested for tests of cell viability, lipid accumulation, and genes markers expression. During the course of 3T3-L1 cells differentiation, DSW treatment decreased lipid accumulation and downregulated expression of adipogenic markers of peroxisome proliferator-activated receptor-γ (*PPAR-γ*), CCAAT/enhancer-binding protein a (*C/EBP-α*), and fatty acid binding protein 4 (*FABP4*). In contrast, DSW at a concentration of 100 hardness increased lipid accumulation and upregulated expression of the adipogenic markers of *PPAR-γ*, *C/EBP-α*, and *FABP4* and promoted thermogenic markers of uncoupling protein 1 (*UCP-1*), peroxisome proliferator-activated receptor gamma co-activator 1-alpha (*PGC-1α*), and cell death-inducing DFFA-like effector A (*CIDEA*) in beige adipocytes. Although, DSW increased browning of SVF cells, not all results are in significant levels, which indicated that DSW only cause tendency in browning of SVF cells. Thus, this study concluded that DSW reduced adipogenesis in WAT, while cause tendency in browning of SVF cells into thermogenic beiges adipocytes. Intake of DSW is suggested to people that would like to counteract obesity because it has potential to reduce WAT and induce browning of WAT into thermogenic adipocytes.

ABSTRAK

Air laut dalam telah dikenal pasti berpotensi merawat pelbagai jenis penyakit termasuk kegemukan, kencing manis, dan penyakit jantung. Terdapat banyak bukti bahawa air laut dalam mampu merawat kegemukan. Kajian sebelum ini menunjukkan ia dapat mengurangkan lemak putih dan berat badan. Ini menarik minat untuk mengkaji kesan air laut dalam terhadap lemak jenis perang. Sel lemak 'beige' adalah sejenis lemak berwarna perang yang muncul dalam lemak putih dan mempunyai potensi untuk menukar tenaga kepada haba. Bila dirangsang oleh faktor tertentu seperti suhu sejuk, β3-adrenergic agonists, atau PPAR-γ agonist, sel lemak beige akan muncul di dalam lemak putih melalui proses dipanggil 'browning'. Kajian ini telah mengkaji kesan air laut dalam terhadap pembentukan sel lemak putih dan sel lemak 'beige' yang di ambil dari bahagian stromal vaskular tikus. Semasa proses pembentukan lemak oleh sel 3T3-L1, air laut dalam telah mengurangkan jumlah lemak putih yang terkumpul, dan mengurangkan gen lemak seperti peroxisome proliferator-activated receptor-*γ* (*PPAR-γ*), CCAAT/enhancer-binding protein a (*C/EBP-α*), dan fatty acid binding protein 4 (*FABP4*). Semasa proses pembentukan sel lemak beige, air laut dalam meningkatkan jumlah lemak perang yang terkumpul, dan menaikan gen lemak seperti *PPAR-γ*, *C/EBP-α*, and *FABP4;* dan meningkatkan gen termogenik seperti uncoupling protein 1 (*UCP-1*), peroxisome proliferator-activated receptor gamma co-activator 1-alpha (*PGC-1α*), dan cell death-inducing DFFA-like effector A (*CIDEA*) di dalam sel lemak beige. Walaupun, air laut dalam meningkatkan lemak perang, gen lemak, dan gen termogenik, tidak semua keputusan menunjukkan nilai 'significant'. Kajian ini merumuskan air laut dalam mengurangkan lemak putih sementara menyebabkan kecenderungan proses 'browning' di dalam lemak putih. Penggunaan air laut dalam adalah disarankan untuk orang yang mahu melawan penyakit obesiti berdasarkan keupayaannya untuk menukar tenaga kepada haba.

TABLE OF CONTENTS

LIST OF TABLES

LIST OF FIGURES

LIST OF ABBREVATIONS

ADIPOQ	-	Adiponectin
ACTA	-	Actin assembly-inducing protein
AGT	-	Angiotensinogen
AIC	-	Adipogenic induction cocktails
AMW	-	Artificial mineral water
B	-	Boron
BAT	-	Brown adipose tissue
BMP7	-	Bone morphogenic factor 7
Ca	-	Calcium
$CaCl_2$	-	Calcium chloride
CD	-	Cluster of differentiation
cDNA	-	Complementary deoxyribonucleic acid
C/EBPIIβ	-	CCAAT/enhancer-binding protein-IIβ
CIDEA	-	Cell death-inducing DFFA-like effector A
COX	-	Cytochrome c oxidase
CO_2	-	Carbon dioxide
Cr	-	Chromium
DEX	-	Dexamethasone
DM	-	Differentiation medium
DMEM	-	Dulbecco's modified eagle's medium
DSW	-	Deep sea water
DIO2	-	Deiodinase, iodothyronine, type II
EBF2	-	Early B-cell factor 2
EN1	-	Engrailed 1
FABP4	-	Fatty acid-binding protein 4
FAS	-	Fatty acid synthase
FGF21	-	Fibroblast growth factor 21

HFD	-	High fat diet
IBMX	-	Methylisobutylxanthine
IC	-	Inhibitory concentration
IL-1β	-	Interlekin-1β
IL-6	-	Interleukin-6
IRS	-	Insulin receptor substrate
K	-	Potassium
LY6A	-	Lymphocyte antigen 6 complex, locus A
Mg	-	Magnesium
MM	-	Maintenance medium
MYH11	-	Smooth muscle cells
MSC	-	Mesenchymal stem cells
MYF	-	Myogenic factor
ORO	-	Oil red oil
PAX7	-	Paired box 7
PBS	-	Phosphate buffer saline
PDGFRA	-	Platelet-derived growth factor receptor
PREF1	-	Preadipocytes factor 1
PGC-1α	-	Peroxisome proliferator-activated receptor gamma coactivator 1- alpha
PPAR-γ	-	Peroxisome proliferator-activated receptor gamma
PPARGC-1α	-	Peroxisome proliferator-activated receptor gamma coactivator 1- alpha
PRDM16	-	PR domain zinc finger protein 16
LD	-	Lethal dose
LEP	-	Leptin
RETN	-	Resistin
ROS	-	Reactive oxygen species
RT-PCR	-	Reverse transcription polymerases chain reaction
Se	-	Selenium
SVF	-	Stromal Vascular Fraction
T3	-	Triiodothyronine
UCP-1	-	Uncoupling protein 1

V	-	Vanadium
WAT	-	White adipose tissue

LIST OF APPENDICES

CHAPTER 1

INTRODUCTION

1.1 Research Background

Water is a crucial component for all living things (Petraccia *et al.* 2006). There are many applications of water including for portable use, irrigation, industrial, and domestic. Most interestingly, water also has therapeutic potential to maintain, cure, and prevent health problems. Generally, human needs water to regulate body functions, such as to enhance body metabolism and provide essential minerals to the body system. Nowadays, there are many types of commercially available drinking water promoted as 'healthy water'. These include deep-sea drinking water, alkaline water, mineral water, electrolyte water, reverse osmosis water, and vitamin water. The sources of this water are vary-; for example, surface water, groundwater, seawater, and deep sea water (DSW).

Nowadays, the uses of seawater are expanding. Water scarcity and large capacity are potential reasons of its exploitation. This leads to the discovery of the potential usages of DSW, especially ones that concern health. DSW is commonly referred to a body of water that has a depth exceeding 200 meters. Cold temperature, pure, and abundant with minerals are the characteristics that are usually associated with it (Hwang et al, 2009). It contains lots of minerals beneficial to health including magnesium (Mg), calcium (Ca), potassium (K), boron (B), chromium (Cr), chloride (Cl), selenium (Se), silica (SiO_2), zinc (Zn), and vanadium (V) (Hwang *et al.* 2009;

Takahashi & Huang 2012; Katsuda *et al.* 2008). Mineral content in DSW is claimed to be very high compared to the other sources of water (Katsuda *et al.* 2008).

DSW is recognized as having the potential to promote health, cure and prevent health problems including obesity, diabetes, skin diseases, cancer, and cardiovascular diseases. Due to its high beneficial mineral content, DSW is being used for many applications such as for agriculture and productions of DSW-byproducts including drinking water, foods, and cosmetic products.

Obesity is a chronic disease of multi-factorial origin that develops from the interaction of social, psychological, behavioral, metabolic, cellular, and molecular factors (Fernández-Sánchez *et al.* 2011). Sedentary living leads people to have less physical activities, while eating becomes a habit that increases fats accumulation in the body, leading to increased prevalence of obesity. Obesity is a currently an alarming disease burdening developing and developed countries. According to World Health Organization (WHO), 600 million adults, 18 years and older, were obese in 2014 (WHO 2013). Meanwhile, 41 million children under the age of 5 were overweight or obese. In Malaysia, National Health and Morbidity Survey of 2015 reported that obesity prevalence has increased to 15.1 per cent in 2011 and continued to increase to 17.7 per cent in 2015 (Institute for Public Health, 2015).

Fighting obesity comes in many ways. These include active physical activities, healthy diets, and good calories intakes. Practicing good diet and lifestyle sometimes can be difficult. As a result, many people prefer dietary supplements or products aimed for weight loss as an instant way in achieving weight loss target. Finding the effective, safe, and reliable source of anti-obesity products could be challenging. There are many kinds of compounds or drugs developed to counteract obesity that target specific pathways including GLP1R agonists liraglutide, orlistat, lorcaserin, and naltrexone bupropion XR. In spite of treating obesity, these kinds of drugs can also cause some adverse health effects such as headache, increased risk of cardiovascular diseases, nausea, dizziness, and hypoglycaemia (Kusminski *et al.* 2016).

There are two classical types of fats in mammals, namely white adipose tissue (WAT) and brown adipose tissue (BAT). Beige adipose tissue is thermogenic fats that emerge in WAT under specified stimuli or exposures such as cold, β3-adrenergic agonists, or PPAR-γ agonist. Excess WAT accumulated in the body leads to the condition that termed as obesity. On the other hands, excess beige adipose tissue and BAT do not cause obesity as these fats function in energy expenditure. There have been many drugs, compounds, supplements, or active substances were developed and introduced to combat obesity by means of decreasing WAT. This leads to the discovery of many potential sources of natural and synthetic anti-obesity agents.

DSW has been recognized as a potential therapeutic compound from nature that combats obesity (Yun 2010). Several lines of scientific evidences have suggested DSW's potential in treating obesity-related pathology. It decreases WAT in ob/ob mice and lipid accumulation in cultured adipocytes (Ha *et al.* 2014a; Ha *et al.* 2013; Hwang, S. H. Kim, *et al.* 2009). This study was done to determine the effects of DSW in development of beige adipose tissue in WAT. The formation of beige adipose tissue so called 'browning' of WAT transforms its function from energy reservation fat into energy utilization fat, thereby provides intervention of obesity treatment. The effects of DSW in WAT were also determined to validate its effects in WAT prior to browning experiment.

1.2 Problem Statement

The applications of DSW to combat obesity have accumulated strong scientific evidences. Previous studies show the effects of DSW in WAT that is recognized as fat that stores energy.DSW reduces lipid accumulation in WAT and down-regulates adipogenic markers such as peroxisome proliferator-activated receptor-γ (*PPAR-γ*), CCAAT/enhancer-binding protein α (*C/EBP-α*), and fatty acid binding protein 4 (*FABP4*), both in *in vitro* and *in vivo* (Hwang *et al.* 2009; Hwang, S. H. Kim, *et al.* 2009; Ha *et al.* 2014a). These findings have encouraged a study

aimed to test the effect of DSW on brown adipogenesis that is involved in energy expenditure.

Brown adipose tissue emerged in WAT under specified stimuli or exposures such as cold, β3-adrenergic agonists, or PPAR-γ agonist. Brown adipose tissue in WAT is also called as beige, inducible brown, brown-in-white, brite, or 'brown-like' adipocytes have ability to perform thermogenesis like classical brown adipocytes (Wang & Seale 2016; Lidell *et al.* 2014; Harms & Seale 2013; Rodríguez *et al.* 2016; Wu *et al.* 2015; Bartelt & Heeren 2014). During browning process, beige adipose tissue express thermogenic genes such as uncoupling protein 1 (*UCP-1*), which is responsible to convert energy to heat (Ricquier 2011; Nedergaard *et al.* 2001; Kozak & Anunciado-Koza 2008; Fedorenko *et al.* 2013). Since its discovery, beige adipose tissue has derived attention due its ability to combat obesity. Therefore, the potential effects of DSW in browning of WAT are interesting to be investigated.

Targeting beige adipose tissues for obesity treatment is useful as classical BAT exist in small portion in the body, which limits its ability in energy utilization. BAT exists during embryonic stages and declines by age (Heaton 1972; Lidell *et al.* 2013). Thus, identifying the effects of DSW in browning of WAT is useful to determine its ability to increase the levels of fats that involved in energy utilization and in adapting loss of BAT.

Excessive lipid accumulation in WAT is a main cause of obesity. Formation of beige adipose tissue in WAT could reduce deleterious effects of WAT (Bartelt & Heeren 2014). Since DSW reduces lipid accumulation in WAT, a research over its potential to develop good fats in WAT through browning process is worth to be carried out. Reduced lipid accumulation in WAT might be associated with formation of beige adipose tissues in WAT.

Beige adipose tissue expresses the thermogenic genes such as *UCP-1*. When activated, beige adipose tissue that contains *UCP-1* utilizes energy and converts it

into heat. Thereby, determining DSW's potential to induce formation of beige adipose tissue may provide a novel therapeutic intervention against obesity.

In previous studies, DSW promotes mitochondrial biogenesis and genes expression which are related to mitochondria functions in liver, skeletal muscle and epididymal fat (Ha *et al.* 2014a)' (Ha *et al.* 2015). Mitochondrial contains *UCP-1* that is responsible for the conversion of energy into heat. From the previous findings it is speculated that DSW would be able to induce thermogenic genes such as *UCP-1*, peroxisome proliferator-activated receptor gamma coactivator 1-alpha (*PGC-1α*), and *CIDEA* that are commonly expressed in beige adipose tissues (Kolumam *et al.* 2015; Shao *et al.* 2016; Vitali *et al.* 2012; Kusminski *et al.* 2016). Thus, this study induced browning of WAT with treatment of DSW during the course of beige adipocyte differentiation.

Up to the present time, there has been only one study regarding the effects of DSW in differentiation of WAT in *in vitro* model ever published (Hwang, S. H. Kim, *et al.* 2009). This study hence aimed to determine the effects of DSW in differentiation of WAT to confirm its effect before performing any experiment regarding the browning of WAT.

Stromal vascular fraction (SVF) cells of WAT are rich source of preadipocytes, macrophages, fibroblast, endothelial cells, smooth muscle cells, and mesenchymal stem cells (MSCs). WAT isolated from SVF cells is a reliable source for inducing browning as it contains lots of preadipocytes, and is easier to differentiate into beige adipose tissue. This study used SVF cells to induce browning of WAT.

To date, the effects of DSW in the browning of WAT have not yet been investigated. The present study investigated the effects of DSW on WAT and browning of WAT from the SVF cells isolated from mice adipose tissue.

1.3 Objectives of the Study

The objectives of this study are to investigate the influence of DSW on adipose tissues that are associated with obesity disease which are white adipose tissue (WAT), and beige adipose tissue.

i. To investigate the effects of DSW in suppressing WAT; and

ii. To investigate the effects of DSW in the browning of SVF cells isolated from mice adipose tissue.

1.4 Scopes of the Study

The scopes this study are divided into three.

i. To determine lipid accumulation in WAT and the SVF cells isolated from mice adipose tissue after being treated with DSW;

ii. To investigate the adipogenic genes expression level in WAT and the SVF cells isolated from mice adipose tissue after being treated with DSW; and

iii. To investigate the thermogenic genes expression level in the SVF cells isolated from mice adipose tissue after being treated with DSW.

1.5 Research Questions

Can DSW induce browning of stromal vascular fraction (SVF) cells into beige adipose tissue?

1.6 Hypotheses

Hypotheses of this study are described as follow.

i. Deep sea water will be able to increase lipid accumulation in beige adipose tissue;

ii. Deep sea water will be able to increase the adipogenic genes expression level in beige adipose tissues;and

iii. Deep sea water will be able to increase the thermogenic genes expression level in beige adipose tissues.

1.7 Significances of the Study

DSW is potential to reduce WAT, an adipocyte that could cause health hazard in excess amount. Induction of adipose tissue browning represents one of important approach that could regulate deleteriously lipid-overloaded WAT into metabolically active and healthy adipose tissue. In this study, DSW has shown potential to reduce WAT, while promoted WAT into beige adipocytes. DSW applications could be suggested to people that has interest in combating obesity.

1.8 Limitation

This study used 3T3-L1 cells to test the effects of DSW in adipocyte differentiation. However, different types of cells were used to test the effects of DSW in browning of WAT, which are SVF cells. It could be more interesting to test the effects of DSW in adipocyte differentiation using SVF cells as the potential the effects of DSW in adipogenesis and browning of SVF cells could be compared.

CHAPTER 2

LITERATURE REVIEW

2.1 Deep Sea Water (DSW)

DSW has many potential health benefits. Its variety types and high mineral content have caused it to gain attention among researchers. It offers exploitation of many byproducts including drinking water, food, and cosmetic products. It can also enhances the quality of foods such as increasing the antioxidant level in green tea (Bae & Lee 2010). It is commonly processed through various technologies such as desalination, blending of minerals, and low vacuum temperature.

2.1.1 Applications of Deep Sea Water

DSW is widely obtainable across the world. However, not all of its locations are accessible due to many factors such as far distance from mainland, lack of essential technologies, and high cost. Nevertheless, with today's advanced development of technologies, many sources of DSW are now reachable. The countries known to pump up DSW for productions of DSW-products include Korea, Japan, Taiwan, China, and the United States of America (USA). The commercialization of DSW-products is expanding, together with extensive

researches regarding the potential health benefits of it. Table 2.1 shows the sources of DSW intake, which are based on the literature of this study.

Table 2.1 Location of deep sea water intake points worldwide.

Country	Location of Deep Sea Water Intake Point	Reference
Korea	Gangwon-Do, Korea	(Ha *et al.* 2014a; Hwang *et al.* 2009a)
Japan	Kochi, Japan	(Katsuda *et al.* 2008; Yoshioka *et al.* 2003)
Taiwan	Hualien County, Taiwan	(Fu *et al.* 2012; Chen *et al.* 2013; Yang *et al.* 2014)
China	Shantou, South China Sea	(Ha *et al.* 2014b)
USA	Hawaii, USA	(Ueshima *et al.* 2003)

As shown in Figure 2.1, the area in colour of yellow, orange, and indicate the selected intake points of DSW worldwide.

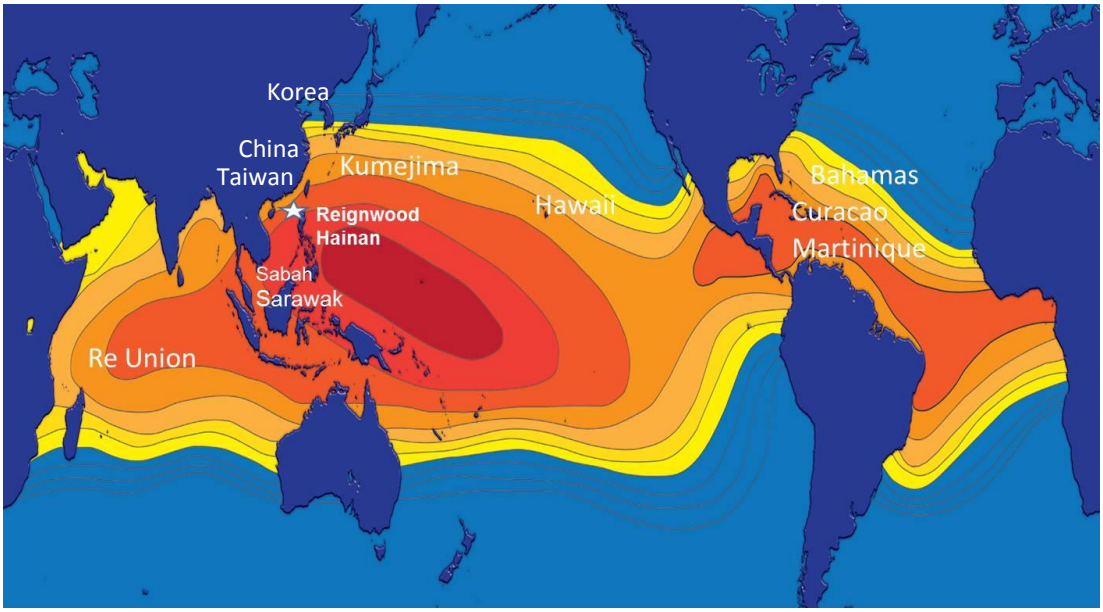

Figure 2.1 Selected intake points of deep sea water worldwide (Jaafar 2016).

2.1.2 Potential Health Benefits of Deep Sea Water

The potential health benefits of DSW have been proven by scientific data. To date, DSW is potential to combat health problems such as obesity, diabetes, cardiovascular diseases, skin diseases, cancer, stomach ulcer, and cataract (Mohd Nani *et al.* 2016). DSW can also improve and increase quality of food such as by increasing good bacteria level in yogurt (Kang *et al.* 2015), and increasing antioxidant level in green tea (Bae & Lee 2010).

2.1.1.1Effects of DSW on Obesity

DSW applications have accumulated strong scientific evidences against combating obesity. It inhibits adipocytes differentiation of 3T3-L1 cells, which means the fats forming are able to be suppressed (Hwang et al., 2009). Anti-obesity activities of it are mediated by modulation of the expression of obesity-specific molecules. In a dose-dependent manner, DSW significantly reduces lipid accumulation in white adipose tissue (WAT), and suppresses the mRNA expression of key adipogenic genes such as peroxisome proliferator-activated receptor-γ (*PPAR-γ*), CCAAT/enhancer-binding protein a (*C/EBP-a*), adipocyte protein-2 (aP2), and fatty acid binding protein 4 (FABP4), both in *in vitro* and *in vivo* (Hwang *et al.* 2009a; Hwang *et al.* 2009b; Ha *et al.* 2014a; Ha *et al.* 2013). It upregulates levels of obesity adipokines which are adiponectin and leptin (Ha *et al.* 2014a; Hwang *et al.* 2009b), whereas decreases levels of resistin, RBP4, and FABP4 (Hwang *et al.* 2009b). In high-fat diet-induced obese mice, DSW inhibited lipogenesis genes such as sterol regulatory element-binding protein 1c (*SREBP1c*) and fatty acid synthase (*FAS*), whereas induced the lipolysis genes such as adipose triglyceride lipase (*ATGL*) and hormone-sensitive lipase (*HSL*) (Ha *et al.* 2014a).

Additionally, DSW promotes mitochondrial biogenesis and genes expression which are related to mitochondria functions in 3T3-L1 preadipocytes, liver, skeletal muscle and epididymal fat (Ha *et al.* 2016; Ha *et al.* 2015; Ha *et al.* 2014a).

In term of fats loss, DSW of 1000 hardness could decreases body weight of high fat diet mice by 7% (Hwang *et al.* 2009). DSW of hardness of 2000 suppresses body weight of mice in a study by Ha *et al.* (2014a). In morphological observation, DSW both hardness of 1000 and 2000 reduce the epididymal adipocytes size of mice (Ha *et al.* 2014a). Electrodialysis deep sea water treatment in mice shows a tendency toward the decreases of visceral fat size in a study by Chang *et al.* (2011).

2.1.3 Minerals in Deep Sea Water

The beneficial health effects from DSW applications are the result of its variety types and high quantity of mineral content. A study by Li *et al.* (2010), showed that the consumption of multivitamin and minerals could improve the lipid profiles, and reduce body weight in obese women. Meanwhile, the combined intakes of Ca, Mg, and Zn in high fat diet mice could reduce body weight, and improve lipid metabolism in high fat diet mice (Pérez-Gallardo *et al.* 2009). This indicates that the intake of various minerals is useful to counteract obesity.

DSW is known to contain various beneficial minerals such as Mg, Ca, K, B, Cr, Cl, Se, Zn, and V (Hwang *et al.* 2009a; Takahashi & Huang 2012; Katsuda *et al.* 2008). Thus, the effort in identifying the underlying molecular mechanisms by which component in DSW that counteract health problems is challenging. The concentration of DSW is determined by water hardness, which calculates the levels of Mg and Ca. For this reason, most studies postulated Mg and Ca ions as major active compounds that counteract health problems. Different types of water which are DSW and artificial mineral water (AMW) that have the same hardness of 1000, contained same concentrations of Mg and Ca have shown albeit different findings. AMW treatment shows less inhibitory effect on 3T3-L1 preadipocytes differentiation compared to DSW treatment (Hwang *et al.* 2009). AMW only contains Mg and Ca, whereas DSW contains Mg and Ca plus other types of minerals, which lead to suggestion that Mg and Ca are not the sole elements in DSW that give benefits to health. The other minerals in DSW, including trace elements such as B, Cr, SiO_2, Se, Zn and V may have potential health benefits, thereby need to be discovered as suggested by many researchers (He *et al.* 2014; Fu *et al.* 2012; Miyamura *et al.* 2004; Katsuda *et al.* 2008; Yoshioka et al., 2003).

Potential of DSW to reduce body weight has inconsistent results. Katsuda *et al.* (2008) reported that Kusanagi-Hypercholesterolemic rabbits were fed for 6 months with DSW with hardness of 1000 did not experience declining body weight. To date, there have been no definite factors of minerals reported to explain different capability of DSW in reducing body weight. Thus, the efforts in determining the

exact minerals or combination of minerals in DSW that combat obesity are remain to elucidate.

The example of types and amount of each minerals that contained in DSW have been estimated based on the average concentrations of it and the total volume of DSW of 1.35×10^{18} m^3as shown in Table 2.2 (Takahashi & Huang 2012).

Table 2.2 Total amount of minerals in deep sea water (Takahashi & Huang 2012).

Element	Total (10^6 ton)	Element	Total (10^6 ton)	Element	Total (10^6 ton)	Element	Total (10^6 ton)
Cl	26,120,000,000	Mo	14,000	Tl	17	Se	0.9
Na	14,550,000,000	U	4,300	W	13	Sm	0.8
Mg	1,728,000,000	V	2,700	Re	11	Sn	0.7
S	1,312,000,000	As	1,600	He	10	Ho	0.5
Ca	556,000,000	Ni	650	Ti	8.8	Lu	0.3
K	538,000,000	Zn	470	La	7.6	Be	0.3
Br	90,000,000	Kr	420	Ge	2.4	Tm	0.3
C	36,000,000	Cs	413	Nb	<7	Eu	0.2
N	11,700,000	Cr	271	Hf	4.6	Hg	0.2
Sr	10,500,000	Sb	270	Nd	4.4	Rh	0.1
B	6,100,000	Ne	216	Ta	<3	Te	0.1
O	3,800,000	Se	209	Ag	2.7	Pd	0.008
Si	3,800,000	Cu	202	Co	1.6	Pt	0.07
F	1,900,000	Cd	94	Ga	1.6	Bi	0.04
Ar	840,000	Xe	89	Er	1.6	Au	0.03
Li	240,000	Fe	40	Yb	1.6	Th	0.02
Rb	160,000	Al	40	Dy	1.5	In	0.01
P	84,000	Mg	27	Gd	1.2	Ru	<0.006
I	78,000	Y	22	Pr	0.9	Os	0.003
Ba	20,000	Zr	20	Ce	0.9	Ir	0.0002

The amount of minerals in DSW is claimed to be among the highest available on earth. The types and amount of minerals in the sea differ depending on seawater depth. According to Sheu *et al.* (2013), DSW has more minerals than the surface seawater. Table 2.3 shows the example of different amount of minerals between surface seawater and DSW.

Table 2.3 Amount of elements in surface seawater and deep sea water (Sheu *et al.* 2013).

Type of Element	Surface Seawater (mg/L)	Deep Sea Water (mg/L)
Na	10800	7240
K	392	10400
Ca	411	39
Mg	1290	96100
Sr	8.1	0.17
B	4.45	320
Fe	0.003	0.25
Li	0.17	11.7
Cu	0.0009	0.22
Co	0.0004	0.26
Mo	0.01	0.62
Ni	0.0066	0.11
Cr	0.0002	0.087
Rb	0.12	1.2
Si	2.9	0.5
V	0.002	1.2
F	13	21.8
Br	67.3	5400
I	0.064	5.5

DSW contains many minerals. The health benefits of several minerals such as Mg, Ca, Cr, K, Se, and V are described as follows:

2.1.3.1 Magnesium

Mg is the most abundant intracellular divalent cation, significant for many physiological processes of the body including energy metabolism and enzyme functions (Michelle & Beerman 2007). Mg is able to reduce the risks of obesity, diabetes, and asthma (Hwang *et al.* 2009b; Watson *et al.* 2014). Mg reduces lipid accumulation in the aorta of subjects that has high cholesterol intake (Ouchi *et al.* 1990). Besides that, it is beneficial for people with cardiovascular disease as it can reduce the potential of heart attack by dilating blood vessels; and stopping spasm in the heart muscle, and vessel walls (Faryadi 2012). Drinking water with high level of Mg content shows inhibitory effects in adipocyte differentiation, which means synthesis of fats are suppressed (Hwang *et al.* 2009b). Mg deficiency in mice significantly increases triglycerides, and free cholesterol in plasma; and increases triglycerides, α-glycerophosphate and lactate levels while decreasing hepatic glycogen content in the liver (Rayssiguier *et al.* 1981).

Molecular mechanisms of Mg in cells especially adipocytes remain unclear. Previous study shows that Mg and Ca enriched DSW upregulated expression of *PGC1-α* in 3T3-L1 adipocytes (Ha *et al.* 2016). *PGC-1α* is an important cofactor for transcriptional activity of major markers in adipocytes differentiation, which is *PPAR-γ* (Puigserver *et al.* 1998; Kleiner *et al.* 2012). Mg appears to play a pivotal role in regulating the PPAR-mediated signaling pathways as a key cofactor in the protein phosphorylation (Fujii 2005).

Mg intake is important to prevent obesity related pathology. Low magnesium status is strongly correlated with increased inflammatory, oxidative stress, and insulin resistance. Inflammatory, oxidative stress, insulin resistance are the main causes of metabolic diseases including obesity (Rayssiguier *et al.* 2010). Oxidative

stress increase reactive oxygen species (ROS). Mg acts as antioxidant compound that could suppress catecholamines release that responsible in ROS production. Mg treatment could suppress the production of acute phase proteins such as C-reactive protein, which is an inflammatory cause (Zheltova *et al.* 2016).

Adiposity is related to interruption in insulin signaling pathway. Insulin signal is responding to levels changes of Mg, both in intracellular and extracellular, respectively (Ishizuka *et al.* 1994). Recent data reveal that Mg supplementation could improve insulin resistance and glucose control, that correlated to obesity (Simental-Mendía *et al.* 2016). Mg deficiency in high fat diet mice has caused decreased of proteins involved in insulin signaling pathway (IR-β, IRS-1 and Akt), which increase insulin resistance (Sales *et al.* 2014). A study by (Venu *et al.* 2008) showed Mg deficient diet has increased in expression of fatty acid synthase and the fatty acid transporter protein 1 in the adipose tissue that cause increased in adiposity. This study has shown that Mg-DSW content suppressed fats formation and decreased adipogenic markers in WAT.

2.1.3.2 Calcium

Ca is one of the major minerals for human that has many health benefits including for bone development, and pivotal cofactor for several enzymes needed in energy metabolism. Adequate intake of Ca can help in reducing risks of cardiovascular disease, obesity, and some forms of cancers (Hwang *et al.* 2009b; Michelle & Beerman 2007; Watson *et al.* 2014).

Intracellular Ca is important to regulate adipocyte lipid metabolism and triglyceride storage as its increases lipogenic gene expression and lipogenesis, and suppress lipolysis. Calcitrophic hormones act on adipocytes to increase Ca influx. Increased of calcitriol level after low calcium diets has stimulated Ca influx in primary cultures of human adipocytes and thereby promotes adiposity (Zemel *et al.* 2000). In contrast, high Ca diet has reduced adipose mass, reduced body weight,

increased lipolysis, and suppressed fatty acid synthase in high fat diet mice (Zemel *et al.* 2000).

Increasing extracellular Ca concentration by means of high Ca supplementation can decrease adipogenic genes. A study by Vergara *et al.* (2016) reported that, decreased extracellular Ca has increased adipocyte differentiation through suppression of calreticulin, a known inhibitor of PPAR-γ.

Diet-induced obesity mice has reduced body and fat mass in response to high Ca intake through induction of apoptosis and activation of Ca^{2+} dependent apoptotic proteases, calpain and caspase-12 (Sergeev & Song 2014). In another study, high dietary Ca in mice has reduced risk of obesity through potential mechanisms including reduced adipose intracellular ROS production, suppressed adipocyte intracellular Ca, and inhibited adipose tissue nicotinamide adenine dinucleotide phosphate oxidase (NADPH) expression while increasing UCP-2 and UCP-3 expression in visceral and subcutaneous adipose tissue, respectively (Sun & Zemel 2006). High Ca intake could also suppress 11β-hydroxysteroid dehydrogenase (11β-HSD) expression in visceral adipose tissue (Sun & Zemel 2006). ROS production is increased in response to obesity. However, high expression of UCP2 and UCP-3 has resulted in the inhibition of ROS production, while NADPH expression has led to ROS production. 11β-HSD is a key enzyme responsible for converting glucocorticoid into its active form, which can alleviate adipogenesis.

2.1.3.3 Chromium

Cr is an essential nutrient that is required for carbohydrates, and lipid metabolism (Lewicki et al. 2014)(Pechova & Pavlata 2007). It has antioxidant properties which are useful to expand the cells life (Krejpcio 2001). Cr is potential to combat obesity. For example, chromic chloride is one of the materials for synthesis of Cr Picolinate; a supplement claiming to aid weight loss (Onakpoya et al. 2013).

2.1.3.4 Potassium

Potassium is an intracellular cationic electrolyte that is necessary for normal cellular function. Prevalence of metabolic syndrome decreased with higher potassium intake. Potassium intake was inversely associated with metabolic syndrome, which are abdominal obesity, high blood pressure, and fasting hyperglycemia (Shin *et al.* 2013). A study by Esmaillzadeh *et al.* (2006) reported that high potassium intake decreases metabolic syndrome though decreased of C-reactive protein, a marker of inflammatory.

2.1.3.5 Selenium

Se is a trace element that plays important role to human health, though it is required only in a small portion in the body. In a study, Se acquired from DSW provides intestinal protection against duodenal ulcers (Yang *et al.* 2014). Se which acts on PPAR-γ is suggested as potential compound to be developed as anti-depressant and anti-obesity agent (Donma & Donma 2016).

2.1.3.6 Vanadium

Vanadium has potential in reducing lipid and has shown effectiveness in inhibiting formation of fats cells. In a study by (Park *et al.* 2013), vanadium-ground water decreases HFD-induced body weight gain and reduces total cholesterol, triglyceride, and glucose levels in the plasma. Its mechanisms are mediated through decreases in mRNA expression levels of *PPAR-γ, C/EBP-α*, fatty acid, lipoprotein lipase, and leptin. Vanadium reduces body fat, body weight, plasma insulin levels, and glucose levels in fatty Zucker rats (Wang *et al.* 2001). It is suggested as anti-obesity agents as it inhibits hypothalamic neuropeptide Y (NPY), which is known to be related to appetite, and increase leptin secretion in adipose tissue (Wang *et al.* 2001). Increased insulin sensitivity in adipose tissue and decreased appetite and body fat correlated with decreasing NPY levels in the hypothalamus (Wang *et al.* 2001).

2.1.4 Cytotoxicity of Deep Sea Water

Cytotoxicity test was conducted for DSW using 3T3-L1 cells in a previous study. Concentration of DSW at below than 1500 hardness has caused no cytotoxicity effect on 3T3-L1 cells (Hwang *et al.* 2009a).

2.2 Adipose Tissue

Adipose tissues are the loose connective tissues that are mainly composed of mature adipocytes and SVF cells. SVF cells contain many types of cells including preadipocytes, macrophages, fibroblasts, endothelial cells, smooth muscle cells, and mesenchymal stem cells (MSCs) (Ruiz-Ojeda *et al.* 2016). It comprises of more than 90% of tissue volume and more than 50% of the total cells number (Zhang *et al.* 2012). Generally, adipose tissue functions to store energy, maintains the energy homeostasis, insulates the body, and protects the internal organs. Adipose tissue is also specialized cells that secrete factors involved in immune system, vascular diseases, and appetite regulation (Fève 2005; Gregoire *et al.* 1998).

2.2.1 Origin of Adipose Tissue

Adipose tissue development begins before birth in most species. The developmental origin or adipocyte lineage of it is derived from an embryonic stem cell precursor with the capacity to differentiate into the mesodermal cell types of adipocytes, myocytes, osteoblasts, and chondrocytes (Gregoire *et al.* 1998). During embryonic development, the cells are restricted by unknown mechanisms to multipotent mesenchymal stem cells (MSCs). Preadipocytes are derived from the MSCs, by directing them toward adipocyte lineage through the process called determination; producing fibroblast-shaped preadipocytes that have capacity for adipocyte differentiation (Bing *et al.* 2004; Avram *et al.* 2007; Gesta *et al.* 2007). Figure 2.2 illustrated by Gesta *et al.* (2007) describes the origin of adipocytes from the embryonic stem cells.

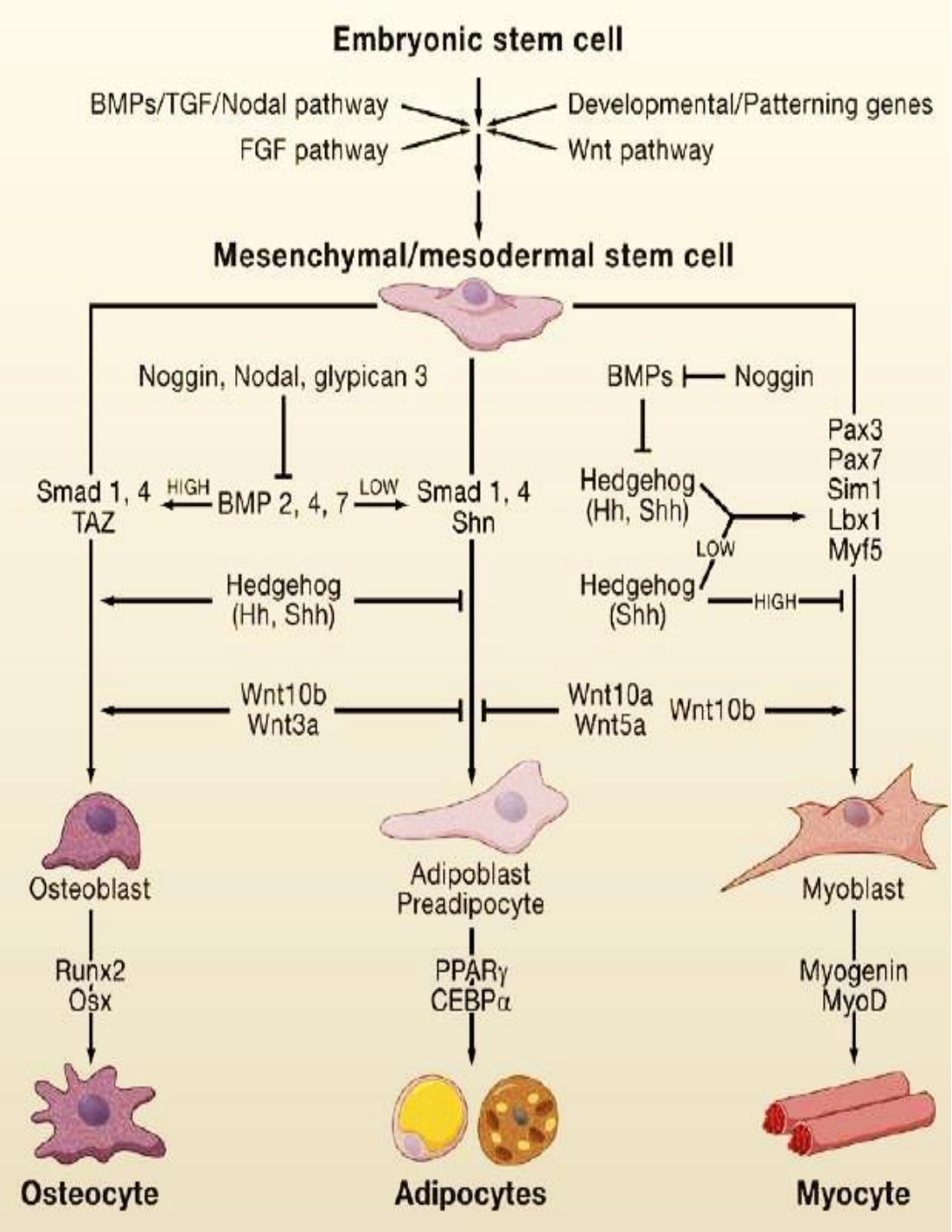

Figure 2.2 Origin of adipose tissue from the embryonic stem cells (Gesta *et al.* 2007).

2.2.2 Types of Adipose Tissues

In mammal, there are two classical types of adipose tissues, known as white adipose tissue (WAT), and brown adipose tissue (BAT). Both types of adipose tissues have different functions. Recently, the brown-like adipocyte emerging in WAT has been identified and is termed as beige adipose tissue. Thus, the types of adipose tissue are classified into three and described as follow.

2.2.2.1 White Adipose Tissue

WAT mainly functions in energy reservation and mobilization. The main cellular components of WAT are mature adipocytes and stromal-vascular cells, which include preadipocytes, macrophage, endothelial cells, and immune cells. An increase in both size (hypertrophy) and number of adipocytes (hyperlasia) during normal development and in obesity causes the expansion of WAT (Dani & Billon 2012). WAT is localized in the various sites of the body, and is majorly found in the abdominal cavity, beneath the skin, and between the skeletal muscles. Excessive lipid accumulation in WAT is a main cause of obesity. WAT in the abdominal cavity is recognized as the visceral fats or the belly fat. Excessive accumulation of visceral fats triggers central obesity or also known as abdominal obesity which has strong association to metabolic diseases (Zhang *et al.* 2012).

2.2.2.2 Brown Adipose Tissue

BAT is specialized in the expenditure of energy. It can be distinguished from WAT by its “brownish” color which is a result of blood vessels enrichment and higher mitochondrial content. In contrast with WAT, BAT is not prioritized to store energy instead of catalyzing energy through thermogenesis (Cannon & Nedergaard 2004; Symonds 2012). As it burns fats, it becomes a target of anti-obesity therapies

(Gnad *et al.* 2014). In adult humans, BAT is usually exists in the neck and upper chest areas. Whereas, in mice, BAT is commonly found in visceral and subcutaneous areas, though, its amount is smaller than WAT (Frontini & Cinti 2010). BAT forms during embryo state and appears before the other adipose types, providing newborn capacity for non-shivering thermogenesis and adaptation to the cold (Wang & Seale 2016). The expression adipogenic markers in differentiated adipocytes for both WAT and BAT are similar, such as *PPAR-γ, CEBP-α*, and *FAB4* (Giralt & Villarroya 2013). However, the distinguishing markers of BAT from the WAT include *UCP1, CIDEA, PGC-1α*, and DIO_2. Note that this type of tissue is not used in this study.

2.2.2.3 Beige Adipose Tissue

WAT and BAT are two general classical classes of adipose tissue in mammals. WAT which is reported to contain small amount of UCP-1 are able to be induced into thermogenic adipocyte called as 'beige' or 'brite' (brown-in-white) adipose tissue (Harms & Seale 2013). This process is called as browning. Browning process refers to the condition where WAT transforms into 'brown-like' adipocytes that have the ability to undergo thermogenesis like brown adipocytes (Wang & Seale 2016; Rodríguez *et al.* 2016; Harms & Seale 2013; Lidell *et al.* 2014). In human, beige adipose tissue is located in the supraclavicular regions, and interspersed within WAT subcutaneous fat in both mice and humans (Ruiz-Ojeda *et al.* 2016).

The discovery of beige adipose tissue introduces a new target for obesity treatment. Under specified stimuli or exposures such as cold, β3-adrenergic agonists, or PPAR-γ agonist, beige adipose tissue is emerged in WAT. Similar to BAT, beige adipose tissue which also expresses *UCP-1*, is able to convert energy into heat (Harms & Seale 2013). Nevertheless, there are many distinguishing characteristics of beige adipose tissues from WAT, and BAT, respectively. Table 2.4 provides the details of BAT, WAT, and beige adipose tissues that can explain their similarities and distinguishing characteristics.

Table 2.4 Characteristics of white adipose tissue, brown adipose tissue, and beige adipose tissue (Wang & Seale 2016).

Type	**Location**	**Developmental origin or precursor type**	**Common marker**		**Brown and beige versus white marker**	
			Adipocyte	Preadipocytes	Adipocyte	Preadipocytes
White	Subcutaneous and visceral	WT1+ mesothelial (visceral)	• ADIPOQ • FABP4 • PPARG • C/EBPIIB	• PDGFRA • LY6A • CD34 • PREF1 • CD29	• LEP • RETN • AGT	• WT1 (visceral fat)
Brown	Interscapular, cervical, axillary and perirenal	$MYF5^{+}$ $PAX7^{+}$ $EN1^{+}$ cells in dermomyotome			• UCP1 • DIO2 • CIDEA • PPARGC1A • PPARA • COX7A1 • COX8B • PRDM16 • *EBF2*	*EBF2*
Beige	WAT depots (more prominent in inguinal than in epididymal)	Inguinal WAT •$EBF2^{+}$ $PDGFRA^{+}$ cells •$ACTA^{2+}$ smooth muscle cells •$MYH11^{+}$ smooth muscle cells •PDGFRB+ mural cells, epididymal WAT •Bipotent $PDGFRA^{+}$ precursor				

2.3 Adipogenesis

Adipogenesis or formation of adipose tissue is a multi-step process involving coordination of many transcription factors, cofactors, and proteins. Mature adipocytes do not divide in vivo. Thus, regeneration and increase of adipocytes number are depending on self-renewal of preadipocytes that exist through lifetime in an adult (Dani & Billon 2012). Meanwhile, BAT is formed during embryonic state and is decreased in adult stage. Formation of beige adipose tissue provides intervention of cell involved in energy utilization instead of BAT. Beige adipose tissue is formed in WAT under specified stimuli or condition such as cold, β3-adrenergic agonists, or PPAR-γ agonist (Wang & Seale 2016; Rodríguez *et al.* 2016; Harms & Seale 2013; Lidell *et al.* 2014). This study focused on WAT, and browning of WAT, termed as beige adipose tissue. Thus, the formation of adipose tissue, expression of genes markers, and types of induction cocktails are described for WAT and beige adipose tissue.

2.3.1 White Adipose Tissue

Adipogenesis of WAT is consisted of two major events. First is the recruitment and proliferation of preadipocytes from sources such as mesenchymal stem cells (MSC) that have the potential to differentiate into many types of cells including adipocytes, osteoblast, and myoblasts. Second event is the subsequent differentiation of preadipocytes into mature adipocytes (Avram *et al.* 2007).

2.3.1.1 Process of Adipocytes Differentiation of WAT

The process of adipocyte differentiation is characterized into two phases, which are determination phase and differentiation phase. Chronological changes in the expression of numerous genes occurred during early, intermediate, and late stage of adipocyte differentiation (Gregoire *et al.* 1998). Figure 2.3 summarizes the process of adipocytes differentiation.

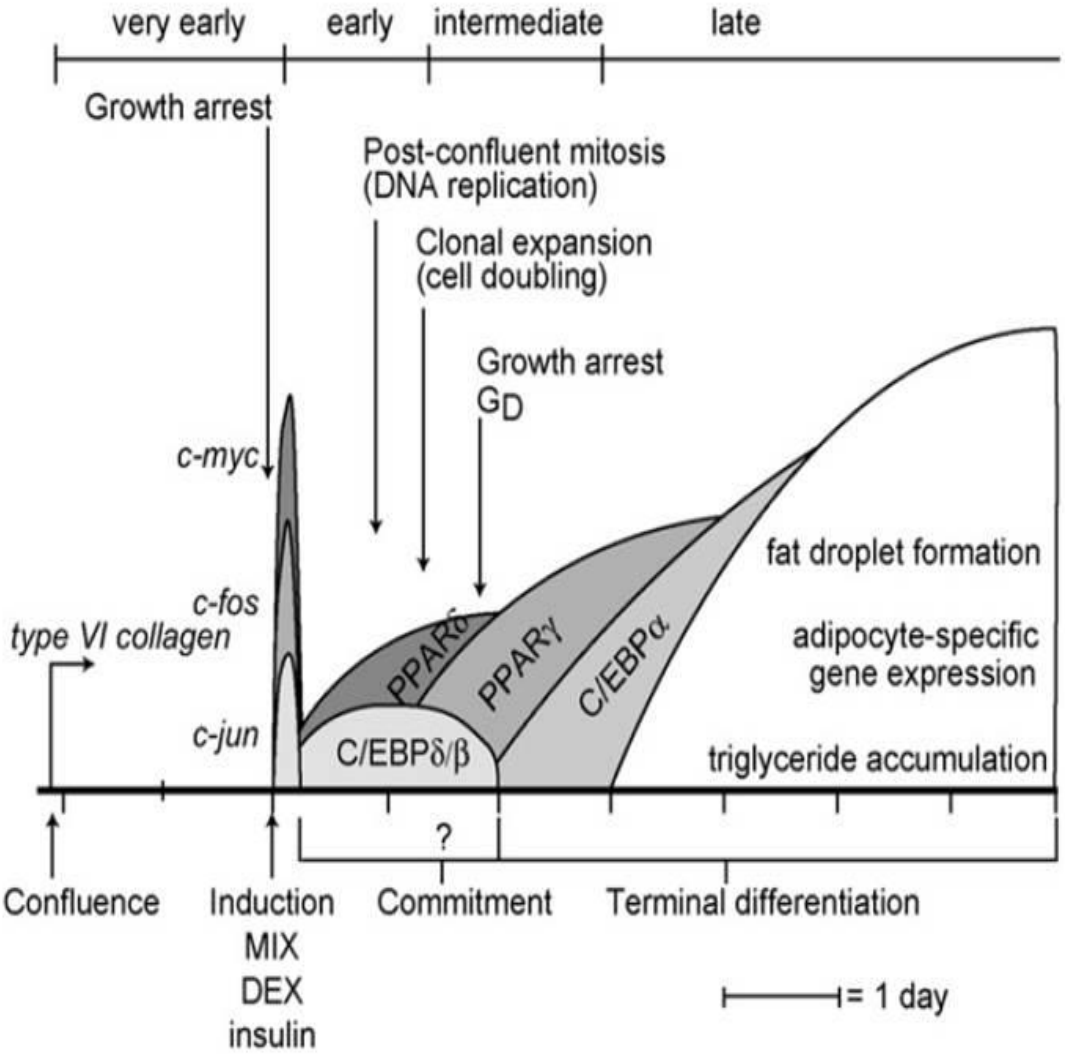

Figure 2.3 Schematic diagram of white adipose tissue differentiation (Avram *et al.* 2007).

2.3.1.1.1 Determination phase

This stage is the determination of the MSC into preadipocytes lineage through mechanisms that are poorly understood (Avram *et al.* 2007). MSCs are then lost potential to differentiate into the other types of cells lineage including myoblast, and osteoblast.

2.3.1.1.2 Differentiation phase

The MSCs that have recruited into preadipocytes lineage can be induced to differentiate into mature adipocytes. The differentiation phase is consisted of several stages (Avram *et al.* 2007; Gregoire *et al.* 1998; Moreno-navarrete & Fernández-real 2012) as follow:

2.3.1.1.3 Growth Arrest

Growth arrest is prerequisite stage in the commitment of all preadipocytes toward terminal differentiation. Preadipocytes have to withdraw from the cell cycle before adipose conversion (Gregoire *et al.* 1998). Once confluence, the proliferation of preadipocytes becomes growth arrested (Avram *et al.* 2007). However, confluence preadipocytes are not prerequisite for adipose conversion, as the confluence preadipocytes that have shifted into suspension are able to undergo differentiation during this phase (Pairault & Green 1979). The transition of cell cycle into differentiation stage is marked with the expression of very early markers of differentiation in cultured cell lines, such as collagen type VI (Avram *et al.* 2007).

2.3.1.1.4 Clonal Expansion

Following the growth arrest is hormonal induction by adipogenic induction cocktails such as IBMX, DEX, and insulin with the presence of DMEM and fetal bovine serum (FBS). Once induced, the transcriptions factors such as C/EBPβ and C/EBPδ are observed, which is important as initiator of post confluent mitosis and clonal expansion (Avram *et al.* 2007). Approximately 24 hours after the induction by adipogenic cocktails, the preadipocytes undergo at least one round of DNA replication and cell doubling (Pairault & Green 1979). 3T3-L1 preadipocytes require at least one doubling prior to differentiation (Moreno-navarrete & Fernández-real 2012). Two days after hormonal induction, 3T3-L1 cells undergo second and final growth arrest event which is required preceding terminal differentiation (Avram *et al.* 2007). *PPAR-γ* and *C/EBP-α* expression are rapidly increased after hormonal induction, and detectable during second day of preadipocytes differentiation (Gregoire *et al.* 1998). These genes expression are having subsequent involvement towards terminal differentiation by transactivation of adipocyte-specific genes (Gregoire *et al.* 1998).

2.3.1.1.5 Terminal Differentiation

During the terminal phase of differentiation, preadipocytes are turned into mature adipocyte. At this phase, adipocytes increase de novo lipogenesis and sensitivity to insulin (Gregoire *et al.* 1998). Cells become able to transport large amount of glucose, synthesize fatty acids, and store triacylglycerol (Fève 2005). Fibroblast shape of preadipocytes are changed into spherical shape which characterizes it as mature adipocytes (Gregoire *et al.* 1998).

PPAR-γ and *C/EBP-α* are key events controlling terminal adipocytes differentiation and are also characterized as the markers of mature adipocytes (Dani & Billon 2012). The associated proteins and mRNA involved in lipid metabolism and glucose metabolism are increased by10 to 100 folds during this phase (Fève

2005; Gregoire *et al.* 1998). The proteins involved in lipid metabolisms include FABP4, FAS, and *β*3 adrenoreceptor (Avram *et al.* 2007). The proteins involved in glucose metabolisms include the insulin receptor rand receptor glucose transporters, such as GLUT4 which increases insulin sensitivity (Avram *et al.* 2007). Mature adipocytes also synthesize adipocyte-secreted proteins such as adiponectin, leptin, resistin, zinc-alpha-glycoprotein, and tumor necrosis factor-α (TNF-α) (Avram *et al.* 2007; Gregoire *et al.* 1998).

2.3.1.2 Types of Cells for Differentiation of WAT

There are many types of cells for adipogenesis study. These include pre-adipocyte cell lines, which are already committed to the adipocyte lineage; and MSCs, which have the potential to commit into various cells lineages including adipocyte, bone and muscle lineage (Moreno-navarrete & Fernández-real 2012). Preadipocytes which are already committed to adipocyte lineage are commonly used to test effects of active compound in adipogenesis as MSCs are needed to be committed into adipocytes lineage before adipocytes differentiation (Avram *et al.* 2007). The examples of preadipocytes lines are 3T3-L1, 3T3-F442A, porcine primary preadipocytes, and feline primary preadipocytes. Whereas, MSCs cell lines include OP9, C3H10T1/2, and primary mouse embryonic fibroblasts (MEFs) (Ruiz-Ojeda *et al.* 2016).

2.3.1.3 3T3-L1 Preadipocytes Cell Lines

3T3-L1 preadipocytes cells lines are the most commonly used preadipocytes lines for adipogenesis studies (Ruiz-Ojeda *et al.* 2016). These cells are isolated from the Swiss 3T3 cells line, derived from disaggregated 17–19-day-old Swiss 3T3 mouse embryos (Moreno-navarrete & Fernández-real 2012). It is originated from MSCs (Scott *et al.* 2011). These clonal cell lines are most suitable for adipogenesis

study as they have homogenous cells population which allow for homogenous treatment, have same cells differentiation stage, high passaging number, less costly, and long life (Moreno-navarrete & Fernández-real 2012; Ruiz-Ojeda *et al.* 2016). This study is used 3T3-L1 cells as *in vitro* model to study the effects of DSW in WAT. 3T3-L1preadipocytes are ready to differentiate into adipocyte with the presence of adipogenic cocktails.

2.3.1.4 Adipogenic Differentiation Cocktails

The commonly used adipogenic induction cocktails for adipocyte differentiation are insulin, dexamethasone (DEX) and methylisobutylxanthine (IBMX),which elevates intracellular cAMP levels, in the presence of fetal bovine serum (Caprio *et al.* 2007; Ruiz-Ojeda *et al.* 2016; Scott *et al.* 2011). DEX is used as glucocorticoids (GCs) to stimulate the GC receptor. DEX is an important agent in early adipocytes differentiation, while its absence inhibits adipocyte differentiation (Caprio *et al.* 2007). IBMX and DEX induce C/EBP-β and C/EBP-δ, which activate expression of transcription factors of PPAR-γ and C/EBP-α (Fève 2005). IBMX promotes protein kinase A (PKA). PKA signaling pathway is required for transcriptional activation of PPAR-γ and other adipogenic gene expressions (Kim *et al.* 2010). Insulin activates p38 MAPK which is required to promote differentiation of preadipocytes into adipocytes (Fève 2005). Insulin also functions to accelerate lipid accumulation in cells (Gregoire *et al.* 1998).

2.3.2 Beige Adipose Tissue

Beige adipose tissue is only emerged in WAT. Thus, its induction requires WAT either from clone lines or from primary preadipocytes.

2.3.2.1 Formation of Beige Adipose Tissue

Beige adipose tissue is emerged in WAT under specified stimuli or exposures such as cold, β3-adrenergic agonists, or PPAR-γ agonist. There are some debates either beige adipose tissue arises from a precursor population or from pre-existing adipocytes. Some study reported that beige adipose tissues emerged in mature WAT in response to cold or β3-adrenergic agonists (Himms-Hagen *et al.* 2000; Vitali *et al.* 2012). However, recent reports showed many evidences that beige adipose tissues are emerged from the specific precursors in preadipocytes.

WAT contains small number of UCP-1, whereas its increase is observed when WAT is stimulated by thermogenic stimulus. Prolonged cold exposures lead to expression of UCP-1 in most WAT depots of mice. Interestingly, beige adipose tissue has reversible characteristics. Beige adipose tissues that formed during cold exposure lose UCP-1 expression but can still exist in WAT after warm exposure. In this state, beige adipose tissues adopt a WAT-like morphology (unilocular). Beige adipose tissues later can be reactivated to have multilocular morphology and UCP-1 expression once stimulated by cold, β3-adrenergic agonists, or PPAR-γ agonist. Beige adipose tissues are a distinctive type of fat cell that expresses UCP-1 and thermogenic components in the activated state and have WAT morphology when no stimuli were introduced (Wu *et al.* 2012). Figure adopted from Wang & Seale (2016) shows the development of beige adipose tissues through the possible mechanisms in both inguinal WAT, and epididymal WAT, respectively.

Accumulating evidences suggested that Prdm 16 is a crucial key component to drive differentiation of beige adipose tissues in WAT (Harms & Seale 2013; Wang & Seale 2016). Transgenic expression of Prdm16 in WAT significantly induces the development of brown-like adipocytes, whereas it reduction cause a decrease in the expression of thermogenic genes, indicating impaired beige adipose tissues development (Seale *et al.* 2011; Lin & Scott 2012). Mechanistic studies indicate that PRDM16 binds and enhances the transcriptional function of PPAR-γ, PPAR-α,

ZFP516, thyroid receptor, PGC-1α, and C/EBP proteins (Kajimura *et al.* 2009; Iida *et al.* 2015; Seale *et al.* 2008; Hondares *et al.* 2011).

Cold exposure increases the expression of transcription factor Early B-Cell Factor-2 (*EBF2*). *EBF2* is identified in the precursor cells, and regulated through differentiation of beige adipose tissues (Wang & Seale 2016). *EBF2* shows important role as it cooperates with PPAR-γ, a master regulator for adipocyte differentiation, to promote adipogenesis (Akerblad *et al.* 2002). *EBF2* induces the expression of UCP-1, whereas mice *EBF2*-knockdown did not induce UCP-1 which promotes the recruitment of beige adipose tissue in WAT (Stine *et al.* 2016). *EBF2*-deficient WAT inhibits browning process, showing that, in addition of it as markers of beige adipose tissue, it is crucial in beige adipose tissue development (Stine *et al.* 2016).

PPAR-α functions in controlling mitochondrial b-oxidation in various cell types. PPAR-α also activates critical brown fat–selective genes, including Ucp1, Prdm16, and *PGC1*-α,which are key drivers of brown fat differentiation (Seale 2015; Hondares *et al.* 2011).

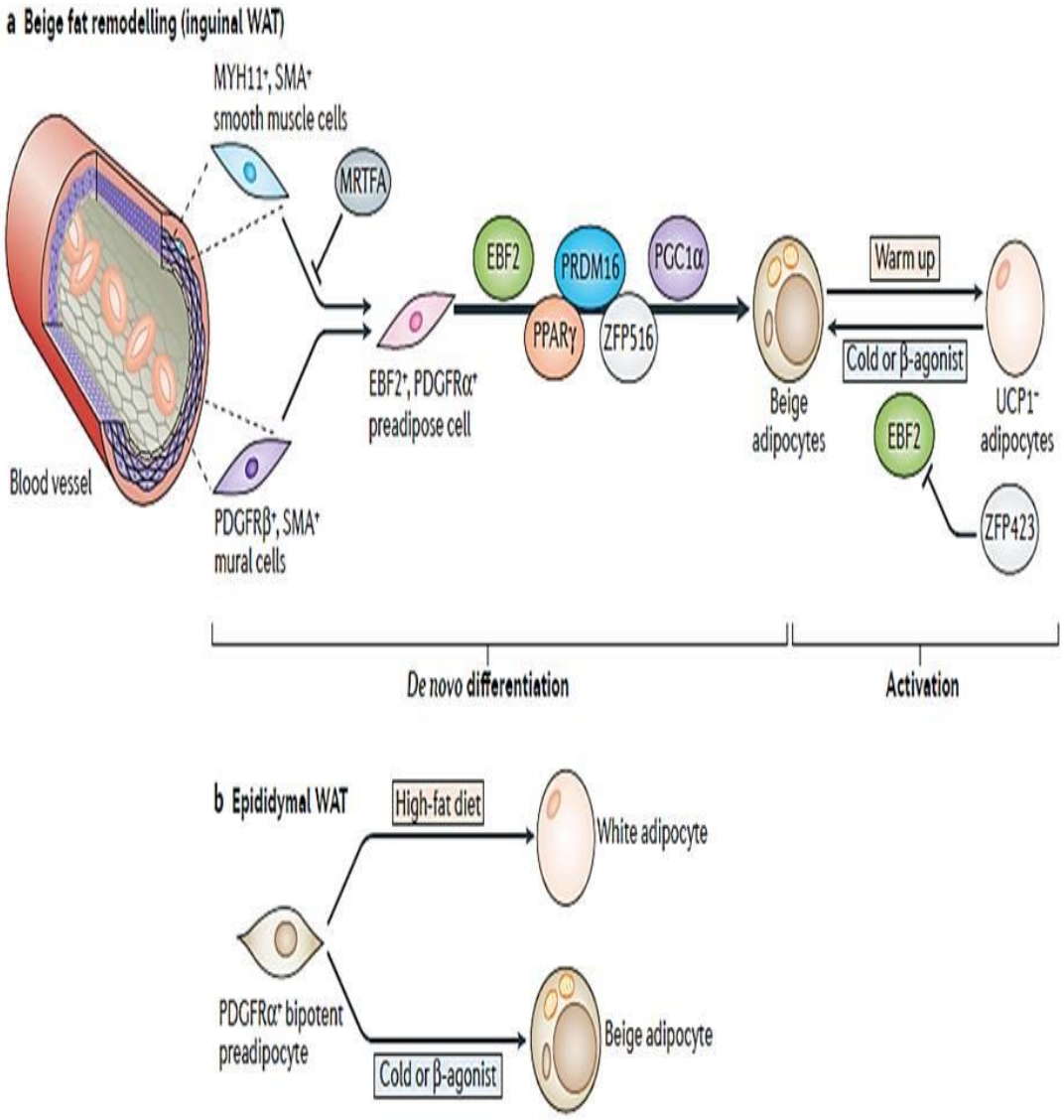

Figure 2.4 Formation of beige adipose tissue (Wang & Seale 2016).

2.3.2.3 Type of Cells for Differentiation of Beige Adipose Tissue

Inguinal WAT (a major subcutaneous depot in rodents) are highly susceptible to browning, compared to other depots such as the epididymal WAT which are quite resistant to it (Wang & Seale 2016). For that, most studies have focused on the inguinal WAT depot in mice to study mechanisms associated with browning. Thus, this study used SVF cells that contain preadipocytes isolated from inguinal depot of mice.

2.3.2.4 Adipogenic Differentiation Cocktails of Beige Adipose Tissue

Preadipocytes can be induced into beige adipose tissue by using the specific medium such as insulin, DEX, IBMX, rosiglitazone, indomethacin, and triiodothyronine (T3) in the specified concentrations (Ruiz-Ojeda *et al.* 2016; Aune *et al.* 2013). Beige adipose tissues express the thermogenic genes only in response to activators such as agonists of the β-adrenergic receptor or PPAR-γ. PPAR-γ agonist such as thiazolidinedione (TZD) has shown important role in beige adipose tissue development. TZDs are particularly potent activators of mitochondrial biogenesis and thermogenic genes including *Ucp1* (Seale 2015). Rosiglitazone is a commonly used TZDs, is a crucial compound which induce thermogenic gene expression in fat cells through stabilization on Prdm16 (Lin & Scott 2012). TZDs also activate SIRT1, an NAD-dependent deacetylase that deacetylates two residues in PPAR-γ which efficiently bind to Prdm 16 (Qiang *et al.* 2012). Increase of SIRT1 activity in adipose tissue promotes WAT browning and combat obesity (Seale 2015). T3 functions to induce the expression of UCP-1 and other thermogenic components (Bianco & Silva 1987; Iida *et al.* 2015). T3 also regulates the expression of PPAR-γ (Symonds 2012). Indomethacin promotes adipogenesis of mesenchymal stem cells through a cyclooxygenase independent mechanism (Styner *et al.* 2010). Indomethacin also play part in activation of PPAR-γ (Lehmann *et al.* 1997).

2.4 Adipogenic Genes Markers

WAT, BAT, and beige adipose tissues are the recognized form of adipocytes until to date. These adipose tissues share common adipogenic genes markers which are *PPAR-γ, C/EBP, adiponectin,* and *FABP4* (Wu *et al.* 2015; Giralt & Villarroya 2013; Seale 2015)**.** *PPAR-γ* is predominantly expressed in adipose tissues and plays a central role in adipose tissue functions. *PPAR-γ* regulates the expression of genes associated with insulin signaling and glucose and lipid metabolism in the mature adipocytes (Taher *et al.* 2015). Reduced expression of *PPAR-γ* and *C/EPB-α* has been shown to inhibit adipogenesis such as in 3T3-L1 cells. SIRT1 shows important role in browning of WAT by deacetylating *PPAR-γ* on Lys268 and Lys293. An acetylation-defective *PPAR-γ* mutant induces a brown phenotype in WAT, whereas an acetylated mimetic fails to induce ‘‘brown’’ genes (Qiang *et al.* 2012). SIRT1-dependent *PPAR-γ* deacetylation is suggested as a form of selective *PPAR-γ* modulation that has potential therapeutic target C/EBP family was the first transcription factors demonstrated to play a major role in adipocyte differentiation (Gregoire *et. al*., 1998).

2.5 Transcriptionals Factors for Thermogenic Genes Programs in Beige Tissue

The key thermogenic genes of beige adipose tissue are similar to BAT in which they include *UCP1*, cell death-inducing DFFA-like effector A (*CIDEA*), peroxisome proliferator-activated receptor-α (*PPAR-α*), and peroxisome proliferator-activated receptor gamma coactivator 1α (*PGC-1α*) (Wang & Seale 2016).

PGC-1α is recognized as a master regulator of mitochondrial biogenesis and oxidative metabolism in many cell types (Harms & Seale 2013). *PGC1-α* is required in *UCP-1* expression and thermogenic genes activation (Seale 2015). Interferon regulatory factor-4 (*IRF4*) is an important transcription factor partner of *PGC-1a* and a critical activator of the thermogenic gene. Increased expression of *IRF4* increases

the *UCP-1* expression. *IRF4* deletion in BAT and beige adipose tissue suppresses the energy dissipation and increases susceptibility to obesity and insulin resistance. *IRF4* presence during browning process is important as *PGC-1α* is unable to activate thermogenic during its absence (Kong *et al.* 2014).

Zinc-finger protein 516 (ZFP516) plays a critical role in both the differentiation and the activation of brown and beige fat cells. ZFP516 is required in general adipogenesis and is also involved in mitochondrial structural and UCP-1 expression (Seale 2015). PRDM16 that binds directly with ZFP516 is proposed as an important co-activator of ZFP516 in fat cells. Overexpression of ZFP516 in adipose tissue that has high level of PRDM16 increases browning of WAT in the inguinal depot and suppresses obesity (Seale *et al.* 2011).

C_2H_2 zinc-finger (ZF) protein, Zfp423 is identified as a transcriptional regulator of pre-adipocyte determination (Gupta *et al.* 2010). It is important in formation of fat and its expression is remains throughout adipocyte differentiation and is present in all mature fat cells (Shao *et al.* 2016). Its presence maintains WAT identity of induced browning of WAT by direct repression of *EBF2* activity (Shao *et al.* 2016). Hence, genetic ablation of Zfp423 in WAT of adult animals leads to a conversion of mature WAT into beige adipose tissue (Shao *et al.* 2016). This provides insight regarding possible mechanisms that are able to block or drive the browning of WAT.

Transcriptions factors and coregulators such as PGC-1α, IRF4, Zfp516, and LSD1 are important in the activation of thermogenic genes in response to cold or β-adrenoceptors stimulation, though, PRDM 16 is not cold inducible (Sambeat *et al.* 2016).

Growth factors such as bone morphogenic factor 7 (BMP7) and fibroblast growth factor 21 (FGF21) also play role in thermogenic gene program. BMP7 is involved in the commitment of MSCs into BAT lineage and also activates thermogenic genes (Sambeat *et al.* 2016). BMP7 disrupts the Zfp423-*EBF2* complex

that can inhibit browning of WAT through induction of a Zfp423-Smad complex. This event provides evidence of cross-talk between BMP7 signaling and *EBF2* signaling pathways in the thermogenic genes program (Shao *et al.* 2016). FF12 is secreted by liver, BAT, and WAT in response to cold exposure that activates the thermogenic genes. FGF12 deletion reduces browning of WAT and impairs cold tolerance in mice (Fisher *et al.* 2012).

Thermogenic adipose tissue program is also affected by epigenetic regulations, which include DNA methylation, and histone modifications. DNA methylation and the histone H3K4 modification involving corepressor receptor-interacting protein 140 (RIP140) silence the UCP-1 expression (Kiskinis *et al.* 2007).

CHAPTER 3

METHODOLOGY

3.1 Introduction

The experimental work of research was started by preparing DSW for uses in experiment. Briefly, the concentrations of minerals in DSW were analyzed, and then were formulated for specified concentrations that required for experiment by using the dilution technique. This study adopted *in vitro* model to test the effects of DSW in adipogenesis. There are two types of adipose tissues were used, which are 3T3-L1 preadipocytes and stromal vascular fraction (SVF) cells that isolated from mice. Both types of adipose tissues were treated with several concentrations of DSW, then, were analyzed for cell viability, intracellular lipid content, and expression of adipogenic genes. As SVF cells were induced into thermogenic adipocytes, the effects of DSW in the expression of thermogenic genes were determined. The flowchart of research is shown in Figure 3.1.

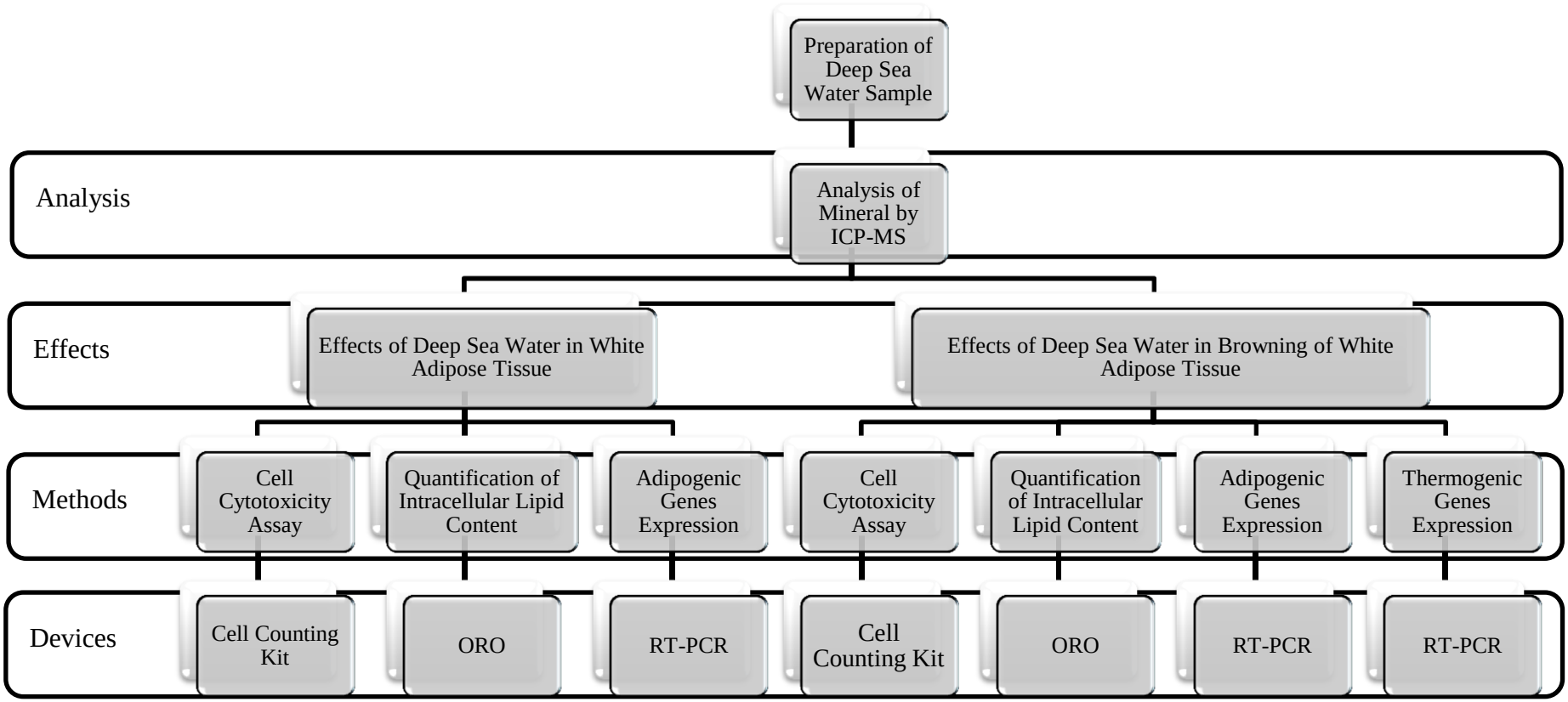

Figure 3.1 Flowchart of research.

3.2 Materials

Materials in this section describe the reagents, apparatus, methods, equipment those used in the research.

3.2.1 Chemicals and Reagents

Dulbecco's modified Eagle's medium (DMEM), DMEM/F12, penicillin-streptomycin, fetal bovine serum (FBS), trypsin, and phosphate buffered saline (PBS) were obtained from Gibco BRL (Grand Island, NY, USA). Insulin, rosiglitazone, 3-isobutyl-1-methylxanthine (IBMX), indomethacin, 3, 3', 5-Triiodo-L-thyronine (T3), and dexamethasone (DEX) were purchased from Sigma Chemical Co. (St. Louis, MO, USA).

3.2.2 Preparation of Deep Sea Water Samples

Concentrated DSW was provided by the unit of Seawater Utilization Plant Research Center (SUPRC) of Korea Research and Ocean Ship Engineering (KRISO) (Gangwon, Korea). In brief, original DSW was pumped up from a depth of 0.5 km and a distance of 6.7 km off Oho-Ri, Goseong (Gangwon-Do, Korea); is filtered using a microfilter system (Synopex Inc., Pohang, Korea) to remove phytoplankton and marine microorganisms. The filtered DSW passed through a reverse osmosis membrane (Vontron Technology Co., Ltd., Beijing, China), then, DSW mineral extracts and desalinated water is obtained. In this experiment, concentrated DSW went through several dilution processes to produce the required concentration, then, known as balanced DSW. The concentration of DSW in this experiment is determined by hardness which calculated by using a formula described in Equation 3.1.

$$\text{Hardness: Mg (mg/L)} \times 4.1 + \text{Ca (mg/L)} \times 2.5 \quad (3.1)$$

Concentrations of minerals in DSW were analyzed using inductively coupled plasma mass spectrometry (ICP-MS) device at the laboratory of University Industry Research Laboratory (UIRL), Universiti Teknologi Malaysia, Johor.

3.2.3 Sources of Cell Lines

3T3-L1 cells were obtained from the American Type Culture Collection (ATCC) (Rockville, MD, USA). The 3T3-L1 cell line is a well-established preadipocyte cell line that was developed from Swiss 3T3 cells mouse embryos, which display a fibroblast-like morphology under appropriate conditions (Ruiz-Ojeda et al. 2016). SVF cells were derived from primary cells isolated from mouse, which were obtained from animal house at Kanazawa University, Graduate School of Medical Sciences, Kanazawa, Ishikawa 920-8641, Japan. The images of untreated 3T3-L1 preadipocytes and SVF cells were photographed using an inverted microscope as shown in Figure 3.2.

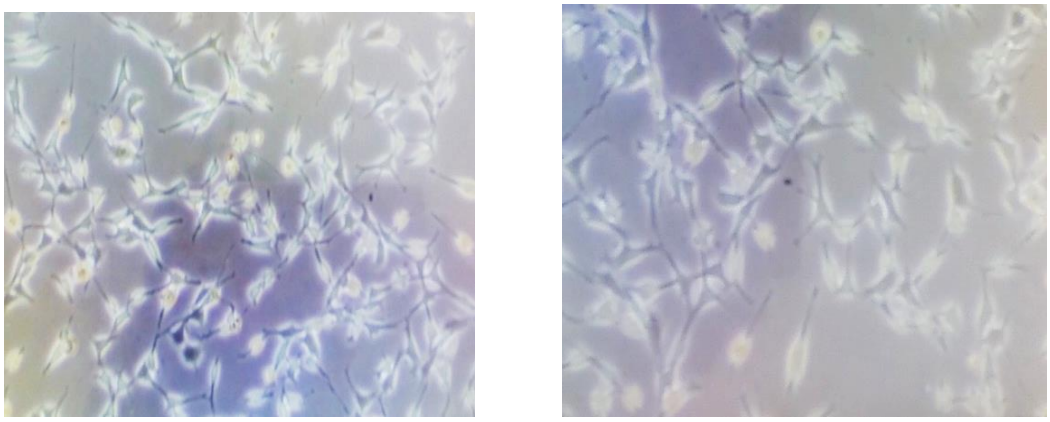

(a) 3T3-L1 Preadipocytes (b) SVF Cells

Figure 3.2 Images of (a) 3T3-L1 preadipocytes and (b) SVF cells were photographed using an inverted microscope by 10 x magnifications.

3.3 Cell Culture Protocol

Cell culture consisted of several procedures include cell thawing, cell maintenance, cell seeding, cell counting, and cell assay. Cell assay is type of experiment or analysis that using cell.

3.3.1 Cell Thawing

Cells were removed from liquid nitrogen tank and outside of the cell vial was cleaned with 70% ethanol. Cells then were thawed in a 37°C water bath for 1 – 2 minutes until it started to defreeze. After that, 1 ml of cells suspension was quickly transferred into 9 ml of pre-warmed complete growth medium (1:10 ratio). Complete growth medium of 3T3-L1 cells was consisted of DMEM containing 10% FBS and 1% penicillin/streptomycin, while complete growth medium of SVF cells was consisted of DMEM/F12 containing 10% FBS and 1% penicillin/streptomycin. Cells were gently mixed and were centrifuged at 1000 x g for about 4 minutes for 3T3-L1 cells and 700 x g for 10 min for SVF cells. Cells then seen as a pellet at bottom of tube. Supernatant was discarded and cells pellet were gently suspended with the particular pre-warmed complete growth medium. Later, cells were transferred into petri dish or flaks for cell culture.

3.3.2 Cell Maintenance

3T3-L1 preadipocytes were cultured in complete growth medium that consisted of DMEM containing 10% FBS and 1% penicillin/streptomycin. It was placed in an incubator at 37°C in a humidified atmosphere of 5% CO_2 until it reached 80% - 90% confluence. SVF cells were cultured in $10cm^3$ petri dish using completed growth medium consisted of DMEM/F12 containing 10% FBS and penicillin/streptomycin at 37ºC in 5% CO_2 in an incubator until it reached 90%

confluent. Cells those reached required percentage of confluent were ready to be seeded in well plates.

3.3.3 Cell Seeding

In this experiment, both of 3T3-L1 cells and SVF cells were seeded in 96-well plates for cell cytotoxicity assay and 24-well plates for adipogenesis assay, respectively. Media were removed from petri dish or flask and PBS was used to wash the cells. Adherent 3T3-L1 cells and SVF cells were detached from petri dish or flask using 5 mL of trypsin and incubated at 37ºC in 5% CO_2 approximately for 5 minutes. Detached cells were confirmed by observation using an inverted microscope, and then, were mixed well with 5 ml of fresh pre-warmed complete growth medium. Later, cells suspension were seeded into well plates. Cells densities and volume of cell culture medium for 3T3-L1 cells and SVF cells in the particular types of well plates are shown in Table 3.1. All tests that used the live cells were conducted in workstation for cell culture as shown in Figure 3.3.

Table 3.1 Protocol of cell seeding.

Cell Type	Plate Type	Cell Density (cell/mL)	Cell Medium Volume (µL)
3T3-L1 Adipocyte	96-well	1.0 x 104	200
	24-well	2.0 x 104	1000
Beige Adipocyte	96-well	1.0 x 104	200
	24-well	2.0 x 104	1000

Figure 3.3 Workstation for cell culture consisted of (a) biological safety cabinet for cell culture, (b) time counter, (c) chair, (d) centrifuge, (e) alcohol, and (f) white board. See appendix B for list of equipment and appliances used.

3.3.4 Cell Counting

The numbers of cultured cells were counted and determined using hemacytometer. These were incorporated by counting and staining cells in suspension. Counting cells with a hemacytometer were prepared by mixing equal volume of both 20 µl of cells and 20 µl of 4% trypan blue, respectively. The mixture was then transferred into both chambers of the hemacytometer. Then, the numbers of cells were counted under microscope. Dead cells take up the blue stain of trypan blue dye while live cells are unstained by the dye. The cell densities are calculated as in Equation 3.2.

$$\text{Cell densities (cells/ml)} = \frac{\text{Total number of viable cells x dilution factor x } 10^4}{\text{Total number of squares calculated}} \quad (3.2)$$

$$\text{Cell viability (\%)} = \frac{\text{Number of live cells}}{\text{Total number of live and dead cells}} \times 100 \quad (3.3)$$

3.4 Cell Cytotoxicity Assay

Cell cytotoxicity assay was conducted to determine viability of cells by using the Cell Counting Kits (CCK)-8 (Dojindo Laboratories, Japan) according to the manufacturer's instruction. Briefly, SVF cells or 3T3-L1 preadipocytes were cultured in complete growth medium that consisted of DMEM containing 10% FBS and 1% penicillin/streptomycin in the incubator at 37°C in a humidified atmosphere of 5% CO_2 until it reached 70 % – 80 % confluence. Pre-confluent SVF cells or 3T3-L1 preadipocytes were seeded in the 96-well plates at a density of $1x10^4$ cells per well for 24 h in the incubator at 37°C in a humidified atmosphere of 5% CO_2. After 24 h, cells were treated with 100 µl of DSW in each well. The cell treatment was conducted for 24 hour. Then, 10 µl CCK-8 reagent was added to each wells, followed by 4 h additional incubation time to stain the living cells. The amount of formazan dye was measured by absorbance at 450 nm using an enzyme-linked

immunosorbent assay (ELISA) microplate reader. Percentage of cell viability is determined by using Equation 3.4.

$$\text{Cell viability (\%)} = \frac{\text{Absorbance of treated group}}{\text{Absorbance of untretaed group}} \times 100 \quad (3.4)$$

3.5 Calculation of Inhibitory Concentration and Lethal Dose

Inhibitory concentration 50 (IC_{50}) is a measure to indicate how much of a particular compound or substance is needed to inhibit half of a given biological response. Lethal Dose 50 (LD_{50}) is the standard measure to determine the concentration of a given compound or chemical that needed in killing half of the tested animals. LD_{50} was estimated based on ICCVAM (2006). In this study, IC_{50} and LD_{50} for DSW using the 3T3-L1 preadipocytes and SVF cells were estimated.

3.6 3T3-L1 Cells Differentiation

Differentiation of 3T3-L1 cells were followed protocol by Taher *et al.* (2015). After preadipocytes reached 80% - 90% confluence, they were seeded in 24-well microplate, and were cultured for two days until reached 100% confluence. DSW treatments on cells in 24-well microplate template layout were as shown in Figure 3.4. Then, the cells were going through post confluence for additional two days (Day 0). Differentiation process is started by stimulated the cells with adipogenic induction cocktails (AIC) consisted of 1 µg/mL of DEX, 100 µg/mL of IBMX, and 1 µg/mL of insulin in the DMEM containing 10% FBS and 1% penicillin-streptomycin for 48 hours (Day 2). Preadipocytes were then cultured in DMEM containing 10% FBS supplemented with 1µg/mL of insulin for two days (Day 4), followed by culturing with DMEM containing 10% FBS which is replaced every two days (Day 6 - Day 8). The preadipocytes differentiations were continued until it gained successful differentiation, which is determined by more than 90% formation of mature

adipocytes. Mature adipocytes are indicated by observable lipid droplets accumulation through microscope. DSW was diluted in DMEM powder, which followed the protocol of ATCC. Then, DSW that was diluted in DMEM powder was diluted with differentiation medium to have concentrations that are required. DSW samples for treatments were prepared freshly in the differentiation medium and supplemented every two days starting from Day 0 until preadipocytes reached mature state.

The protocol of adipocytes differentiation treated with DSW using 3T3-L1 preadipocytes was illustrated in Figure 3.4. The experiments were conducted in Tissue Culture Engineering Research Laboratory, Faculty of Chemical Engineering, Universiti Teknologi Malaysia, 81310 Skudai, Johor. Genes expression analysis were conducted in Department of Endocrinology and Metabolism, Kanazawa University Graduate School of Medical Sciences, Kanazawa, Ishikawa 920-8641, Japan.

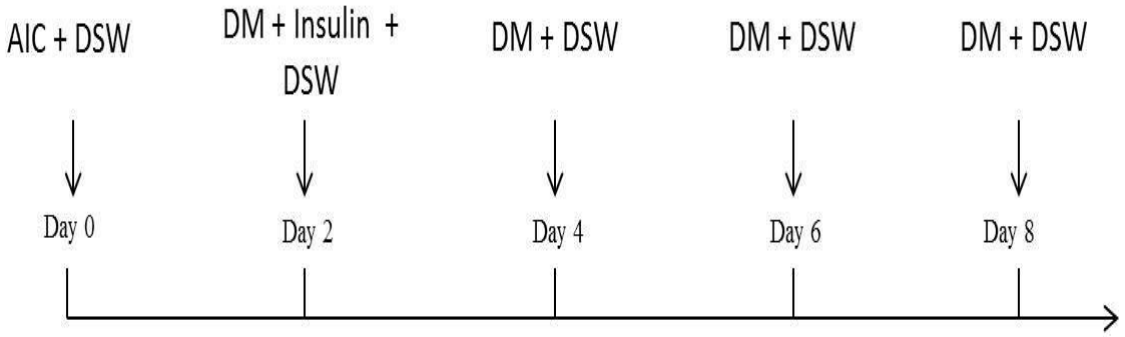

Figure 3.4 Protocol of adipocytes differentiation treated with DSW using 3T3-L1 preadipocytes (AIC - adipogenic induction cocktails; DM – differentiation medium; DSW – deep sea water).

	Control 1	DSW 100	DSW 500	DSW 1000	DSW 1500
	Control 2	DSW 100	DSW 500	DSW 1000	DSW 1500
	Control 3	DSW 100	DSW 500	DSW 1000	DSW 1500

Well plate untreated with cells and DSW

Well plate treated with cells and DSW

Figure 3. 5 Diagram of DSW treatment on cells in 24-well plate template layout. Cells were cultured using 24-well plate and placed in an incubator. See appendix B for specifications of 24-well plate.

3.7 Ethical Statement

The animal use was carried out in accordance with the Guidelines on the Care and Use of Laboratory Animals issued by Kanazawa University. The protocol has received the approval from the ethical committee of Kanazawa University (Approval No. 143206).

3.8 Isolation of Stromal Vascular Fraction Cells from Mice

Isolation of SVF cells from mice was followed the protocol described by Aune *et al.* (2013). Briefly, SVF cells were isolated from inguinal depot of 6 - 8 weeks of C57Bl/6 male mice. SVF cells then were minced into small pieces in digestion medium that consisted of collagenase D, dispase II, PBS and 10 mM $CaCl_2$ and digested at 37°C with constant agitation at 150 rpm for 40-50 min. Digestion

was stopped by adding complete growth medium (DMEM/F12 containing 10% FBS and P/S), and mixed well. Then, it was centrifuged at 700 x g for 10 min. Later, SVF cells were seen as a brownish pellet on the bottom of the tube. Oily mature adipocyte layer was aspirated, and the pellet was dissolved in 10 ml complete growth medium, and mixed well. Cell suspension was filtered through a cell strainer (50 - 70 μm diameters) over a new 50 ml tube. After that, cell suspension was transferred to a 15 ml tube and centrifuged at 700 x g for 10 min. Media was aspirated and the pellet were re-suspend in 10 ml complete medium. Cells then were plated on 10mm collagen coated dishes in complete growth medium. After 1-2 hr plating the cells, media was aspirated, and twice washed with PBS and added with fresh medium to remove red blood cells, immune cells and other contaminants. The locations of adipose tissues in mice are illustrated in Figure 3.6.

The experiments were conducted in Department of Endocrinology and Metabolism, Kanazawa University Graduate School of Medical Sciences, Kanazawa, Ishikawa 920-8641, Japan.

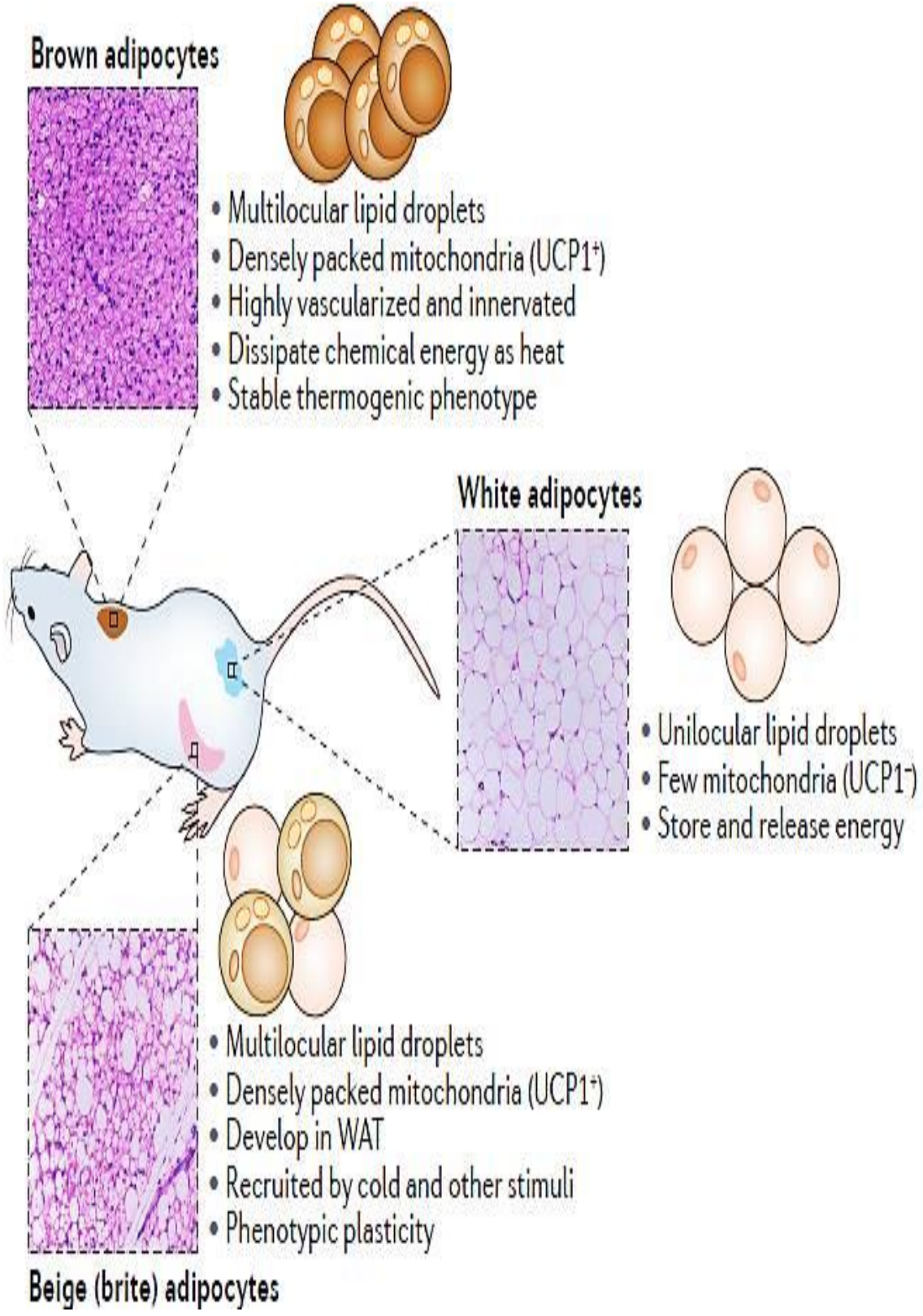

Figure 3.6 Location of adipose tissues in mice (Wang & Seale 2016).

3.9 Beige Adipocytes

Differentiation of beige adipocytes were followed protocol described by Aune *et al.* (2013). After reached 90% confluent, SVF cells were plated in 24-well plates and were differentiated until it reached 90-95% confluence. Induction of beige adipose tissue was initiated with the induction medium (IM) and maintenance medium (MM). Induction medium was consisted of 125 μM indomethacin, 2 μg/ml of DEX, 0.5 mM of IBMX, and 0.5 μM of rosiglitazone. Maintenance medium was contained the complete medium that supplemented with 5μg/ml of insulin, and 1 nM of T3. After 48 hours (Day 2) of beige adipose tissue induction, cells were maintained in fresh maintenance medium that contained 5 μM of rosiglitazone. At day 4, the medium was changed to fresh maintenance medium that contained 1μM of rosiglitazone and cells were cultured for additional 2 - 3 days until it reached confluence. DSW was diluted in powder DMEM that specified for beige adipocytes. The treatment samples of DSW are diluted with induction medium or maintenance medium and are prepared freshly during experiment. The protocol of beige adipocytes differentiation treated with DSW using SVF cells preadipocytes is illustrated in Figure 3.7. The experiments were conducted in Department of Endocrinology and Metabolism, Kanazawa University Graduate School of Medical Sciences, Kanazawa, Ishikawa 920-8641, Japan.

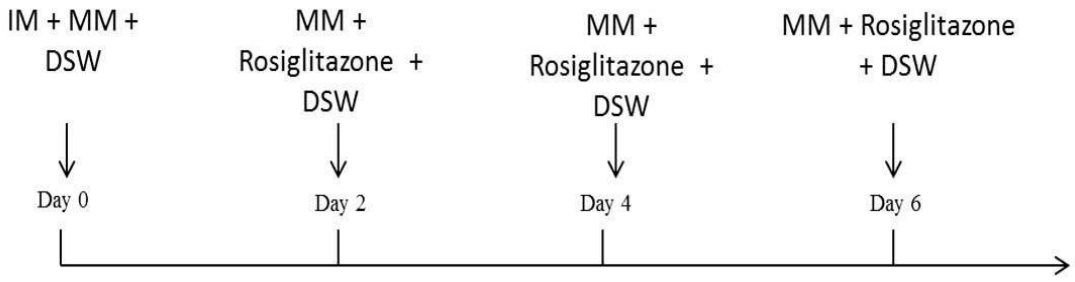

Figure 3.7 Protocol of adipocytes differentiation treated with DSW using SVF cells (DSW - deep sea water; IM - induction medium; MM - maintenance medium).

3.10 Quantification of Intracellular Lipid Content by Oil Red O Staining

Oil Red O (ORO) staining was followed protocol prepared by the Department of Endocrinology and Metabolism, Kanazawa University. Intracellular lipid accumulation was stained using ORO. Cells were washed with phosphate buffer saline (PBS) twice, and fixed with 4% formaldehyde at room temperature for 60 min. After washing with 60% isopropanol, and PBS, cells were stained with ORO solution for 30 min at room temperature. Cells then were washed with distilled water for several times until no visible pink color were observed. The images of stained cells were photographed using an Olympus inverted microscope (Olympus, Tokyo, Japan). Following microscopic observation, the stained cells were extracted with isopropanol and measured spectrophotometrically at 510 nm using a microplate reader as shown in Figure 3.8. Percentage of lipid accumulation was calculated based on Equation 3.5.

Lipid Accumulations (%):

$$= 100 - \frac{(\text{Average control} - \text{average blank}) - (\text{OD value} - \text{Average Blank})}{(\text{Average control} - \text{average blank}) \times 100} \qquad (3.5)$$

Figure 3.8 Microplate reader used for absorbance reading. See appendix B for specifications of microplate reader used.

3.11 Quantitative Genes Expression Analysis using Reverse Transcription Polymerase Chain Reaction (RT-PCR)

Total RNA was extracted from cultured cells using a High Pure RNA Isolation Kit (Roche Diagnostics), according to the manufacturer's protocol. Briefly, total RNA (10ng/µl) was converted to cDNA using a High-Capacity cDNA Reverse Transcription Kit (Life Technologies), according to the manufacturer's instructions. 10 µl of premix reagent prepared as shown in Table 3.2 were dispensed to each well of 96-well PCR plate. Then, 10 µl of 10 ng/µl RNA solution were added to each well and gently mixed with premix reagent. This cDNA conversion process was done using the thermal cycler device as shown in Figure 3.9, with settings of 25℃ for 10 min, 37℃ for 120 min, 85℃ for 5 min and 4℃ for storing time.

Table 3.2 Preparation of premix reagent for cDNA conversion.

Premix Reagent	Sample (µl)
Nuclease free water	4.2
10X RT buffer	2
25X dNTP	0.8
10X Random primer	2
Enzyme	1
Total	10

Standard series and PCR premix reagent was prepared as shown in Table 3.3. Then, 19 µl of premix reagent and 1 µl of cDNA were dispensed to each well. The cDNA population was amplified using a PCR premix kit and concurrently performed using TaqMan probes with references genes of β-actin and 18s. To control for variation in the amount of DNA available for PCR in the different samples, gene expression of the target sequence was normalized in relation to the expression of an endogenous control, 18s (TaqMan Control Reagent Kit; Applied Biosystems). The PCR conditions were one cycle at 50°C for 2 min, 95°C for 10 min, followed by 50 cycles at 95°C for 15 s and 58°C for 1 min.

Table 3.3 Preparation of (a) standard series and (b) PCR premix reagent for genes expression analysis.

	1	0.2	0.04	0.008	0.0016
cDNA	20	4 µl	4 µl	4 µl	4 µl
Nuclease free water	-	16 µl	16 µl	16 µl	16 µl

(a) Standard series.

Premix reagent	Sample (µl)
Nuclease free water	7
2X master mix	10
Target gene	1
Reference gene	1
Total	19

(b) Preparation of PCR premix reagent for genes expression analysis.

PCR products were measured with a StepOnePlus Real-Time RT-PCR System as shown in Figure 3.10. The relative gene expression was calculated based on the comparative CT method using the StepOne software (Applied Biosystems, Foster City, CA, USA). The resulting cDNA was amplified by PCR using the following primer pairs as shown in Table 3.4 (National Center for Biotechnology Information 2017). The sets of primers and TaqMan probes were proprietary to Applied Biosystems (TaqMan Gene Expression Assays product). The experiments were conducted at Department of Endocrinology and Metabolism, Kanazawa University Graduate School of Medical Sciences, Kanazawa, Ishikawa 920-8641, Japan.

Figure 3.9 Thermal cycler device for cDNA conversion. See appendix B for specifications of thermal cycler.

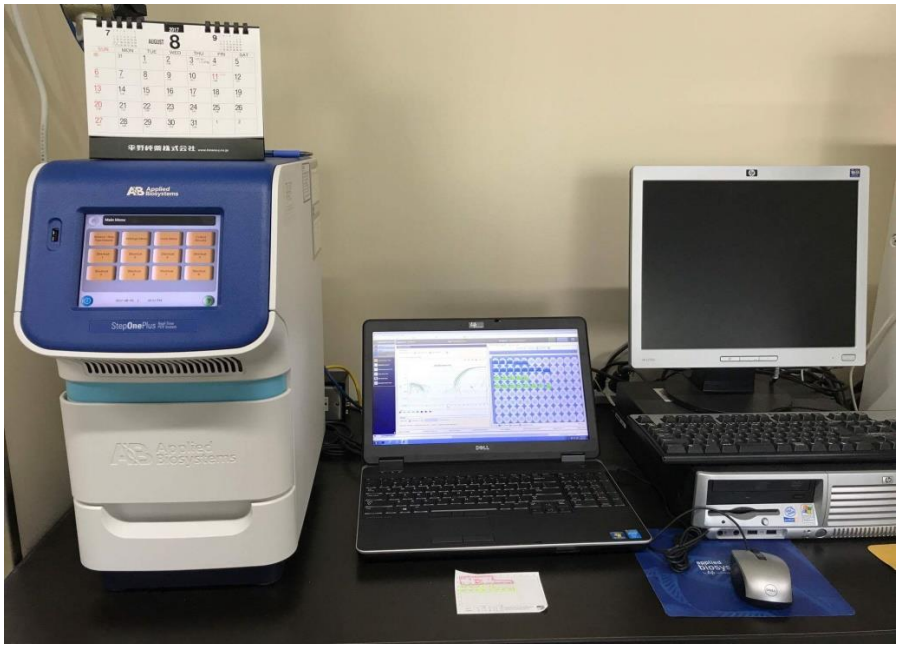

Figure 3.10 Reverse-transcription polymerase chain reaction (RT-PCR) devices. See appendix B for specifications of RT-PCR used.

Table 3.4 The primer sequences used for RT-PCR (National Center for Biotechnology Information 2017).

Target gene	Primer sequence
PPAR-γ	5' – TTCGCTGATGCACTGCCTAT - 3' (forward) 5' – GGCATTGTGAGACATCCCCA - 3' (reverse)
C/EBP-α	5' - CTAGGAGATTCCGGTGTGGC - 3' (forward) 5' – CCCGAGAGGAAGCAGGAATC - 3' (reverse)
CIDEA	5' – CGGGAATAGCCAGAGTCACC - 3' (forward) 5' - GTATCCACGCAGTTCCCACA - 3' (reverse)
FABP4	5' – GGATTTGGTCACCATCCGGT - 3' (forward) 5' - CCAGCTTGTCACCATCTCGT - 3' (reverse)
PGC-1α	5' - AGACAGGTGCCTTCAGTTCAC - 3' (forward) 5' - CTGTGGGTTTGGTGTGAGGA - 3' (reverse)
UCP-1	5' - CATGGGATCAAACCCCGCTA - 3' (forward) 5' - ACCCGAGTCGCAGAAAAGAA - 3' (reverse)
B-actin	5' - AGGCATTGTGATGGACTCCG - 3' (forward) 5' – AAACGCAGCTCAGTAACAGTC - 3' (reverse)
18s	5' - CGCGGTTCTATTTTGTTGGT - 3' (forward) 5' – AGTCGGCATCGTTTATGGTC - 3' (reverse)

3.12 Statistical Analysis

All experimental results were expressed as the means ± standard error (S.EM). Data were analyzed using a one-way analysis of variance (ANOVA) to define the significant values ($P < 0.05$) among the multiple groups using the Graph Pad Prism 6.0 software. ANOVA test is used for sample is more than three. Graph pad prism is the software that easy to use, best for graphing data, less technical, and lower price than other software. It is easier to use the software to import and export of data or graph, many automatic sets up, user-friendly interface and fast data output.

CHAPTER 4

RESULTS AND DISCUSSIONS

4.1 Overview

This chapter presents the results and discussions about the effects of DSW treatments on 3T3-L1 cells and SVF cells. Concentrations of minerals in DSW were analyzed to determine the types and amount of particular minerals in it. DSW samples were prepared for several concentrations and were treated to the particular cells in the dose dependent manner. 3T3-L1 cells present as a model of WAT, the adipocytes that could pose health hazard such as obesity in excess amount. SVF cells are model, which used to study the browning mechanisms of WAT. Cytotoxicity effects of DSW on both 3T3-L1 cells and SVF cells were evaluated, respectively. Metabolic activities such as quantification of intracellular lipid accumulation, and expressions of adipogenic genes with and without DSW treatments on cells were determined. Expressions of thermogenic genes in SVF cells treated with DSW and without DSW were reported.

4.2 Concentrations of Minerals in Deep Sea Water

Concentrations of minerals in DSW were analyzed using inductively coupled plasma mass spectrometry (ICP-MS) device at University Industry Research Laboratory (UIRL), Universiti Teknologi Malaysia, Johor as shown in Table 4.1. Hardness of DSW was measured as in Equation 3.1.

Table 4.1 Concentrations of minerals in deep sea water.

Type of Mineral	Original Deep Sea Water (mg/L)	Balanced Deep Sea Water (mg/L)
Mg	1141.9	1041.0
Ca	388.3	354.4
Bromide	48.8	NA
Chloride	4336.8	NA
Fluoride	0.6	NA
Potassium	314.5	NA
Na	573.7	NA
Nitrate	1.6	NA
Sulfate	2825.3	NA
Hardness	5652.6	5154.2

(NA – Not analyzed)

Original DSW is the original DSW that was supplied by Seawater Utilization Plant Research Center (SUPRC) of Korea Research and Ocean Ship Engineering (KRISO). Balanced DSW is the original DSW that was diluted with DMEM powder as to prepare it for experiment uses. Due to financial limitations the minerals in the original DSW were measured only for Mg and Ca. Accordingly, the balanced DSW was diluted with complete media to produce several concentrations of DSW which are 100, 500, 1000, and 1500 hardness for uses in experiment.

Study by Li *et al.* (2010) showed that, consumption of multivitamin and minerals could improve lipid profiles, and reduce body weight in the obese women. Meanwhile, intake combination of Ca, Mg, and Zn could reduce body weight, and improve lipid metabolism in high fat diet mice (Pérez-Gallardo *et al.* 2009). DSW contains lots of minerals including Mg, Ca, K, B, Cr, Cl, Se, Zn, and V (Hwang *et al.* 2009; Takahashi & Huang 2012; Katsuda *et al.* 2008). Each type of mineral has its own benefits to health. Thus, many minerals combination in DSW has cause efforts to identify underlying molecular mechanism by which components combat particular health problems are challenging. In this experiment, concentration of DSW was determined by hardness of water, which calculated the levels of Mg and Ca presence. Thus, Mg and Ca could be the major components that play roles in combating health problems together with others minerals. Previous studies emphasized that Mg and Ca presence in DSW are the major minerals that counteract the particular diseases include obesity, diabetes, and ulcer (Mohd Nani *et al.* 2016).

Mg is significant for many physiological processes in a body include in lipid metabolism, glucose metabolism, and enzyme functions (Michelle & Beerman 2007). Mg is able to reduce the risks of obesity, diabetes, and asthma (Hwang *et al.* 2009b; Watson *et al.* 2014). A study by Hwang *et al.* (2009a) reported, treatment with high level of Mg shows inhibitory effects in adipocytes differentiation, which means suppressed of fats synthesis. Molecular mechanisms of Mg in cells especially adipocytes remains unclear. Previous study shows that Mg and Ca enriched DSW upregulated expression of *PGC1-α* in 3T3-L1 adipocytes (Ha *et al.* 2016). *PGC-1α* is an important cofactor for transcriptional activity of major markers in adipocytes differentiation, which is *PPAR-γ* (Puigserver *et al.* 1998; Kleiner *et al.* 2012). Mg appears to play a pivotal role in regulating the PPAR-mediated signaling pathways as a key cofactor in the protein phosphorylation (Fujii 2005).

Mg intake is important to prevent obesity related pathology. Mg deficiency in mice has cause significant increase of triglycerides, and free cholesterol in plasma; and increase of triglycerides, α-glycerophosphate and lactate levels, meanwhile decrease of hepatic glycogen content in liver (Rayssiguier *et al.* 1981). Inflammatory, oxidative stress, and insulin resistance are increased in obesity state

(Rayssiguier *et al.* 2010). Oxidative stress causes increase of reactive oxygen species (ROS). Mg acts as antioxidant compound that could suppress catecholamines release that responsible in ROS production. Mg treatment could suppress the production of acute phase proteins such as C-reactive protein, which is an inflammatory cause (Zheltova *et al.* 2016).

Adiposity is related to interruption in insulin signaling pathway. Insulin signal is responding to levels changes of Mg, both in intracellular and extracellular, respectively (Ishizuka *et al.* 1994). Recent data reveals that Mg supplementations could improve insulin resistance and glucose control, that correlated to obesity (Simental-Mendía *et al.* 2016). Mg deficiency in high fat diet mice has caused decreased of proteins involved in insulin signaling pathway (IR-β, IRS-1 and Akt), which increase insulin resistance (Sales *et al.* 2014). A study by (Venu *et al.* 2008) showed Mg deficient diet has increased expression of FAS and fatty acid transporter protein 1 in the adipose tissue that cause increased in adiposity. This study has shown that Mg-DSW content suppressed fats formation and decreased adipogenic markers in WAT.

Adequate intake of Ca can help to reduce risks of cardiovascular disease, obesity, and some form of cancers (Hwang *et al.* 2009b; Michelle & Beerman 2007; Watson *et al.* 2014). Intracellular Ca is important to regulate adipocyte lipid metabolism and triglyceride storage as its increased stimulated lipogenic gene expression and lipogenesis, and suppressed lipolysis. Moreover, calcitrophic hormones act on adipocytes to increase Ca influx. Increased of calcitriol level after low calcium diets has stimulates Ca influx in in primary cultures of human adipocytes and thereby promotes adiposity (Zemel *et al.* 2000). In contrast, high Ca diet reduces adipose mass, reduces body weight, increases lipolysis, and suppresses fatty acid synthase in high fat diet mice (Zemel *et al.* 2000).

Increasing extracellular Ca concentration by means of high Ca supplementation could decreases the adipogenic genes. A study by Vergara *et al.* (2016) reported that, decreased extracellular Ca has increased adipocyte

differentiation through suppression of calreticulin, a known inhibitor of PPAR-γ. Reduced lipid accumulations and adipogenic markers in response to DSW treatment in this experiment could be linked with suppressed adipocyte intracellular Ca or increased adipocyte extracellular Ca; that can attenuate obesity risk through energy metabolism modulation.

Diet-induced obesity mice has reduction in body and fat mass in response to high Ca intake, which could mediated through induction of apoptosis and activation of Ca^{2+-} dependent apoptotic proteases, calpain and caspase-12 (Sergeev & Song 2014). In a study, high dietary Ca mice reduced the risk of obesity through potential mechanisms include reduced adipose intracellular ROS production, suppressed adipocyte intracellular Ca, and inhibited adipose tissue nicotinamide adenine dinucleotide phosphate oxidase (*NADPH*) expression; and increased *UCP-2* and *UCP-3* expression both in visceral and subcutaneous adipose tissue, respectively (Sun & Zemel 2006). ROS production is increased in response to obesity. Meanwhile, increased expressions of UCP2 and UCP-3 have caused inhibition of ROS production. High Ca intake could suppressed 11*β*-hydroxysteroid dehydrogenase (11*β*-HSD) expression in visceral adipose tissue (Sun & Zemel 2006). 11*β*-HSD is a key enzyme responsible for converting glucocorticoid into its active form that can alleviate adipogenesis. DSW used in this study containing Ca as one of the major mineral. The possible mechanisms of Ca to counteract obesity that described above could explain its roles in decreasing lipid accumulation and adipogenic genes in WAT in this study.

DSW contains many minerals include Mg, Ca, K, B, Cr, Cl, Se, Zn, and V which has potential to combat obesity (Hwang *et al.* 2009; Takahashi & Huang 2012; Katsuda *et al.* 2008). For instances, Se that acts on PPAR-γ is suggested as potential compound to be developed as anti-depressant and anti-obesity agent (Donma & Donma 2016). Chromic chloride is the major materials used in synthesis of Cr Picolinate, a supplement that claimed to aid weight loss (Onakpoya *et al.* 2013). V has potential in reducing lipid and has shown effectiveness in inhibiting formation of fats cells (Seale *et al.* 2006). Though, molecular mechanism of minerals such as Mg, and Ca in suppressing obesity remain limited.

4.3 Cytotoxicity Effects of Deep Sea Water on 3T3-L1 Cells

Cell viability assay is a prerequisite step for each experiment or analysis that using cells is conducted. It purposes to determine the suitable or safe concentration of compound, which do not cause potential toxic effects to the particular cells. The cell cytotoxicity assay was conducted to determine the effects of DSW in the 3T3-L1 preadipocytes viability. 3T3-L1 preadipocytes were treated with DSW in dose dependent manner at concentrations of 100, 500, 1000, 1500, 2000, 3000, 4000, and 5000 hardness. The percentage of cell viability for DSW-treated cells and untreated cells (control) were determined. The absorbance of control group and treatment group were subtracted with absorbance of blank, respectively. The percentages of cell viability were calculated by using Equation 3.4. Data are expressed as means of three replicates and are shown in Figure 4.1.

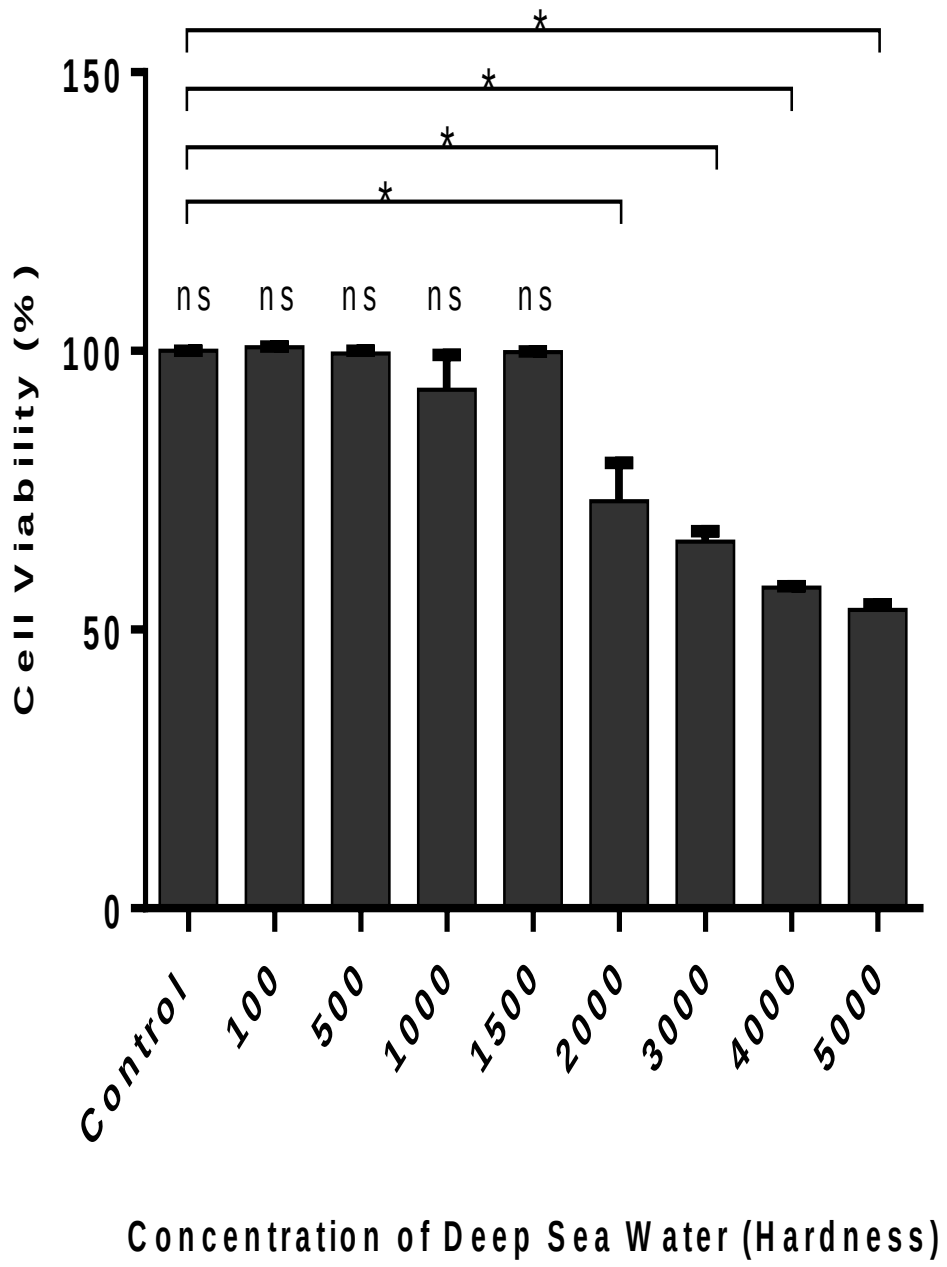

Figure 4.1 Effects of deep sea water on cell viability using 3T3-L1 preadipocytes, means ± S.E.M (n = 3). Where * $P < 0.05$, was considered a statistically significant difference from the differentiated control (ns – not significant).

DSW at concentrations of 100, 500, 1000, and 1500 hardness did not significantly reduced the 3T3-L1 preadipocytes viability which indicated that these concentration are suitable for uses in experiment. Thus, these concentrations of DSW were used in the experiment to test its effects in adipogenesis and genes expression. DSW at concentrations of 2000, 3000, 4000, and 5000 hardness has significantly reduced 3T3-L1 preadipocytes viability, are potential to lead the cells death. Inhibitory concentration 50 (IC_{50}) is a measure to indicate how much of a particular compound or substance is needed to inhibit half of a given biological response. IC_{50} value for DSW using 3T3-L1 preadipocytes is at concentration of more than 5000 hardness. Lethal Dose 50 (LD_{50}) is a standard measure to determine the concentration of a given compound or chemical that needed in killing half of the tested animals. LD_{50} value for DSW using 3T3-L1 preadipocytes is estimated based on ICCVAM (2006), which is concentration of more than 2511.9 mg/kg.

4.4 Effects of DSW on Intracellular Lipid Accumulation in 3T3-L1 Adipocytes

Differentiated preadipocytes could easily detected through observation of lipid accumulation. To determine the effects of DSW in adipocytes differentiation, 3T3-L1 preadipocytes were treated with DSW at concentrations of 100, 500, 100, and 1500 hardness for 8 days. After fixation with 10% formalin, lipid droplets were stained with Oil Red O and imaged. The captured images are shown in Figure 4.2.

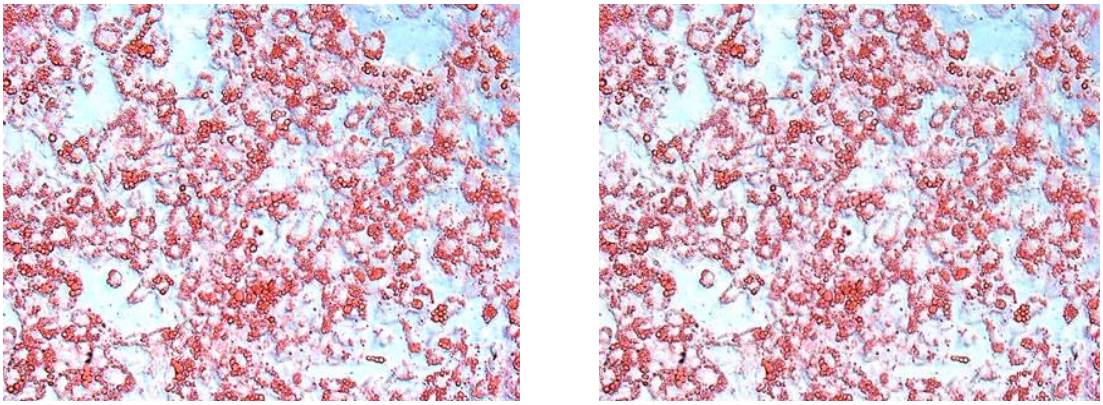

(a) (b)

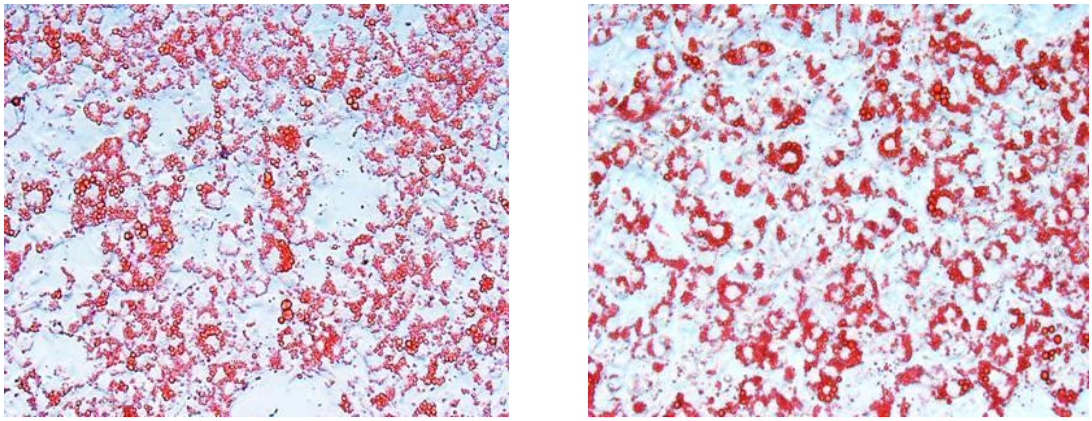

(c) (d)

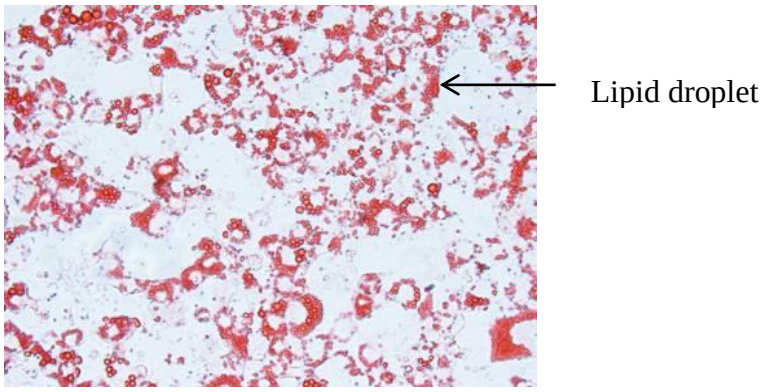

(e)

Figure 4.2 Intracellular lipid accumulation in 3T3-L1 adipocytes treated with deep sea water (a) Control, (b) 100 hardness, (c) 500 hardness, (d) 1000 hardness, and (e) 1500 hardness. Images were photographed using an Olympus inverted microscope by 10 x magnifications.

Mature 3T3-L1 adipocytes that untreated with DSW were served as the control group is contained many lipid droplets. As shown in Figure 4.2, lots of red lipid droplets in mature 3T3-L1 adipocytes of control group indicated that differentiation of preadipocytes into mature adipocytes was successful. Whereas, DSW at concentration of 100, 500, 1000, and 1500 hardness in dose dependent manner has reduced the lipid accumulation in mature 3T3-L1 adipocytes, indicated by reduced red lipid droplets. Reduced red lipid accumulation in DSW-treated group cells represented the inhibition of adipocytes differentiation.

4.5 Quantification of Intracellular Lipid Content in 3T3-L1 Adipocytes

Observable lipid accumulation in differentiated 3T3-L1 adipocytes can be analyzed for percentage of lipid accumulations. Briefly, 3T3-L1 adipocytes were differentiated in the specified medium for adipogenesis, as described in chapter of methodology part. 3T3-L1 adipocytes were harvested after it reached confluence approximately after 8 days. After fixation with 10% of formalin, 3T3-L1 adipocytes were stained with Oil Red O. Then, stained cells were dissolved with isopropanol which then producing red colour solution. The red colour solutions were measured at absorbance 490 nm. Figure 4.3 show the percentage of lipid accumulation in 3T3-L1 adipocytes after treated with various concentration of DSW and control group, respectively.

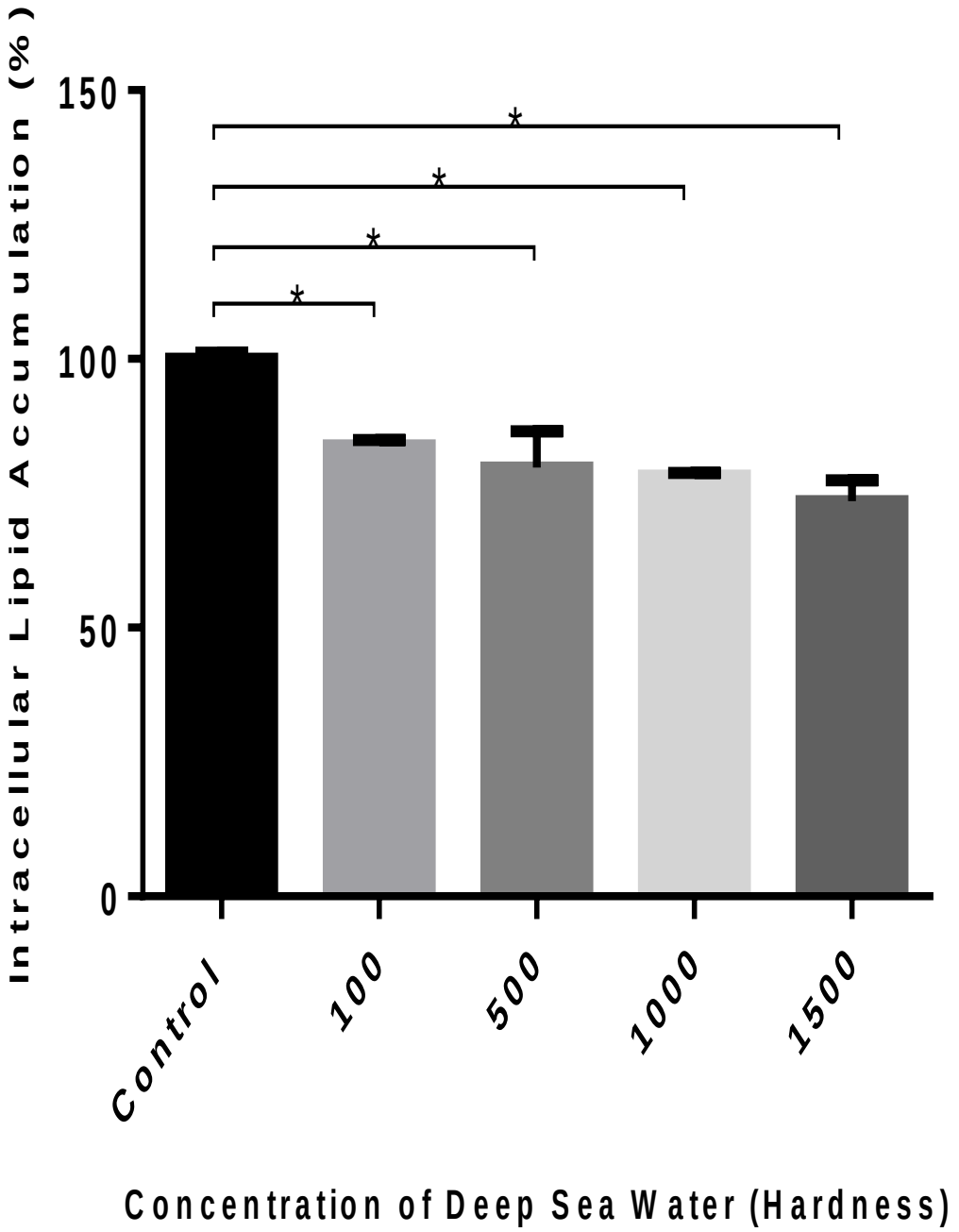

Figure 4.3 Percentage of intracellular lipid accumulation in 3T3-L1 adipocytes treated with deep sea water, means ± S.E.M (n = 3). Where * $P < 0.05$ was considered a statistically significant difference from the differentiated control.

DSW treatments in dose dependent manner of 100, 500, 1000, and 1500 hardness significantly reduced percentage of lipid accumulation in 3T3-L1 adipocytes as shown in Figure 4.3. The control group, which untreated with DSW, shows higher percentage of lipid accumulation than the DSW-treated group. Reduced percentage of lipid accumulation by DSW-treated groups indicated that the differentiations of 3T3-L1 preadipocytes into mature adipocytes were inhibited. Suppressed lipid accumulation in 3T3-L1 adipocytes could be linked with presence of minerals such as Mg and Ca in DSW. A study by Hwang *et al.* (2009) indicated that Mg and Ca could suppress adipocytes differentiation, and lipid accumulation.

4.6 Effects of DSW on mRNA Expression of Adipogenic Genes in 3T3-L1 Adipocytes

Understanding molecular mechanisms such as types of gene expression involved in a biology system could provide comprehensive insight regarding it. In adipogenesis, adipogenic genes such as *PPAR-γ, C/EBP-α*, and *FABP4* are useful to provide scientific indicators of this event. These genes are the common adipogenic markers that were evaluated in determining successful adipocytes differentiation. In this study, 3T3-L1 preadipocytes were differentiated with presence or absence of various concentrations of DSW, which are 100, 500, 1000, and 1500 hardness, respectively. During day 8, mature adipocytes were harvested and its mRNA was isolated. After reverse transcription, cells were analyzed for genes expression using the RT-PCR device. Data shown in Figure 4.4 are expressed as the means of three replicates.

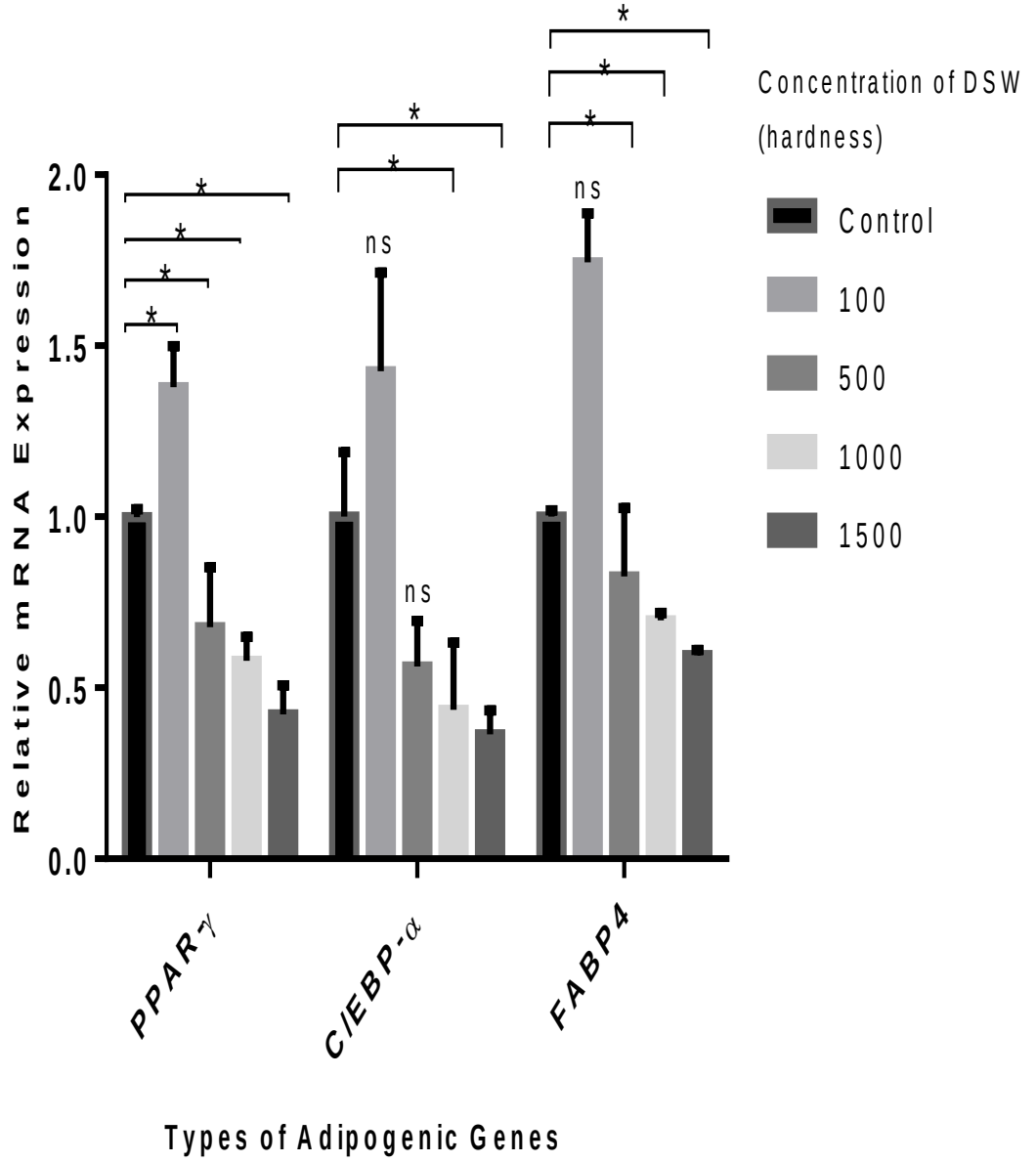

Figure 4.4 Effects of deep sea water on mRNA expression of adipogenic genes in 3T3-L1 adipocytes, means ± S.E.M (n = 3). Results were expressed relative to control group after normalization to β-actin. Where * $P < 0.05$ was considered a statistically significant.

DSW at concentrations of 500, 1000, and 1500 hardness reduced the adipogenic genes markers which are *PPAR-γ, C/EBP-α*, and *FABP4* in 3T3-L1 adipocytes. In contrast, DSW at a concentration of 100 hardness increased the expression levels of *PPAR-γ, C/EBP-α,* and *FABP4* in 3T3-L1 adipocytes. Though, 3T3-L1 adipocytes those treated with DSW of 100, 500, 1000, and 1500 hardness show the reduction of lipid in captured images of lipid droplets (Figure 4.2) and percentage of lipid accumulation (Figure 4.3), respectively. DSW 100 hardness that has increased adipogenic markers (*PPAR-γ, C/EBP-α,* and *FABP4*), but decreased lipid accumulation in the 3T3-L1 cell may indicated the 3T3-L1 cells potential to underwent browning. Decreased lipid in photographed images and decreased percentage of lipid accumulation, which are contrast results with increased adipogenic markers after treated with DSW of 100 hardness could be associated with detached lipid droplets during experiment. Lots of lipid accumulation in it could be detached because the mature 3T3-L1 adipocytes are loose connective tissue that easily to detach (Zhang *et al.* 2012).

Differentiated adipocytes are characterized by lots of lipid accumulation and with the presence of adipogenic markers include *PPAR-γ, C/EBP-α,* adiponectin, and *FABP4*. In this experiment, 3T3-L1 preadipocytes were induced with adipogenic cocktails and untreated with DSW (control group) has showed lots of lipid accumulation and expressed mRNA of *PPAR-γ, C/EBP-α,* and *FABP4*, indicated successful adipocytes differentiation. Thus, DSW-untreated 3T3-L1 cells were used as the control group to determine the effects of DSW in adipogenesis. DSW of 500, 1000, and 1500 hardness reduced lipid accumulation and downregulated expression of *PPAR-γ, C/EBP-α,* and *FABP4* postulated the inhibition of adipocytes differentiation. Thus, it was summarized that DSW able to suppress formation of fats or adipogenesis in WAT by reducing lipid accumulation and suppressing the adipogenic genes. Metabolic mechanims of Mg in cells especially adipocytes remains unclear. Previous study shows that Mg and Ca enriched DSW upregulated expression of *PGC1-α* in 3T3-L1 adipocytes (Ha *et al.* 2016). *PGC-1α* is an important cofactor for transcriptional activity of major markers in adipocytes differentiation, which is *PPAR-γ* (Puigserver *et al.* 1998; Kleiner *et al.* 2012).

In this experiment, DSW has proven to suppress adipogenesis in WAT through *in vitro* model using 3T3-L1 preadipocytes. Beige adipocytes are inducible WAT that induced to browning under specified stimuli such as cold, β3-adrenergic agonists, or PPAR-γ agonist. As DSW reduced lipid in WAT, it is interesting to know either DSW promotes browning of WAT. Beige adipocytes could perform thermogenesis likes BAT as it contains UCP-1, which enable it to convert energy into heat (Wang & Seale 2016; Rodríguez *et al.* 2016; Harms & Seale 2013; Lidell *et al.* 2014). Thus, it is worthy to determine the potential of DSW in inducing browning of WAT, as thermogenic adipocytes.

Furthermore, classical BAT is reduced in adult, making effort to identify the potential stimuli for beiges adipocytes differentiations are necessary to adapt decreasing of thermogenic adipocytes. Previous studies revealed that DSW promotes mitochondrial and functions (Ha *et al.* 2015; Ha *et al.* 2016). UCP-1 is located in mitochondrial, uncouples respiration of ATP to produce heat. Beiges adipocytes that contain UCP-1, has potential to counteract obesity. Thus, this study determined the effects of DSW in inducing browning of SVF cells that isolated from mice.

4.7 Cytotoxicity Effect of DSW on Stromal Vascular Fractions Cells

The cell cytotoxicity assay was conducted to determine the effects of DSW on cell viability using SVF cells. SVF cells were treated with DSW in dose dependent manner for the concentrations of 100, 500, 1000, 1500, 2000, 3000, 4000, and 5000 hardness, respectively. As comparison, DSW-treated cells were compared with DSW-untreated cells. The absorbance of control group and treatment groups were subtracted with absorbance of blank, respectively. The percentages of cell viability were calculated by using Equation 3.4. Data are expressed as means of three replicates and shown in Figure 4.5.

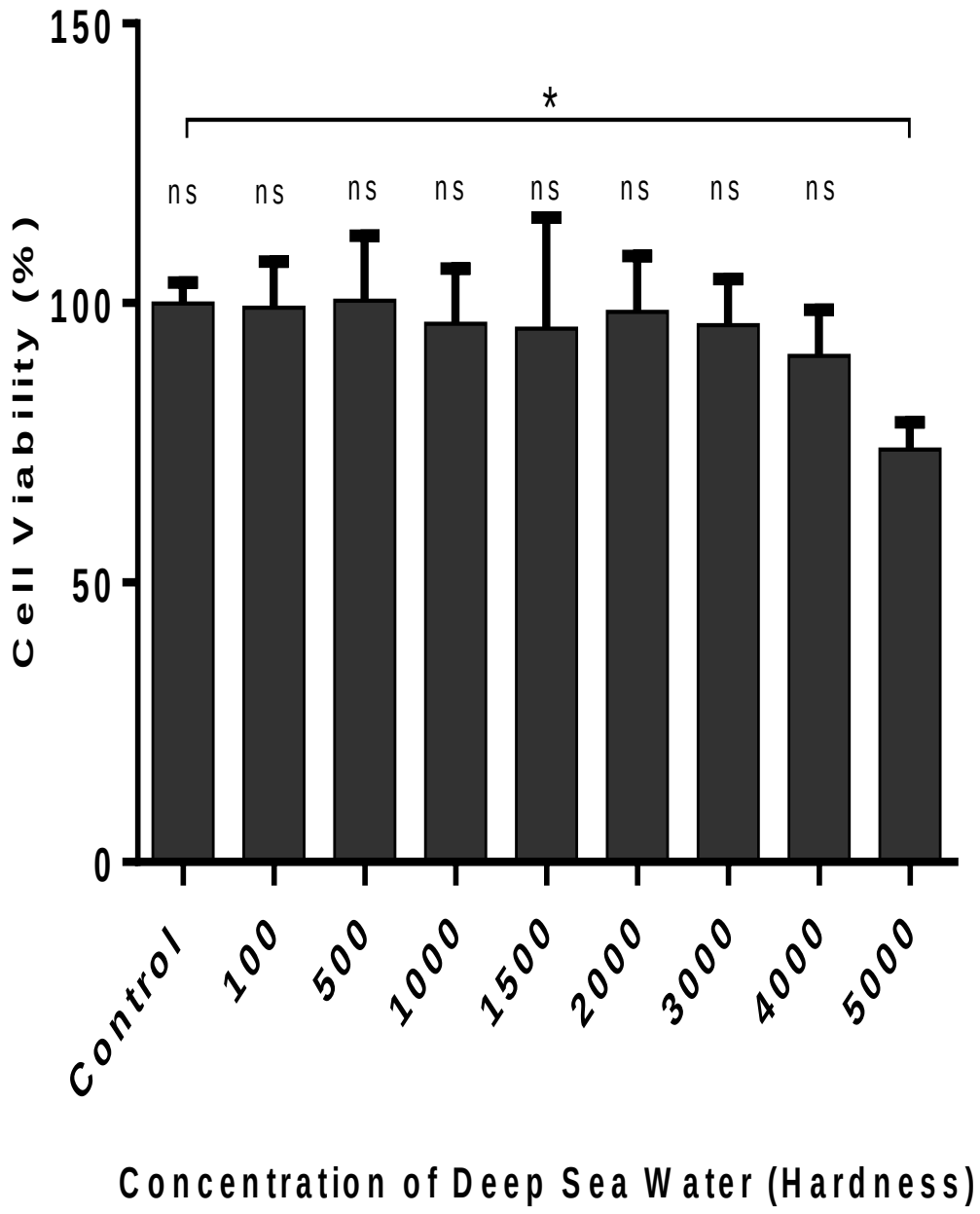

Figure 4.5 Effects of deep sea water on cell viability using stromal vascular fractions cells, means ± S.E.M (n = 3). Where * $P < 0.05$, was considered a statistically significant difference from the differentiated control (ns - not significant).

DSW at concentrations of 100, 500, 1000, 1500, 2000, 3000, and 4000 hardness did not significantly reduced cell viability of SVF cells, which indicated its suitability for use in experiment. DSW hardness of 5000 significantly reduced cells viability of SVF cells. DSW at concentrations of 100, 500, 1000, and 1500 hardness were used in experiment to determine the effects of DSW in adipogenesis and genes expression.

IC_{50} value for DSW using SVF cells was calculated, which at concentration of more than 4500 hardness. LD_{50} value for DSW using SVF cells was estimated based on ICCVAM (2006), which is at concentration of more than 2415.4 kg/mg.

4.8 Effects of DSW on Intracellular Lipid Accumulation in Beige Adipocytes

Lots of lipid accumulation in beige adipocytes marked the successful differentiation of beige adipocytes. To determine the effects of DSW in browning of WAT, SVF cells were induced into beige adipocytes in the absence or presence of DSW at various concentrations, which are 100, 500, 100, and 1500 hardness for 6 days, respectively. After fixation with 10% of formalin, lipid droplets were stained with Oil Red O. Staining with Oil Red O has caused lipid appeared in red colour and then were imaged. The pictures of red lipid accumulation in the differentiated beige adipocytes are shown as in Figure 4.6.

.

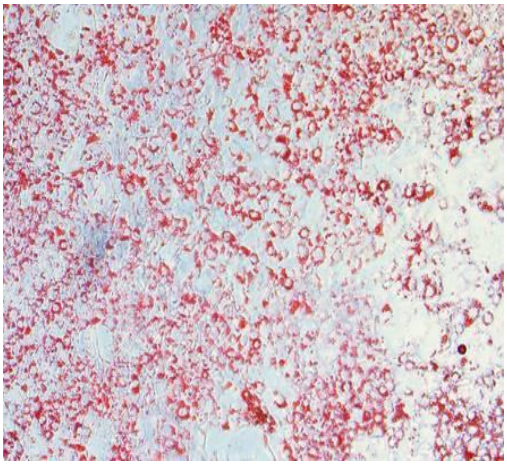

(a)

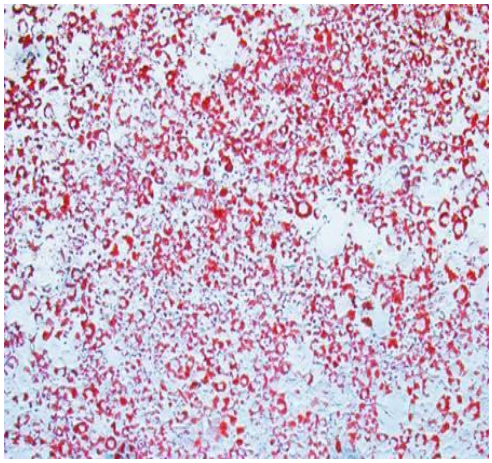

(b)

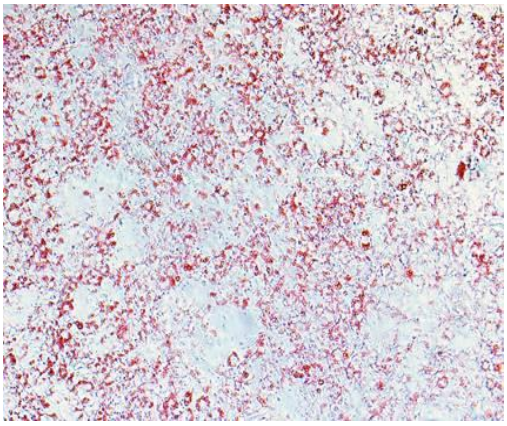

(c)

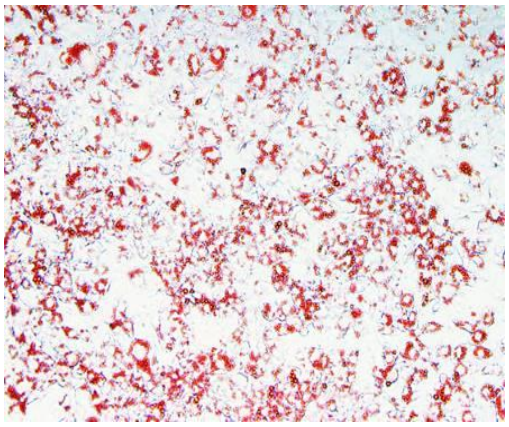

(d)

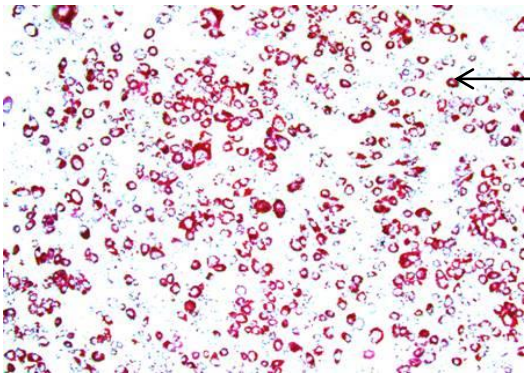

(e)

Figure 4.6 Intracellular lipid accumulation in beige adipocytes treated with deep sea water (a) Control, (b) 100 hardness, (c) 500 hardness, (d) 1000 hardness, and (e) 1500 hardness. Images were photographed using an Olympus inverted microscope (10 x magnifications).

As shown in Figure 4.6, DSW of 100 hardness significantly promoted lipid accumulation in differentiated beige adipocytes. DSW of 500, 1000, and 1500 hardness suppressed lipid accumulation in differentiated SVF cells.

4.9 Quantification of Intracellular Lipid Content in Beige Adipocytes

Primary SVF preadipocytes were treated with DSW at several concentrations of 100, 500, 1000, and 1500 hardness. Differentiated beige adipocytes were then were fixed with 10 % of formalin before were stained with Oil Red Oil. Stained differentiated beige adipocytes were dissolved with isopropanol that produced red colour solution. The absorbance of red colour solutions was measured at 450 nm using the microplate reader. Data shown in Figure 4.7 are expressed as means of three replicates.

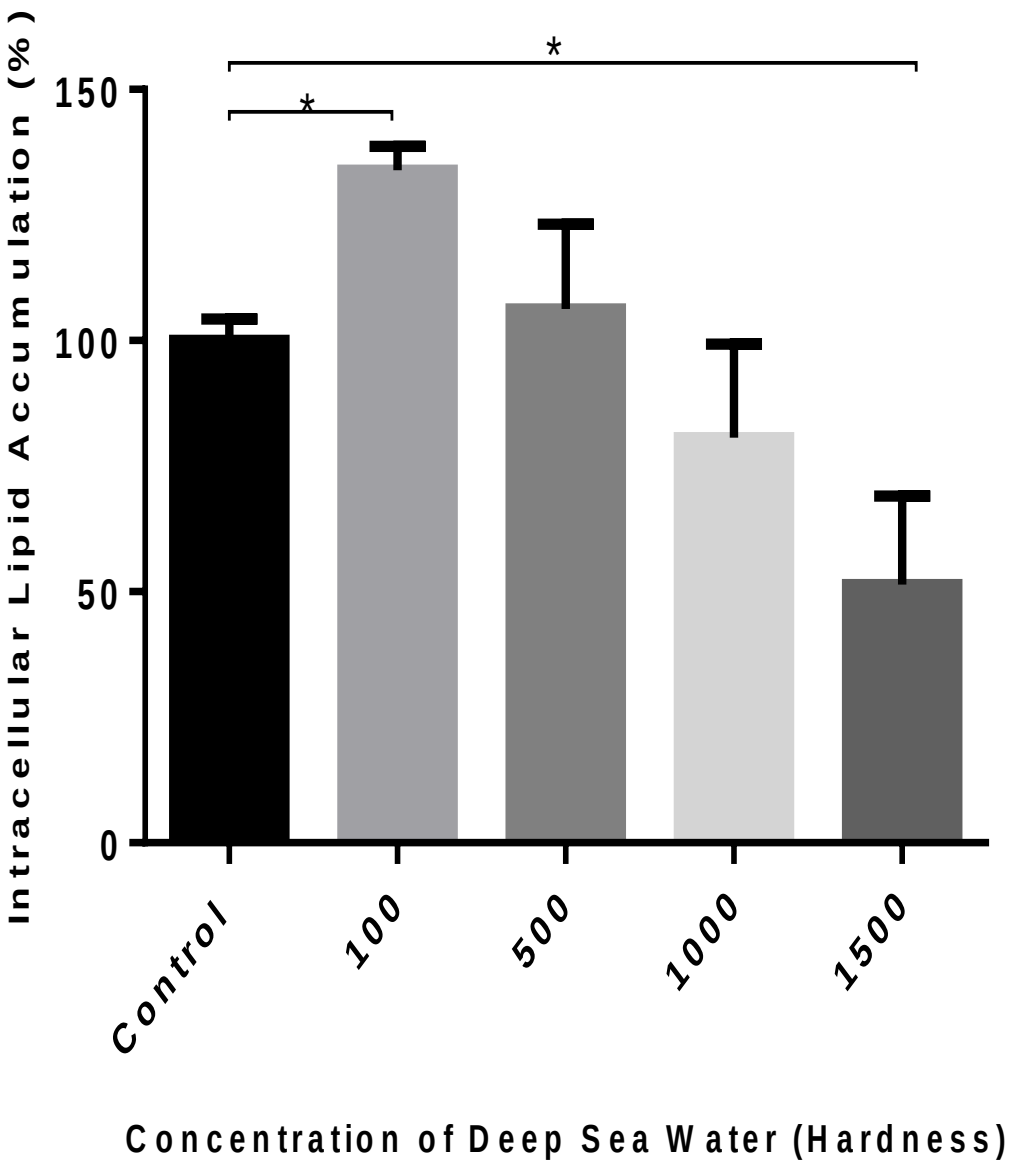

Figure 4.7 Effects of deep sea water on intracellular lipid accumulation in differentiated beige adipocyte, means ± S.E.M (n = 3). Where * $P < 0.05$ was considered a statistically significant difference from the differentiated control.

4.10 Effects of DSW on mRNA Expression of Adipogenic Genes in Differentiated Beige Adipocytes

The adipogenic markers in differentiated beige adipocytes are similar with others differentiated adipocytes which are *PPAR-γ, CEBP-α* and *FABP4*. Primary preadipocytes of SVF cells were treated with various DSW concentrations (100, 500, 1000, 1500 hardness) for 6 days. At day 6, differentiated beige adipocytes were harvested for mRNA measurement. *PPAR-γ*, *C/EBP-α*, and *FABP4* expressions were evaluated by quantitative real-time RT-PCR. Data in Figure 4.8 are expressed as means of three replicates. Results were expressed relative to untreated cells (control) after normalization to 18s.

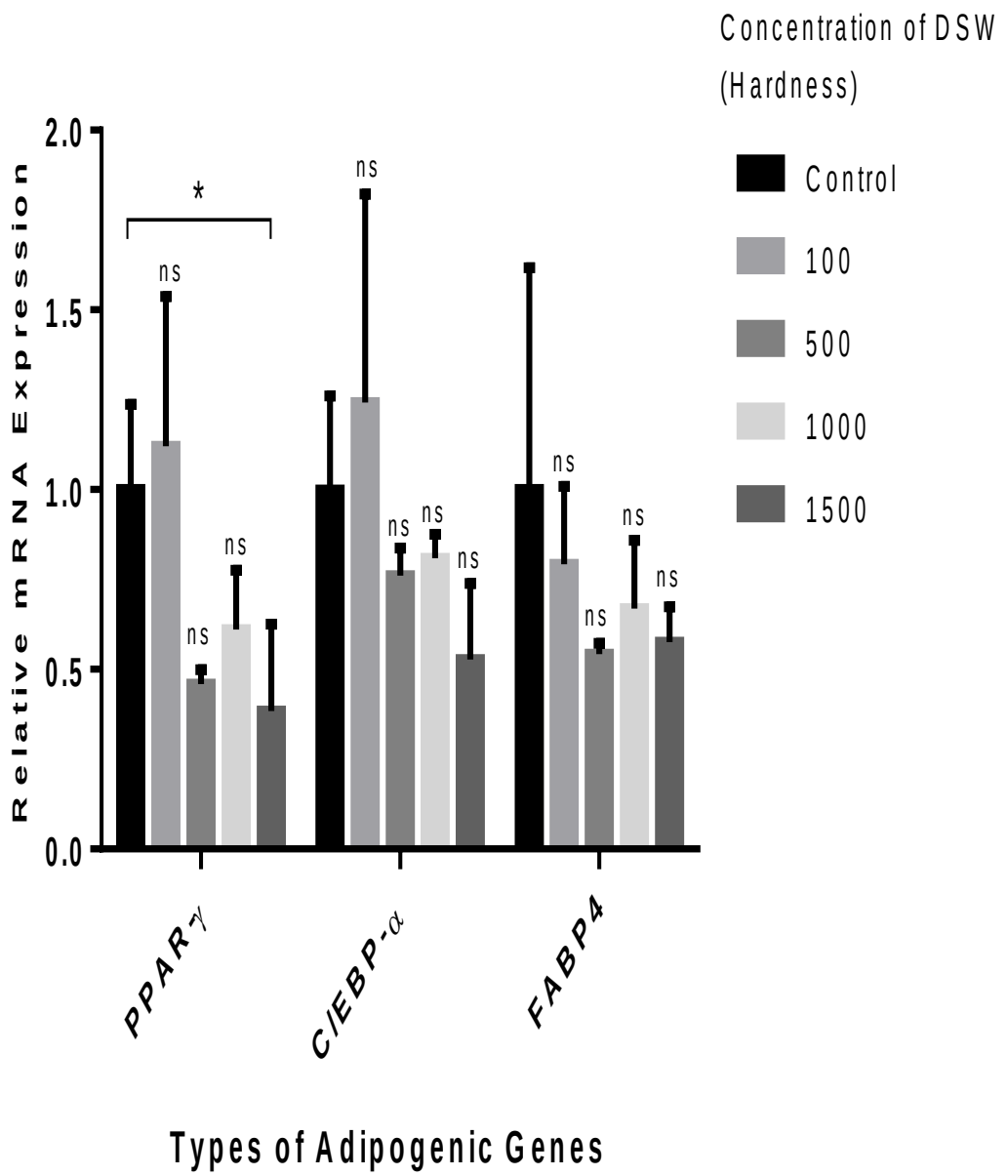

Figure 4.8 Effects of deep sea water on mRNA expression of adipogenic geness in differentiated beige adipocytes, means ± S.EM (n = 3). Results were expressed relative to control group after normalization to 18s. Where * $P < 0.05$ was considered a statistically significant difference from the differentiated control (ns – not significant).

DSW of 100 hardness increased the mRNA expression levels of *PPAR-γ*, and *C/EBP-α* in differentiated beige adipocytes. Though, the others concentrations of DSW did not increased mRNA expression levels of *PPAR-γ*, *C/EBP-α*, and *FABP4* in differentiated beige adipocytes after compared to the control group. Increased of *PPAR-γ*, and *C/EBP-α* expression level after treatment with DSW hardness of 100 in differentiated beige adipocytes could indicated tendency of WAT to undergo browning. As shown in Figure 4.6 and Figure 4.7, DSW hardness of 100 significantly promoted lipid accumulation and significantly increased the percentage of lipid accumulation in beiges adipocytes. PPAR-γ is a master regulator for adipocyte differentiation, to promote adipogenesis (Akerblad *et al.* 2002). *PPAR-γ* is also an important transcription factor that coordinates with *EBF2* during course of beige adipocytes differentiation. *EBF2* is identified in the precursor cells, and regulated through differentiation of beige adipose tissues to promote the recruitment of beige adipose tissue in WAT (Wang & Seale 2016).

4.11 Effects of DSW on mRNA Expression of Thermogenic Genes in Differentiated Beige Adipocytes

The key thermogenic genes of beige adipose tissue are similar with the classical thermogenic adipocytes, BAT, in which including *UCP1*, *PGC-1α*, and *CIDEA* (Wang & Seale 2016). These genes were expressed in differentiated beige adipocytes (Wang & Seale 2016; Harms & Seale 2013). Thus, this study tests the effects of DSW during the course of beige adipocytes differentiation for 6 days. After 6 days, differentiated beige adipocytes were harvested for mRNA measurement. The mRNA expressions of *UCP-1*, *PGC-1α,* and *CIDEA* were evaluated by quantitative RT-PCR. Results were expressed relative to untreated cells (control) after normalization to 18s.

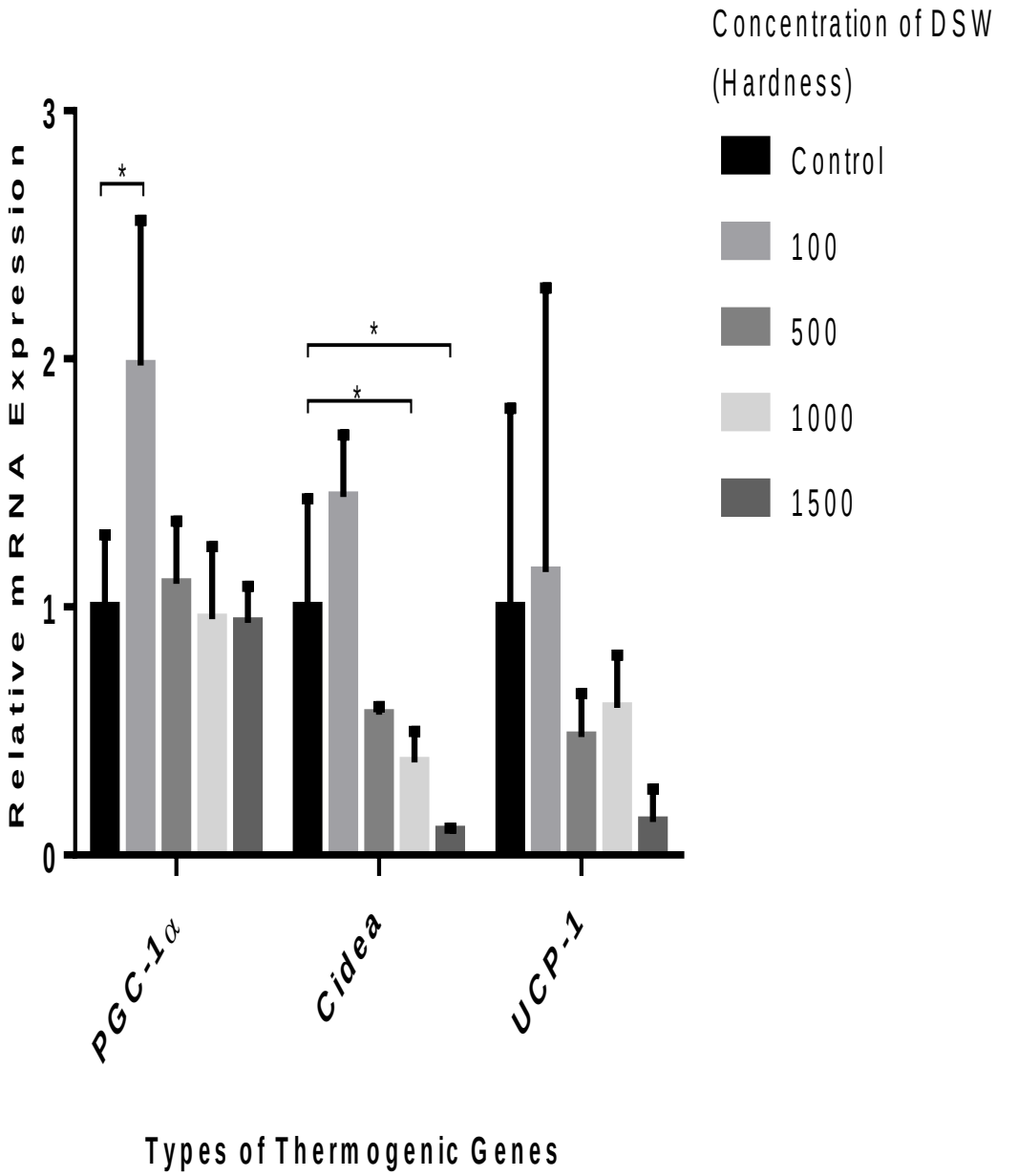

Figure 4.4.9 Effects of deep sea water on mRNA expression of thermogenic genes in differentiated beige adipocytes, mean ± S.EM (n = 3). Results were expressed relative to control group after normalization to 18s. Where * $P < 0.05$ was considered a statistically significant difference from the differentiated control.

In differentiated beige cells, DSW at a concentration of 100 hardness has increased mRNA expression of the thermogenic genes, which are *PGC-1α, CIDEA*, and *UCP-1* as shown in Figure 4.9. In concert with the findings in the browning of SVF cells into beige cells, the concentrations of DSW at 500, 1000, and 1500 hardness (Figure 4.8) did not increased mRNA expression of the thermogenic genes in the differentiated beige adipocytes.

Beige adipose tissue formed in WAT under specified stimuli or condition such as cold, β3-adrenergic agonists, or PPAR-γ agonist (Wang & Seale 2016; Rodríguez *et al.* 2016; Harms & Seale 2013; Lidell *et al.* 2014). Thiazolidinedione (TZDs) is a PPAR-γ agonist that are particularly potent activators of mitochondrial biogenesis and thermogenic genes including *UCP1* (Seale 2015). Rosiglitazone is a commonly used type of thiazolidinedione, is a crucial compound that induce thermogenic gene expression in the fat cells through stabilization of PRDM16 (Lin & Scott 2012). Accumulating evidences suggested that PRDM16 is a crucial key component to drive differentiation of beige adipose tissues in WAT (Harms & Seale 2013; Wang & Seale 2016). Transgenic expression of PRDM16 in WAT significantly induce the development of brown-like adipocytes, whereas it reduction cause decreased in the expression of thermogenic genes, indicated impaired beige adipose tissues development (Seale *et al.* 2011; Lin & Scott 2012). Mechanistic studies indicate that PRDM16 binds and enhances the transcriptional function of PPAR-γ, PPAR-α, ZFP516, thyroid receptor, PGC-1α, and C/EBP proteins (Kajimura *et al.* 2009; Iida *et al.* 2015; Seale *et al.* 2008; Hondares *et al.* 2011). In this experiment, rositaligtazone was used as PPAR-γ agonist to induce browning of WAT. TZDs also activate SIRT1, an NAD-dependent deacetylase that deacetylates two residues in PPAR-γ which efficiently bind to PRDM16 (Qiang *et al.* 2012). Increase of SIRT1 activity in adipose tissue promotes WAT browning and combat obesity (Seale 2015).

Untreated SVF cells that was induced with the specified medium for beige adipocytes differentiation was served as the control group. It has expressed the thermogenic genes which are *PGC-1α, CIDEA*, and *UCP-1* that indicated the successful beige adipocytes differentiation in this experiment (Wang & Seale 2016).

CIDEA and *UCP-1* are the important thermogenic markers of beige adipocytes as these genes constantly expressed and significantly increased in 'browning' induced-WAT. Expression levels of *CIDEA*, and *UCP-1* provide the rigid evidence to differentiate between WAT and beige adipocytes (Garcia *et al.* 2016).

PGC-1α is recognized as a master regulator for mitochondrial biogenesis and oxidative metabolism in many cell types (Harms & Seale 2013). *PGC-1α* is important in mitochondria biogenesis (Ha *et al.* 2014a) to contribute in activation of thermogenic genes (Hondares *et al.* 2011). In this experiment, the functions of *PGC-1α* to activate the thermogenic genes such as *UCP-1* and *CIDEA* were proven, when both of these genes were expressed in differentiated beige adipocytes. *PGC-1α* induces the expression of *UCP-1* by stimulate *Irisin* hormone that led to browning of WAT in culture and *in vivo* studies (Boström *et al.* 2012). *PGC-1α* is also important cofactor for transcriptional activity of *PPAR-γ* which induces the expression of *UCP-1* and other thermogenic component (Puigserver *et al.* 1998; Kleiner *et al.* 2012). Interferon regulatory factor-4 (*IRF4*) is an important transcription factor partner of *PGC-1α* and a critical activator of thermogenic genes. Increased expression of *IRF4* increases the *UCP-1* expression. *IRF4* deletion in BAT and beige adipose tissue suppresses energy dissipation and increase susceptibility to obesity and insulin resistance. *IRF4* presence during browning process is important as *PGC-1α* is not able to activate thermogenic during its absence (Kong *et al.* 2014). Previous study showed that Mg and Ca enriched DSW upregulated expression of *PGC1-a*, *NRF1*, and *TFAM* genes in 3T3-L1 adipocytes (Ha *et al.* 2016). In this experiment, *PGC-1α* was significantly upregulated with DSW at concentration of 100 hardness after compared to control group (Figure 4.9).

UCP-1 is a thermogenic marker that expressed in differentiated beige adipocytes. It functions to uncouple respiration from energy production. One important means of *UCP-1* expression is though regulation of *EBF2*. A study by Stine *et al.* (2016), showed the expression of *EBF2* induced the expression of *UCP-1*, while mice *EBF2*-knockdown did not induced *UCP-1*. *EBF2*-deficient WAT inhibits browning process, shows that, in addition of it as a marker of beige adipose tissue, it is crucial in beige adipose tissue development (Stine *et al.* 2016). Previous

studies show that DSW promotes mitochondrial biogenesis and genes expression that are related to mitochondria functions in the 3T3-L1 preadipocytes, liver, skeletal muscle and epididymal fat (Ha *et al.* 2016; Ha *et al.* 2015; Ha *et al.* 2014a). In the present study, *UCP-1* that expressed in mitochondria was upregulated with treatment of DSW at a concentration of 100 hardness. Increased of *UCP-1* might combat obesity, whereas lack of *UCP-1* may cause disruption of metabolic system (Nedergaard *et al.* 2001; Fedorenko *et al.* 2013; Ricquier 2011; Kozak & Anunciado-Koza 2008). *UCP-1*, when activated, catalyses the leak of protons across the mitochondrial membrane, which uncouples oxidative respiration from ATP synthesis. Resulting energy derived from substrate oxidation is then dissipated as heat (Fedorenko *et al.* 2013; Ricquier 2011). In this experiment, DSW of 100 hardness promoted the expression of UCP-1 although not in the significant level.

CIDEA is consistently expressed in thermogenic adipocytes and recognized as markers in thermogenic adipocytes including beige adipocytes (Garcia *et al.* 2016). It functions to modulates uncoupling action of UCP1 (Garcia *et al.* 2016). In this experiment, DSW of 100 hardness promoted the expression of *CIDEA* although not in the significant level.

Concentrations of DSW used in this study were determined by hardness of water that calculated Mg and Ca as main minerals. A study by (Ha *et al.* 2016) shows that DSW promotes mitochondrial biogenesis by AMPK-activated signals pathway in 3T3-L1 preadipocytes, in which associated with Mg and Ca-enriched content. Mg content in DSW could contribute in mitochondria biogenesis as it is the main component for mitochondria functions, while its deficiencies could cause mitochondria decay (Ames *et al.* 2005). Ca induces increases mitochondrial biogenesis and *PGC-1α* by a pathway leading to p38 mitogen-activated protein kinase activation (Wright *et al.* 2007). Mitochondrial biogenesis is correlated with expression of thermogenic markers such as *UCP-1* and *PGC-1α*, and could combat metabolic disease including obesity.

A study by Sun & Zemel (2006) shows high dietary Ca in mice increase *UCP-2* and *UCP-3* expression both in visceral and subcutaneous adipose tissue, respectively. Increased expression of *UCP-2* and *UCP-3* resulted in inhibition of ROS production. ROS production increased in response to obesity. Mg and Ca applications has provided the evidences in counteract obesity, though, their potential mechanisms in browning of WAT remain limited. Metabolic roles and mechanisms of minerals such as Mg, Ca, Cr, Se, K, and V in obesity remains limited and available data have been described in section 2.1.3 and section 4.2.

CHAPTER 5

CONCLUSION AND RECOMMENDATIONS

5.1 Conclusion

This study tests the effects of DSW in two types of adipocytes, which are 3T3-L1 cells and SVF cells. In this study, DSW has reduced WAT, which were determined by quantification of lipid accumulation and expression of adipogenic genes in 3T3-L1 cells. DSW could be suggested to counteract WAT, the adipocytes that could cause health hazard in excess amount. SVF cells are preadipocytes that could be induced into healthy form of adipocytes called as 'beige'. The present study shows first that DSW promoted induction of beige adipocytes from mouse adipose tissue-derived SVF cells. Beige adipocytes are distinctive type of fat cells which can be distinguished from WAT and BAT (Wu *et al.* 2012). In this experiment, DSW at a concentration of 100 hardness significantly promoted lipid accumulations, increased adipogenic genes, and upregulated thermogenic genes in beige adipocytes. Though, DSW at concentration of 100 hardness increased adipogenic genes and thermogenic genes not in the significant levels, instead of *PGC-1α* mRNA. This study concluded that DSW only cause tendency in browning of WAT.

Active components in DSW in reduced WAT and induced browning of SVF cells could be linked with presence of many beneficial minerals especially Mg and Ca. Metabolic roles and mechanisms of mineral such as Mg, Ca, Cr, Se, K, and V in obesity have been described in section 2.1.3 and section 4.2. Induction of adipose

tissue browning represents one of important approach that could regulate deleteriously lipid-overloaded WAT into metabolically active and healthy adipose tissue. Beige adipocytes are thermogenic adipocytes that can convert energy into heat. In this study, DSW has shown potential to reduce WAT, while promoted WAT into beige adipocytes. DSW applications could be suggested to people that has interest in combating obesity.

5.2 Recommendations

This study used SVF cells as WAT model to test its potential in browning. SVF cells that differentiated into beige adipocytes will express the *UCP-1*, a gene that can convert energy into heat. However, *UCP-1* required activation in order for it to functions. As mention by Harms & Seale (2013), therapeutic approaches for browning of WAT without activation of *UCP-1* could be less productive. Thus, this study suggests to determine the effects of DSW in activating *UCP-1* in differentiated beige adipocytes in the future study. In addition, the potential effects of DSW through *in vivo* test are suggested. Proposed treatment to target beige adipocytes for obesity treatment is useful, as its thermogenic ability is potential to counteract obesity.

In this study, there are two major types of experiments, which are adipogenesis of WAT and browning of WAT. Adipogenesis of WAT used 3T3-L1 cells and browning of WAT used SVF cells. The 3T3-L1 preadipocytes lines were used as representative of WAT in this experiment due to several factors include it has homogenous population, high passaging number, low cost, and are frequently uses adipocytes lines in adipogenesis study. Moreover, the used of 3T3-L1 preadipocytes to confirm one previous finding that DSW has inhibited adipocytes differentiation of 3T3-L1 preadipocytes. SVF cells are recommended depot to study the browning effects of WAT as it is has high susceptibility to browning. In this study, the effects of DSW in adipogenesis only were investigated in 3T3-L1 cells. Thus, this study also

recommends using SVF cells as WAT model, to study the effects of DSW in adipogenesis in the future.

REFERENCES

Akerblad, P. et al., 2002. Early B-cell factor (O/E-1) is a promoter of adipogenesis and involved in control of genes important for terminal adipocyte differentiation. *Molecular and Cellular Biology*, 22(22), pp.8015–25. Available at: http://www.pubmedcentral.nih.gov/articlerender.fcgi?artid=134715&tool=pmcentrez&rendertype=abstract.

Ames, B.N., Atamna, H. & Killilea, D.W., 2005. Mineral and vitamin deficiencies can accelerate the mitochondrial decay of aging. *Molecular Aspects of Medicine*, 26(4–5 SPEC. ISS.), pp.363–378.

Aune, U.L., Ruiz, L. & Kajimura, S., 2013. Isolation and differentiation of stromal vascular cells to beige/brite cells. *Journal of Visualized Experiments : JoVE*, (73), pp.1–6. Available at: http://www.pubmedcentral.nih.gov/articlerender.fcgi?artid=3641667&tool=pmcentrez&rendertype=abstract.

Avram, M.M., Avram, A.S. & James, W.D., 2007. Subcutaneous fat in normal and diseased states. 3. Adipogenesis: From stem cell to fat cell. *Journal of the American Academy of Dermatology*, 56, pp.472–492.

Bae, M. & Lee, S., 2010. Effect of deep sea water on the antioxidant activity and catechin content of green tea. *Journal of Medicinal Plants Research*, 4(16), pp.1662–1667.

Bartelt, A. & Heeren, J., 2014. Adipose tissue browning and metabolic health. *Nature Reviews. Endocrinology*, 10(1), pp.24–36. Available at: http://www.ncbi.nlm.nih.gov/pubmed/24146030.

Bianco, A.C. & Silva, J.E., 1987. Optimal response of key enzymes and uncoupling protein to cold in BAT depends on local T3 generation. *American Journal of Physiology - Endocrinology and Metabolism*, 253(3).

Bing, C. et al., 2004. Zinc-alpha2-glycoprotein, a lipid mobilizing factor, is

expressed in adipocytes and is up-regulated in mice with cancer cachexia. *Proceedings of the National Academy of Sciences of the United States of America*, 101(8), pp.2500–5. Available at: http://www.pubmedcentral.nih.gov/articlerender.fcgi?artid=356979&tool=pmcentrez&rendertype=abstract.

Boström, P. et al., 2012. A PGC1a dependent myokine that derives browning of white fat and thermogenesis. *Nature*, 481(7382), pp.463–468.

Cannon, B. & Nedergaard, J. a N., 2004. Brown Adipose Tissue: Function and Physiological Significance. *Physiological Reviews*, 84(1), pp.277–359. Available at: http://physrev.physiology.org/content/84/1/277.abstract.

Caprio, M. et al., 2007. Pivotal role of the mineralocorticoid receptor in corticosteroid-induced adipogenesis. *The FASEB journal : official publication of the Federation of American Societies for Experimental Biology*, 21(9), pp.2185–2194.

Chang, M.-H. et al., 2011. Effects of Deep-Seawater on Blood Lipids and Pressure in High-Cholesterol Dietary Mice. *Journal of Food Biochemistry*, 35(1), pp.241–259. Available at: http://doi.wiley.com/10.1111/j.1745-4514.2010.00379.x [Accessed February 17, 2014].

Chen, I.S. et al., 2013. Alleviative effects of deep-seawater drinking water on hepatic lipid accumulation and oxidation induced by a high-fat diet. *Journal of the Chinese Medical Association*, 76(2), pp.95–101. Available at: http://www.ncbi.nlm.nih.gov/pubmed/23351420 [Accessed February 17, 2014].

Dani, C. & Billon, N., 2012. Adipocyte Precursors: Developmental Origins, Self-Renewal, and Plasticity. In M. E. Symonds, ed. *Adipose Tissue Biology*. New York, NY: Springer New York, pp. 1–16. Available at: http://link.springer.com/10.1007/978-1-4614-0965-6.

Donma, M.M. & Donma, O., 2016. Promising link between selenium and peroxisome proliferator activated receptor gamma in the treatment protocols of obesity as well as depression. *Medical Hypotheses*, 89, pp.79–83. Available at: http://dx.doi.org/10.1016/j.mehy.2016.02.008.

Esmaillzadeh, A. et al., 2006. Fruit and vegetable intakes, C-reactive protein, and the metabolic syndrome. *The American Journal of Clinical Nutrition*, 84(6), pp.1489–97. Available at: http://www.ncbi.nlm.nih.gov/pubmed/17158434

[Accessed August 9, 2017].

Faryadi, Q., 2012. The Magnificent Effect of Magnesium to Human Health : A Critical Review. *International Journal of Applied Science and Technology*, 2(3), pp.118–126.

Fedorenko, A., Lishko, P. V. & Kirichok, Y., 2013. Mechanism of Fatty-Acid-Dependent UCP1 Uncoupling in Brown Fat Mitochondria. *Cell*, 151(2), pp.400–413.

Fernández-Sánchez, A. et al., 2011. Inflammation, oxidative stress, and obesity. *International Journal of Molecular Sciences*, 12(5), pp.3117–32. Available at: http://www.pubmedcentral.nih.gov/articlerender.fcgi?artid=3116179&tool=pmcentrez&rendertype=abstract [Accessed April 29, 2014].

Fève, B., 2005. Adipogenesis: cellular and molecular aspects. *Best Practice & Research. Clinical Endocrinology & Metabolism*, 19(4), pp.483–499.

Fisher, M. et al., 2012. adaptive thermogenesis FGF21 regulates PGC-1a and browning of white adipose tissues in adaptive thermogenesis. , pp.271–281.

Frontini, A. & Cinti, S., 2010. Distribution and Development of Brown Adipocytes in the Murine and Human Adipose Organ. *Cell Metabolism*, 11(4), pp.253–256. Available at: http://linkinghub.elsevier.com/retrieve/pii/S1550413110000744.

Fu, Z.-Y. et al., 2012. Drinking deep seawater decreases serum total and low-density lipoprotein-cholesterol in hypercholesterolemic subjects. *Journal of Medicinal Food*, 15(6), pp.535–41. Available at: http://www.pubmedcentral.nih.gov/articlerender.fcgi?artid=3359629&tool=pmcentrez&rendertype=abstract [Accessed February 17, 2014].

Fujii, H., 2005. [Nuclear Receptor PPARs and magnesium]. *Clinical Calcium*, 15(11), pp.52–64. Available at: http://www.ncbi.nlm.nih.gov/pubmed/16272614 [Accessed August 9, 2017].

Garcia, R.A., Roemmich, J.N. & Claycombe, K.J., 2016. Evaluation of markers of beige adipocytes in white adipose tissue of the mouse. *Nutrition & Metabolism*, 13(1), p.24. Available at: http://nutritionandmetabolism.biomedcentral.com/articles/10.1186/s12986-016-0081-2.

Gesta, S., Tseng, Y.-H. & Kahn, C.R., 2007. Developmental Origin of Fat: Tracking Obesity to Its Source. *Cell*, 131(2), pp.242–256. Available at:

http://linkinghub.elsevier.com/retrieve/pii/S009286740701272X.

Giralt, M. & Villarroya, F., 2013. White, brown, beige/brite: Different adipose cells for different functions. *Endocrinology*, 154(9), pp.2992–3000.

Gnad, T. et al., 2014. Adenosine activates brown adipose tissue and recruits beige adipocytes via A2A receptors. *Nature*, 516(7531), pp.395–399. Available at: http://dx.doi.org/10.1038/nature13816.

Gregoire, F.M., Smas, C.M. & Sul, H.S., 1998. Understanding adipocyte differentiation. *Physiological reviews*, 78(3), pp.783–809.

Gupta, R.K. et al., 2010. Transcriptional control of preadipocyte determination by Zfp423. *Nature*, 464(7288), pp.619–623. Available at: http://www.nature.com/doifinder/10.1038/nature08816 [Accessed January 13, 2017].

Ha, B.G. et al., 2013. Anti-diabetic effect of balanced deep-sea water and its mode of action in high-fat diet induced diabetic mice. *Marine Drugs*, 11, pp.4193–212. Available at: http://www.ncbi.nlm.nih.gov/pubmed/24172214.

Ha, B.G. et al., 2014a. Effects of balanced deep sea water on adipocyte hypertrophy and liver steatosis in high-fat diet-induced obese mice. *Obesity (Silver Spring)*, 22(7), pp.1669–1678. Available at: http://www.ncbi.nlm.nih.gov/pubmed/24634394.

Ha, B.G. et al., 2016. Magnesium and calcium-enriched deep-sea water promotes mitochondrial biogenesis by AMPK-activated signals pathway in 3T3-L1 preadipocytes. *Biomedicine & Pharmacotherapy*, 83, pp.477–484. Available at: http://linkinghub.elsevier.com/retrieve/pii/S0753332216306321.

Ha, B.G. et al., 2014b. Modulation of glucose metabolism by balanced deep-sea water ameliorates hyperglycemia and pancreatic function in streptozotocin-induced diabetic mice. *PLoS ONE*, 9(7), p.e102095. Available at: http://dx.plos.org/10.1371/journal.pone.0102095.

Ha, B.G. et al., 2015. Stimulatory Effects of Balanced Deep Sea Water on Mitochondrial Biogenesis and Function. *Plos One*, 10(6), p.e0129972. Available at: http://dx.plos.org/10.1371/journal.pone.0129972.

Harms, M. & Seale, P., 2013. Brown and beige fat: development, function and therapeutic potential. *Nature Medicine*, 19(10), pp.1252–1263. Available at: http://www.nature.com/doifinder/10.1038/nm.3361.

Heaton, J.M., 1972. The distribution of brown adipose tissue in the human. *Journal of Anatomy*, 112(Pt 1), pp.35–39.

Himms-Hagen, J. et al., 2000. Multilocular fat cells in WAT of CL-316243-treated rats derive directly from white adipocytes. *American Journal of Physiology. Cell Physiology*, 279(3), pp.C670–C681.

Hondares, E. et al., 2011. Peroxisome proliferator-activated receptor α (PPARα) induces PPARγ coactivator 1α (PGC-1α) gene expression and contributes to thermogenic activation of brown fat: Involvement of PRDM16. *Journal of Biological Chemistry*, 286(50), pp.43112–43122.

Hwang, H.S., Kim, H.A., et al., 2009. Anti-obesity and antidiabetic effects of deep sea water on ob/ob mice. *Marine Biotechnology (New York, N.Y.)*, 11(4), pp.531–9. Available at: http://www.ncbi.nlm.nih.gov/pubmed/19083059 [Accessed February 17, 2014].

Hwang, H.S., Kim, S.H., et al., 2009. Inhibitory effect of deep-sea water on differentiation of 3T3-L1 adipocytes. *Marine Biotechnology (New York, N.Y.)*, 11(2), pp.161–8. Available at: http://www.ncbi.nlm.nih.gov/pubmed/18654820 [Accessed March 3, 2014].

ICCVAM, 2006. *In Vitro Cytotoxicity Test Methods for Estimating Starting Doses for Acute Oral Systemic Toxicity Test*, Available at: ICCVAM, 2006. In Vitro Cytotoxicity Test Methods for Estimating Starting Doses for Acute Oral Systemic Toxicity Test.

Iida, S. et al., 2015. PRDM16 enhances nuclear receptor-dependent transcription of the brown fat-specific Ucp1 gene through interactions with Mediator subunit MED1. *Genes & Development*, 29(3), pp.308–21. Available at: http://www.pubmedcentral.nih.gov/articlerender.fcgi?artid=4318147&tool=pmcentrez&rendertype=abstract.

Institute for Public Health, 2015. National Health and Morbidity Survey 2015 (NHMS 2015). Vol. II: Non-Communicable Diseases, Risk Factors & Other Health Problems. *Ministry of Health*, II, pp.1–291. Available at: http://www.iku.gov.my/images/IKU/Document/REPORT/nhmsreport2015vol2.pdf.

Ishizuka, J. et al., 1994. In vitro relationship between magnesium and insulin secretion. *Magnesium Research*, 7(1), pp.17–22. Available at:

http://www.ncbi.nlm.nih.gov/pubmed/8054257 [Accessed January 18, 2017].

Jaafar, A.B., 2016. Proceedings 2nd National Workshop on Ocean Enery 2016. In A. B. Jaafar & A. Mahadzir, eds. *Ocean Energy and Ocean Thermal Energy: An Overview*. Kuala Lumpur: Perpustakaan Negara, p. 40. Available at: https://drive.google.com/file/d/0B64iEN8o2-1UZWVhT2RpZ05DZjQ/view.

Kajimura, S. et al., 2009. Initiation of myoblast/brown fat switch through a PRDM16-C/EBP-b transcriptional complex. *Nature*, 460(7259), pp.1154–1158. Available at: http://www.ncbi.nlm.nih.gov/pmc/articles/PMC2754867/.

Kang, S.M. et al., 2015. Effect of yogurt containing deep sea water on health-related serum parameters and intestinal microbiota in mice. *Journal Dietary Science*. Available at: http://www.journalofdairyscience.org/article/S0022-0302(15)00454-3/references.

Katsuda, S.-I. et al., 2008. Deep-sea water improves cardiovascular hemodynamics in Kurosawa and Kusanagi-Hypercholesterolemic (KHC) rabbits. *Biological & Pharmaceutical Bulletin*, 31(1), pp.38–44. Available at: http://www.ncbi.nlm.nih.gov/pubmed/18175939.

Kim, S. et al., 2010. Transcriptional activation of peroxisome proliferator-activated receptor-gamma requires activation of both protein kinase A and Akt during adipocyte differentiation. *Biochemical and Biophysical Research communications*, 399(1), pp.55–59. Available at: http://dx.doi.org/10.1016/j.bbrc.2010.07.038 [Accessed January 10, 2017].

Kiskinis, E. et al., 2007. RIP140 directs histone and DNA methylation to silence Ucp1 expression in white adipocytes. *The EMBO Journal*, 26(23), pp.4831–40. Available at: http://www.ncbi.nlm.nih.gov/pubmed/17972916 [Accessed January 14, 2017].

Kleiner, S. et al., 2012. Development of insulin resistance in mice lacking PGC-1 in adipose tissues. *Proceedings of the National Academy of Sciences*, 109, pp.9635–9640. Available at: http://www.ncbi.nlm.nih.gov/pubmed/22645355.

Kolumam, G. et al., 2015. Sustained Brown Fat Stimulation and Insulin Sensitization by a Humanized Bispecific Antibody Agonist for Fibroblast Growth Factor Receptor 1/βKlotho Complex. *EBioMedicine*, 2(7), pp.730–743. Available at: http://dx.doi.org/10.1016/j.ebiom.2015.05.028.

Kong, X. et al., 2014. IRF4 is a key thermogenic transcriptional partner of PGC-1??

Cell, 158(1), pp.69–83.

Kozak, L.P. & Anunciado-Koza, R., 2008. UCP1: Its involvement and utility in obesity. *International Journal of Obesity (2005)*, 32 Suppl 7, pp.S32-8. Available at: http://www.pubmedcentral.nih.gov/articlerender.fcgi?artid=2746324&tool=pmcentrez&rendertype=abstract.

Kusminski, C.M., Bickel, P.E. & Scherer, P.E., 2016. Targeting adipose tissue in the treatment of obesity-associated diabetes. *Nature Publishing Group*, 15(9), pp.639–660. Available at: http://dx.doi.org/10.1038/nrd.2016.75.

Lehmann, J.M. et al., 1997. Peroxisome Proliferator-activated Receptors and Are Activated by Indomethacin and Other Non-steroidal Anti-inflammatory Drugs. *Journal of Biological Chemistry*, 272(6), pp.3406–3410. Available at: http://www.jbc.org/cgi/doi/10.1074/jbc.272.6.3406 [Accessed January 30, 2017].

Li, Y. et al., 2010. Effects of multivitamin and mineral supplementation on adiposity, energy expenditure and lipid profiles in obese Chinese women. *International Journal of Obesity (2005)*, 34(6), pp.1070–1077.

Lidell, M.E. et al., 2013. Evidence for two types of brown adipose tissue in humans. *Nature Medicine*, 19(5), pp.631–634. Available at: http://www.nature.com/doifinder/10.1038/nm.3017 [Accessed January 30, 2017].

Lidell, M.E., Betz, M.J. & Enerbäck, S., 2014. Brown adipose tissue and its therapeutic potential. *Journal of Internal Medicine*, 276(4), pp.364–377.

Lin, G.G. & Scott, J.G., 2012. PPAR agonists induce a white-to-brown fat conversion through stabilization of PRDM16 protein. *Cell Metabolism*, 100(2), pp.130–134.

Michelle, M. & Beerman, K.A., 2007. The Major Minerals and Water. In *Nutritional Sciences: From Fundamentals to Food*. USA: Peter Marshall, pp. 517–525.

Mohd Nani, S.Z. et al., 2016. Potential Health Benefits of Deep Sea Water : A Review. *Evidence-based Complementary and Alternative Medicine*, 2016.

Moreno-navarrete, J.M. & Fernández-real, J.M., 2012. Adipocyte Differentiation. In M. E. Symonds, ed. *Adipose Tissue Biology*. New York, NY: Springer New York, pp. 17–39. Available at: http://link.springer.com/10.1007/978-1-4614-

0965-6.

National Center for Biotechnology Information, 2017. Primer designing tool Primer designing tool. *U.S. National Library of Medicine*. Available at: https://www.ncbi.nlm.nih.gov/tools/primer-blast/index.cgi?ORGANISM=10090&INPUT_SEQUENCE=NM_024406.2&LINK_LOC=nuccore [Accessed August 9, 2017].

Nedergaard, J. et al., 2001. UCP1: The only protein able to mediate adaptive non-shivering thermogenesis and metabolic inefficiency. *Biochimica et Biophysica Acta - Bioenergetics*, 1504(1), pp.82–106.

Onakpoya, I., Posadzki, P. & Ernst, E., 2013. Chromium supplementation in overweight and obesity: A systematic review and meta-analysis of randomized clinical trials. *Obesity Reviews*, 14(6), pp.496–507.

Ouchi, Y. et al., 1990. Effect of dietary magnesium on development of atherosclerosis in cholesterol-fed rabbits. *Arteriosclerosis, Thrombosis, and Vascular Biology*, 10(5), pp.732–737. Available at: http://atvb.ahajournals.org/cgi/doi/10.1161/01.ATV.10.5.732 [Accessed November 19, 2014].

Pairault, J. & Green, H., 1979. A study of the adipose conversion of suspended 3T3 cells by using glycerophosphate dehydrogenase as differentiation marker. *Proceedings of the National Academy of Sciences of the United States of America*, 76(10), pp.5138–42. Available at: http://www.pubmedcentral.nih.gov/articlerender.fcgi?artid=413095&tool=pmcentrez&rendertype=abstract.

Park, S.J. et al., 2013. The anti-obesity effect of natural vanadium-containing jeju ground water. *Biological Trace Element Research*, 151(2), pp.294–300. Available at: http://link.springer.com/10.1007/s12011-012-9557-8 [Accessed August 10, 2017].

Pérez-Gallardo, L. et al., 2009. Effect of calcium-enriched high-fat diet on calcium, magnesium and zinc retention in mice. *The British Journal of Nutrition*, 101(10), pp.1463–6. Available at: http://www.ncbi.nlm.nih.gov/pubmed/18986597.

Petraccia, L. et al., 2006. Water, mineral waters and health. *Clinical Nutrition (Edinburgh, Scotland)*, 25(3), pp.377–85. Available at:

http://www.sciencedirect.com/science/article/pii/S0261561405001792 [Accessed May 8, 2014].

Puigserver, P. et al., 1998. A cold-inducible coactivator of nuclear receptors linked to adaptive thermogenesis. *Cell*, 92(6), pp.829–839.

Qiang, L. et al., 2012. Brown remodeling of white adipose tissue by SirT1-dependent deacetylation of Pparγ. *Cell*, 150(3), pp.620–632.

Rayssiguier, Y. et al., 2010. Magnesium deficiency and metabolic syndrome: Stress and inflammation may reflect calcium activation. *Magnesium Research*, 23(2), pp.73–80.

Rayssiguier, Y., Gueux, E. & Weiser, D., 1981. Effect of magnesium deficiency on lipid metabolism in rats fed a high carbohydrate diet. *The Journal of Nutrition*, 111(11), pp.1876–83. Available at: http://www.ncbi.nlm.nih.gov/pubmed/7299488 [Accessed January 18, 2017].

Ricquier, D., 2011. Uncoupling protein 1 of brown adipocytes, the only uncoupler: A historical perspective. *Frontiers in Endocrinology*, 2(DEC), pp.1–7.

Rodríguez, A. et al., 2016. Cross-talk between adipokines and myokines in fat browning. *Acta Physiologica (Oxford, England)*, pp.1–20. Available at: http://www.ncbi.nlm.nih.gov/pubmed/27040995.

Ruiz-Ojeda, F. et al., 2016. Cell Models and Their Application for Studying Adipogenic Differentiation in Relation to Obesity: A Review. *International Journal of Molecular Sciences*, p.1040.

Sales, C.H. et al., 2014. Magnesium-deficient high-fat diet: Effects on adiposity, lipid profile and insulin sensitivity in growing rats. *Clinical Nutrition*, 33(5), pp.879–888. Available at: http://dx.doi.org/10.1016/j.clnu.2013.10.004.

Sambeat, A. et al., 2016. Epigenetic Regulation of the Thermogenic Adipose Program. *Trends in Endocrinology and Metabolism: TEM*, xx, pp.1–13. Available at: http://www.ncbi.nlm.nih.gov/pubmed/27692461.

Scott, M. a. et al., 2011. Current Methods of Adipogenic Differentiation of Mesenchymal Stem Cells. *Stem Cells and Development*, 20(10), pp.1793–1804.

Seale, A.P. et al., 2006. Vanadium and insulin increase adiponectin production in 3T3-L1 adipocytes. *Pharmacological Research*, 54(1), pp.30–38.

Seale, P. et al., 2008. NIH Public Access. *Pharmacological Research*, , 454(7207), pp.617–632.

Seale, P. et al., 2011. Prdm16 determines the thermogenic program of subcutaneous white adipose tissue in mice. *The Journal of Clinical Investigation*, 121(1), pp.53–56. Available at: http://web.a.ebscohost.com.pallas2.tcl.sc.edu/ehost/pdfviewer/pdfviewer?sid=24beb4c7-21d9-462f-967f-c98434c26670%40sessionmgr4005&vid=1&hid=4114.

Seale, P., 2015. Transcriptional regulatory circuits controlling brown fat development and activation. *Diabetes*, 64(7), pp.2369–2375.

Sergeev, I.N. & Song, Q., 2014. High vitamin D and calcium intakes reduce diet-induced obesity in mice by increasing adipose tissue apoptosis. *Molecular Nutrition & Food Research*, 58(6), pp.1342–1348. Available at: http://doi.wiley.com/10.1002/mnfr.201300503 [Accessed January 18, 2017].

Shao, M. et al., 2016. Zfp423 Maintains White Adipocyte Identity through Suppression of the Beige Cell Thermogenic Gene Program. *Cell Metabolism*, 23(6), pp.1167–1184. Available at: http://dx.doi.org/10.1016/j.cmet.2016.04.023.

Sheu, M.-J. et al., 2013. Deep Sea Water Modulates Blood Pressure and Exhibits Hypolipidemic Effects via the AMPK-ACC Pathway: An in Vivo Study. *Marine Drugs*, 11(6), pp.2183–202. Available at: http://www.ncbi.nlm.nih.gov/pubmed/23774889 [Accessed February 17, 2014].

Shin, D. et al., 2013. Benefits of potassium intake on metabolic syndrome: The fourth Korean National Health and Nutrition Examination Survey (KNHANES IV). *Atherosclerosis*, 230(1), pp.80–85. Available at: http://linkinghub.elsevier.com/retrieve/pii/S0021915013003912 [Accessed August 9, 2017].

Simental-Mendía, L.E. et al., 2016. A systematic review and meta-analysis of randomized controlled trials on the effects of magnesium supplementation on insulin sensitivity and glucose control. *Pharmacological Research*, 111, pp.272–282. Available at: http://www.ncbi.nlm.nih.gov/pubmed/27329332 [Accessed January 18, 2017].

Stine, R.R. et al., 2016. EBF2 promotes the recruitment of beige adipocytes in white adipose tissue. *Molecular Metabolism*, 5(1), pp.57–65. Available at: http://dx.doi.org/10.1016/j.molmet.2015.11.001.

Styner, M. et al., 2010. Indomethacin promotes adipogenesis of mesenchymal stem

cells through a cyclooxygenase independent mechanism. *Journal of Cellular Biochemistry*, 111(4), pp.1042–50. Available at: http://www.ncbi.nlm.nih.gov/pubmed/20672310 [Accessed January 30, 2017].

Sun, X. & Zemel, M.B., 2006. Dietary calcium regulates ROS production in aP2-agouti transgenic mice on high-fat/high-sucrose diets. *International Journal of Obesity (2005)*, 30, pp.1341–1346.

Symonds, M.E. ed., 2012. *Adipose Tissue Biology* 2012th ed., New York, NY: Springer New York. Available at: http://www.springerlink.com/index/10.1007/978-1-4614-0965-6 [Accessed November 10, 2015].

Taher, M. et al., 2015. Mangostin improves glucose uptake and inhibits adipocytes differentiation in 3T3-L1 cells via PPAR , GLUT4, and leptin expressions. *Evidence-based Complementary and Alternative Medicine*, 2015.

Takahashi, M. Mac & Huang, P., 2012. Novel Renewable Natural Resource of Deep Ocean Water (DOW) and Their Current and Future Practical Applications. *Kuroshio Science*, pp.101–113.

Ueshima, S. et al., 2003. Suppression of the release of type-1 plasminogen acti v ator inhibitor from human v ascular endothelial cells by Hawaii deep sea water. *Pathophysiology*, 9, pp.103–109.

Venu, L. et al., 2008. Long-term effects of maternal magnesium restriction on adiposity and insulin resistance in rat pups. *Obesity (Silver Spring, Md.)*, 16(6), pp.1270–1276.

Vergara, E.J.S. et al., 2016. Increased adipocyte differentiation may be mediated by extracellular calcium levels through effects on calreticulin and peroxisome proliferator activated receptor gamma expression in intramuscular stromal vascular cells isolated from Hanwoo beef cattle. *Italian Journal of Animal Science*, 15(2), pp.256–263. Available at: http://www.tandfonline.com/doi/full/10.1080/1828051X.2016.1186503.

Vitali, a. et al., 2012. The adipose organ of obesity-prone C57BL/6J mice is composed of mixed white and brown adipocytes. *The Journal of Lipid Research*, 53(4), pp.619–629.

Wang, J., Yuen, V.G. & McNeill, J.H., 2001. Effect of vanadium on insulin sensitivity and appetite. *Metabolism*, 50(6), pp.667–673. Available at:

http://www.ncbi.nlm.nih.gov/pubmed/11398143 [Accessed August 10, 2017].

Wang, W. & Seale, P., 2016. Control of brown and beige fat development. *Nature Reviews Molecular Cell Biology*, 17(11), pp.691–702. Available at: http://www.nature.com/doifinder/10.1038/nrm.2016.96.

Watson, R.R. et al., 2014. *Nutrition in the Prevention and Treatment of Abdominal Obesity*, Elsevier. Available at: http://www.sciencedirect.com/science/article/pii/B9780124078697000118 [Accessed December 9, 2014].

WHO, 2013. WHO | Obesity and overweight. *Who*. Available at: http://www.who.int/mediacentre/factsheets/fs311/en/.

Wright, D.C. et al., 2007. Calcium induces increases in peroxisome proliferator-activated receptor coactivator-1α and mitochondrial biogenesis by a pathway leading to p38 mitogen-activated protein kinase activation. *Journal of Biological Chemistry*, 282(26), pp.18793–18799.

Wu, J. et al., 2012. Beige adipocytes are a distinct type of thermogenic fat cell in mouse and human. *Cell*, 150(2), pp.366–376.

Wu, J., Jun, H. & McDermott, J.R., 2015. Formation and activation of thermogenic fat. *Trends in Genetics*, 31(5), pp.232–238. Available at: http://dx.doi.org/10.1016/j.tig.2015.03.003.

Yang, C.-C. et al., 2014. Deep-sea water containing selenium provides intestinal protection against duodenal ulcers through the upregulation of Bcl-2 and thioredoxin reductase 1. *PloS One*, 9(7), p.e96006. Available at: http://www.pubmedcentral.nih.gov/articlerender.fcgi?artid=4077573&tool=pmcentrez&rendertype=abstract [Accessed December 14, 2014].

Yoshioka, S. et al., 2003. Pharmacological activity of deep-sea water: examination of hyperlipemia prevention and medical treatment effect. *Biological & Pharmaceutical Bulletin*, 26(11), pp.1552–1559.

Yun, J.W., 2010. Possible anti-obesity therapeutics from nature - A review. *Phytochemistry*, 71(14–15), pp.1625–1641.

Zemel, M.B. et al., 2000. Regulation of adiposity by dietary calcium. *FASEB journal : official publication of the Federation of American Societies for Experimental Biology*, 14(9), pp.1132–8. Available at: http://www.ncbi.nlm.nih.gov/pubmed/10834935 [Accessed January 18, 2017].

Zhang, Y., Zeng, X. & Jin, S., 2012. Autophagy in adipose tissue biology. *Pharmacology*, 66(6), pp.505–512. Available at: http://www.ncbi.nlm.nih.gov/pubmed/23017672%5Cnhttp://ac.els-cdn.com/S1043661812001685/1-s2.0-S1043661812001685-main.pdf?_tid=c266c9d0-1fce-11e3-9053-00000aacb35f&acdnat=1379446043_3291a6d6ab1da2aec417354f741359b4.

Zheltova, A.A. et al., 2016. Magnesium deficiency and oxidative stress: an update. *BioMedicine*, 6(4), p.20. Available at: http://www.ncbi.nlm.nih.gov/pubmed/27854048 [Accessed August 9, 2017].

APPENDIX A

RESULT CALCULATION SHEETS

Table A.1 Absorbance readings for effects of deep sea water on cell viability test using 3T3-L1 cells.

Concentration of DSW (hardness)	Blank	0	100	500	1000	1500	2000	3000	4000	5000
OD 1	0.041	5.974	6.008	5.931	5.979	5.96	4.012	4.007	3.469	3.187
OD 2	0.041	5.97	6.008	5.975	5.28	5.96	4.808	4.012	3.452	3.19
OD 3	0.041	5.962	6.008	5.919	5.423	5.96	4.304	3.813	3.429	3.282
Average	0.041	5.968667	6.008	5.941667	5.560667	5.96	4.374667	3.944	3.45	3.219667

Table A.2 Normalized readings for effects of deep sea water on cell viability test using 3T3-L1 cells.

Concentration of DSW (hardness)	0	100	500	1000	1500	2000	3000	4000	5000
OD Value - Blank	5.933	5.967	5.89	5.938	5.919	3.971	3.966	3.428	3.146
	5.929	5.967	5.934	5.239	5.919	4.767	3.971	3.411	3.149
	5.921	5.967	5.878	5.382	5.919	4.263	3.772	3.388	3.241
Average	5.928	5.967	5.900	5.520	5.919	4.334	3.903	3.409	3.18

Table A.3 Percentage of cell viability for effects of deep sea water using 3T3-L1 cells.

Concentration of DSW (hardness)	0	100	500	1000	1500	2000	3000	4000	5000
Percentage	100.09	100.6646	99.365	100.174	99.854	66.990	66.907	57.830	53.073
	100.0225	100.664	100.107	88.382	99.854	80.420	66.990	57.544	53.124
	99.888	100.664	99.162	90.795	99.854	71.917	63.634	57.156	54.676
Average of Percentage	100	100.6636	99.545	93.117	99.854	73.109	65.844	57.510	53.624
Error Bar (S.E.M)	2.579	2.579	2.579	2.579	2.579	2.579	2.579	2.579	2.579

Table A.4 ANOVA calculations for effects of deep sea water on cell viability test using 3T3-L1 Cells.

Source of Variation	SS	df	MS	F	P-value
Between groups	9493	8	1187	118.9	P < 0.0001
Within groups	179.6	18	9.980		
Total	9673	26			

Table A.5 Absorbance readings for effects of deep sea water on percentage of lipid accumulation using 3T3-L1 cells.

Concentration of DSW (hardness)	Blank	0	100	500	1000	1500
OD 1	0.038	0.331	0.289	0.284	0.272	0.248
OD 2	0.038	0.334	0.288	0.252	0.269	0.251
OD 3	0.038	0.338	0.283	0.288	0.269	0.269
Average	0.038	0.334	0.287	0.275	0.270	0.256
Average OD - blank	0	0.296	0.249	0.237	0.232	0.218

Percentage of Lipid Accumulation
= 100 – ((Average control – average blank) - (OD value – Average Blank) / (Average control – average blank) x 100

Table A.6 Percentage reading for effects of deep sea water on lipid accumulation in 3T3-L1 cells.

Concentration of Deep Sea Water	0	100	500	1000	1500
OD 1	98.875	84.702	83.015	78.965	70.866
OD 2	99.888	84.364	72.216	77.953	71.879
OD 3	101.237	82.677	84.364	77.953	77.953
Average Percentage	100.0	83.915	79.865	78.290	73.566
Error bar (S.E.M)	0.6842	0.6263	3.844	0.3375	2.213

Table A.7 ANOVA calculations for effects of deep sea water on percentage of lipid accumulation in 3T3-L1 cells.

Source of Variation	SS	df	MS	F	P-value
Between groups	1232	4	308.1	24.87	$P < 0.0001$
Within groups	123.9	10	12.39		
Total	1356	14			

Table A.8 Absorbance readings for effects of deep sea water on adipogenic genes markers in 3T3-L1 cells.

Type of Adipogenic Genes	Concentration of DSW	0	100	500	1000	1500
PPAR-γ	OD 1	1.321	1.940	1.123	0.824	0.459
	OD 2	1.309	1.806	0.843	0.783	0.672
	OD 3	1.267	1.633	0.676	0.648	0.517
CEBP-α	OD 1	3.080	3.105	2.006	1.872	0.806
	OD 2	3.210	4.441	1.254	0.812	1.162
	OD 3	2.225	4.593	1.530	1.022	1.133
FABP4	OD 1	1.160	2.222	1.155	0.800	0.685
	OD 2	1.199	2.027	0.705	0.806	0.720
	OD 3	1.159	1.890	1.047	0.846	0.695

Table A9 Normalized absorbance readings for effects of deep sea water on adipogenic genes markers in 3T3-L1 cells.

Type of Adipogenic Genes	Concentration of DSW	0	100	500	1000	1500
PPAR-γ	OD 1	1.017	1.492	0.864	0.634	0.353
	OD 2	1.008	1.390	0.649	0.602	0.518
	OD 3	0.975	1.260	0.520	0.499	0.398
	Average	1	1.380	0.678	0.580	0.423
	Error bar (S.E.M)	0.0126	0.068	0.100	0.041	0.0491
CEBP-α	OD 1	1.085	1.094	0.707	0.659	0.284
	OD 2	1.131	1.565	0.442	0.286	0.409
	OD 3	0.784	1.618	0.539	0.360	0.399
	Average	1	1.426	0.563	0.435	0.364
	Error bar (S.E.M)	0.1089	0.1666	0.07734	0.114	0.0401
FABP4	OD 1	0.989	1.894	0.985	0.683	0.584
	OD 2	1.022	1.728	0.601	0.687	0.613
	OD 3	0.989	1.611	0.892	0.721	0.592
	Average	1	1.744	0.826	0.697	0.597
	Error bar (S.E.M)	0.01098	0.08227	0.1158	0.01218	0.009

Table A.10 ANOVA calculations for effects of deep sea water on mRNA *PPAR-γ* in 3T3-L1 cells.

Source of Variation	SS	df	MS	F	P-value
Between groups	1.745	4	0.4362	38.24	P < 0.0001
Within groups	0.1141	10	0.01141		
Total	1.859	14			

Table A.11 ANOVA Calculations for effects of deep sea water on mRNA *CEBP-α* in 3T3-L1 cells.

Source of Variation	SS	df	MS	F	P-value
Between groups	2.405	4	0.6012	16.64	P < 0.0021
Within groups	0.3613	10	0.03613		
Total	2.766	14			

Table A.12 ANOVA calculations for effects of deep sea water on mRNA *FABP4* in 3T3-L1 cells.

Source of Variation	SS	df	MS	F	P-value
Between groups	2.505	4	0.6263	50.86	P < 0.0001
Within groups	0.1231	10	0.01231		
Total	2.628				

Table A.13 Percentage of cell viability for effects of deep sea water on stromal vascular fractions cells.

Concentration of DSW (hardness)	Blank	0	100	500	1000	1500	2000	3000	4000	5000
Percentage	0.041	2.479	2.138	2.101	2.123	2.368	2.251	2.311	1.962	1.642
	0.041	2.362	2.471	2.449	2.56	2.69	2.614	2.475	2.345	1.859
	0.041	2.312	2.483	2.637	2.207	1.774	2.181	2.092	2.182	1.811
Average of Percentage	0.041	2.384	2.364	2.396	2.297	2.277	2.349	2.293	2.163	1.770

Table A.14 Percentage of cell viability for effects of deep sea water using stromal vascular fractions cells.

Concentration of DSW (hardness)	0	100	500	1000	1500	2000	3000	4000	5000
Percentage	2.438	2.097	2.06	2.082	2.327	2.21	2.27	1.921	1.601
	2.321	2.43	2.408	2.519	2.649	2.573	2.434	2.304	1.818
	2.271	2.442	2.596	2.166	1.733	2.14	2.051	2.141	1.77
Average of Percentage	2.343	2.323	2.355	2.256	2.236	2.308	2.252	2.122	1.730

Table A.15 Normalized percentage of cell viability for effects of deep sea water using stromal vascular fractions cells.

Concentration of DSW (hardness)	0	100	500	1000	1500	2000	3000	4000	5000
Percentage	104.040	89.488	87.909	88.848	99.303	94.310	96.870	81.977	68.321
	99.047	103.698	102.760	107.496	113.044	109.801	103.869	98.321	77.581
	96.913	104.210	110.782	92.432	73.954	91.323	87.525	91.366	75.533
Average of Percentage	100	99.132	100.484	96.259	95.434	98.478	96.088	90.555	73.812
Error Bar	2.112	4.824	6.700	5.713	11.45	5.727	4.734	4.736	2.808

Table A.16 ANOVA Calculations for effects of deep sea water on percentage of cell viability using stromal vascular fractions cells.

Source of Variation	SS	df	MS	F	P-value
Between groups	1660	8	0.07151	1.934	P < 0.1168
Within groups	1931	18	0.02999		
Total	3591	26			

Table A.17 Absorbance readings for effects of deep sea water on percentage of lipid accumulations using stromal vascular fractions cells.

Concentration of DSW (hardness)	Blank	0	100	500	1000	1500
OD 1	0.038	0.776	0.852	0.673	0.522	0.299
OD 2	0.038	0.716	1.019	0.794	0.55	0.371
OD 3	0.038	0.755	0.999	0.914	0.764	0.542
Average	0.038	0.749	0.95666667	0.79366667	0.612	0.404
Average OD - blank	0	0.711	0.91866667	0.75566667	0.574	0.366

Percentage of Lipid Accumulation
= 100 – ((Average control – average blank) - (OD value – Average Blank)/ (Average control – average blank) x 100

Table A.18 Normalized reading for effects of deep sea water on percentage of lipid accumulation using stromal vascular fractions cells.

Concentration of Deep Sea Water	0	100	500	1000	1500
OD 1	103.797	124.487	89.311	68.0731	36.709
OD 2	95.359	137.974	106.330	72.0113	46.840
OD 3	100.844	135.162	123.207	102.1097	70.886
Average Percentage	100	132.541	106.282	80.731	51.477
Error bar (S.E.M)	2.472	2.793	9.785	10.75	10.14

Table A.19 ANOVA calculations for effects of deep sea water on cell viability using stromal vascular fractions cells.

Source of Variation	SS	df	MS	F	P-value
Between groups	11285	4	2821	14.34	$P < 0.0004$
Within groups	1968	10	196.8		
Total	13253	14			

Table A.20 Absorbance readings for effects of deep sea water on adipogenic genes markers in stromal vascular fraction cells.

Type of Adipogenic Genes	Concentration of DSW	0	100	500	1000	1500
PPAR-γ	OD 1	3.224	4.423	1.1975	2.190	0.321
	OD 2	2.048	2.097	1.267	1.717	1.648
	OD 3	3.184	2.952	1.418	1.254	1.275
CEBP-α	OD 1	1.752	2.477	1.028	1.204	0.424
	OD 2	1.059	1.692	0.936	1.065	0.997
	OD 3	1.270	0.899	1.143	1.029	0.735
FABP4	OD 1	3.913	2.345	1.166	1.708	1.560
	OD 2	1.444	1.371	1.258	1.035	1.263
	OD 3	1.4977	1.740	1.296	1.842	1.119

Table A.21 Normalized absorbance readings for effects of deep sea water on adipogenic genes markers in stromal vascular fraction cells.

Type of Adipogenic Genes	Concentration of DSW	0	100	500	1000	1500
PPAR-γ	OD 1	1.144	1.569	0.425	0.777	0.114
	OD 2	0.727	0.744	0.450	0.609	0.585
	OD 3	1.130	1.047	0.503	0.445	0.452
	Average	1	1.120	0.459	0.610	0.384
	Error bar (S.E.M)	0.1367	0.2410	0.02305	0.09589	0.1401
CEBP-α	OD 1	1.288	1.821	0.756	0.885	0.312
	OD 2	0.778	1.24383	0.688	0.783	0.733
	OD 3	0.934	0.661	0.841	0.757	0.540
	Average	1	1.242	0.762	0.808	0.528
	Error bar (S.E.M)	0.1508	0.3349	0.04411	0.03930	0.1218
FABP4	OD 1	1.713	1.027	0.510	0.748	0.683
	OD 2	0.632	0.600	0.551	0.453	0.553
	OD 3	0.655	0.753	0.5673	0.806	0.490
	Average	1	0.793	0.543	0.669	0.575
	Error bar (S.E.M)	0.3566	0.1247	0.01698	0.1093	0.0568

Table A.22 ANOVA Calculations for effects of deep sea water on mRNA *PPAR-γ* in stromal vascular fraction cells.

Source of Variation	SS	df	MS	F	P-value
Between groups	1.295	4	0.3237	5.084	P = 0.0169
Within groups	0.6367	10	0.06367		
Total	1.932	14			

Table A.23 ANOVA Calculations for effects of deep sea water on mRNA *CEBP-α* in stromal vascular fraction cells.

Source of Variation	SS	df	MS	F	P-value
Between groups	0.8631	4	0.2158	2.348	P = 0.1248
Within groups	0.9191	10	0.09191		
Total	1.782	14			

Table A.24 ANOVA Calculations for effects of deep sea water on mRNA *FABP4* in stromal vascular fraction cells.

Source of Variation	SS	df	MS	F	P-value
Between groups	0.4160	4	0.1040	1.096	P = 0.4098
Within groups	0.9489	10	0.09489		
Total	1.365	14			

Table A.25 Absorbance readings for effects of deep sea water on thermogenic genes markers in stromal vascular fraction cells.

Type of Adipogenic Gene	Concentration of DSW	0	100	500	1000	1500
UCP-1	OD 1	2.840	19.736	4.334	6.525	0.054
	OD 2	6.009	3.971	4.873	3.150	2.181
	OD 3	15.184	3.715	2.215	4.600	0.989
PGC-1α	OD 1	1.926	3.741	1.265	1.864	1.136
	OD 2	1.145	2.057	1.502	1.104	1.357
	OD 3	1.266	2.758	1.982	1.160	1.566
CIDEA	OD 1	6.614	7.351	2.592	1.376	0.393
	OD 2	3.070	5.175	2.337	2.2853	0.491
	OD 3	3.533	6.553	2.563	1.263	0.378

Table A.26 Normalized absorbance readings for effects of deep sea water on thermogenic genes markers in stromal vascular fraction cells.

Type of Adipogenic Gene	Concentration of DSW	0	100	500	1000	1500
UCP-1	OD 1	0.355	2.464	0.541	0.815	0.007
	OD 2	0.750	0.496	0.608	0.393	0.272
	OD 3	1.895	0.464	0.277	0.574	0.123
	Average	1	1.141	0.475	0.594	0.134
	Error bar (S.E.M)	0.4620	0.6613	0.1013	0.1220	0.07681
PGC-1α	OD 1	1.332	2.588	0.875	1.290	0.785
	OD 2	0.791	1.423	1.039	0.764	0.939
	OD 3	0.876	1.908	1.370	0.802	1.083
	Average	1	1.973	1.095	0.952	0.936
	Error bar (S.E.M)	0.1678	0.3378	0.1459	0.1693	0.0869
CIDEA	OD 1	1.501	1.669	0.588	0.312	0.089
	OD 2	0.697	1.175	0.531	0.519	0.112
	OD 3	0.802	1.488	0.582	0.287	0.086
	Average	1	1.444	0.567	0.373	0.096
	Error bar (S.E.M)	0.2525	0.1443	0.01827	0.07346	0.0080

Table A.27 ANOVA Calculations for effects of deep sea water on mRNA *UCP-1* in stromal vascular fraction cells.

Source of Variation	SS	df	MS	F	P-value
Between groups	1.985	4	0.4962	1.213	P = 0.3645
Within groups	4.091	10	0.4091		
Total	6.076	14			

Table A.28 ANOVA Calculations for effects of deep sea water on mRNA *PGC-1α* in stromal vascular fraction cells.

Source of Variation	SS	df	MS	F	P-value
Between groups	2.338	4	0.5844	4.881	P = 0.0192
Within groups	1.197	10	0.1197		
Total	3.535	14			

Table A.29 ANOVA Calculations for effects of deep sea water on mRNA *CIDEA* in stromal vascular fraction cells.

Source of Variation	SS	df	MS	F	P-value
Between groups	3.399	4	0.8499	15.68	P = 0.0003
Within groups	0.5421	10	0.05421		
Total	3.942	14			

APPENDIX B

LIST OF EQUIPMENT AND APPARATUS

Table B.1 List of equipment and materials in Figure 3.3.

List of equipment and material	**Function**	**Catalog No.**
Time counter	To set time	PTC-1A
Centrifuge device	To centrifuge suspension	75007205
70% Alcohol	To sterile apparatus and work environment	CAS 67-63-0
Chair	To seat	-

Table B.2 Specifications of 24-well plate.

Product Name	24-well plate
Catalog No.	12684049
Classification	Animal Origin-Free
Form	Lyophilized
Format	24-well plate
Phenol Red Indicator	No Phenol Red
Product Line	Algimatrix™, Gibco®
Product Size	4 x 24 well plates
Purity or Quality Grade	Cell Culture Grade
Serum Level	Serum-Free
Sterility	Sterile
Shipping Condition	Room Temperature

Table B.3 Specifications of biological safety cabinet.

Product Name	Biosafety Cabinet, Class II, Type A2
Catalog No.	MHE-N600A2-PE
External Dimensions (W x D x H)	1972 x 799 x 1572 mm
Internal Dimensions (W x D x H)	1788 x 654 x 724 mm
Net Weight	290 kg
Crated Shipping Weight	313 kg
Product Protection	EN 12469
Classification	Class II Type A2
Style of Cabinet	Benchtop/console with base stand/storage cabinet
Cabinet Construction	All welded stainless steel 16/18 gauge Type 304 pressure tight design
Cabinet Depth with Armrest Removed	799 mm
Minimum Cabinet Height for Transport	1499 mm
Work Access Opening (standard height)	254 mm
Standard Inflow Velocity 2)	0.53 m/s
Diffuser for Air Supply (Non-flammable Metal)	Included
HEPA Supply Filter	99.995% effective on 0.3 microns neoprene gasket type H14
HEPA Exhaust Filter	99.995% effective on 0.3 microns neoprene gasket type H14
Gas Valve / Service Coupling (3/8x NPT)	1 right sidewall
Service Coupling (3/8x NPT)	1 right sidewall, 2 left sidewall
Power Socket	2 back wall
Ultraviolet Light (included)	1 back wall
Viewing Window Opening Range(tempered safety plate sliding glass)	533 open mm
Exhaust Opening	254 mm
Required Exhaust Canopy Variable Flow Thimble(MHE-NAC11)	363-588 | 617-1000 CFM | CMH
Required Exhaust Canopy Fixed Flow Thimble(MHE-NAC07)	426 | 724 CFM | CMH
Duct Static Pressure	1.27-2.54 mm H2O
Heat Rejected non-vented	1140 BTU/hour
Heat Rejected vented	157 BTU/hour
Power Supply	230 V
Frequency	50 Hz
Amps: Rated	10
Power Cord	3.7 m,14 gauge - 3 Wire, 15A
Sound pressure level per ISO 4871 4)	not to exceed 56 dB (A)

Table B.4 Specifications of microplate reader.

Product Name	Microplate reader
Catalog No.	ELx808
Detection modes	Absorbance
Read methods	End point, kinetic, linear scanning
Microplate types	96-well plates
Temperature control	4-Zone incubation to 50 °C ±0.2 °C at 37 °C
Shaking	Linear
Software	Gen5 Reader Control Software Gen5 Secure for 21 CFR Part 11 compliance (option)
Light source	Tungsten halogen
Detector	photodiode
Wavelength selection	filters
Wavelength range	380 to 900 nm 340 to 900 nm (ELx808IU)
Dynamic range	0 to 4.0 OD
Resolution	0.001 OD
Pathlength correction	No
Filter wheel capacity	6 positions
Filters supplied	4 filters (5 with UV option)
OD accuracy	< 1% at 2.5 OD < 2% at 3.5 OD
OD linearity	<1% at 2.5 OD
OD repeatability	< 0.5% at 2.5 OD < 1.5% at 3.5 OD
Reading speed (kinetic)	96 wells: 8 seconds
Power	100 - 240 Volts AC. 50/60 Hz
Dimensions	15.5"W x 16"D x 8.75"H<="" td="" style="box-sizing: border-box;">
Weight	30 lbs (13.6 kg)
Regulatory	For In Vitro Diagnostic use. CE and TUV marked, RoHS Compliant.

Table B.5 Specifications of thermal cycler.

Product Name	SimpliAmp™ Thermal Cycler
Catalog No.	A24811
Capacity	96-well 3 zones VeriFlex
For Use With (Equipment)	2720 Thermal Cycler, GeneAmp® 2700, GeneAmp™ 9700, Veriti® Thermal Cycler
Format	0.2 ml tubes, 96-well plate
High Throughput Compatibility	Not High Throughput-Compatible (Manual)
Product Size	1 instrument

Table B.6 Specifications of Real Time PCR.

Product Name	StepOnePlus™ Real-Time PCR System
Catalog No.	4376598
Calibrated Dye	FAM™, JOE™, NED, ROX™, SYBR® Green I, TAMRA™, VIC®
Capacity	1 x 96-well plate, 12 x 8-tube strips, 96 x 0.1 ml tubes
Detection Method	Primer-Probe Detection, SYBR
Dimensions	24.6 cm/9.7 in.(W) x 42.7 cm/16.8 in.(D) x 51.2 cm/20.2 in.(H)
Dynamic Range	Linear Dynamic Range greater than 9 log units (detection)
External Computer	Notebook
For Use With (Equipment)	StepOnePlus™
Format	0.1 ml tubes, 8-tube strips, 96-well plate
Green Features	Sustainable packaging
High Throughput Compatibility	Multiplexing
Optics	4 emission filters, Blue LED excitation source, photodiode
Passive Reference Dye	No ROX, ROX (Pre-mixed), ROX (Separate Tube)
Peak Block Ramp Rate	4.6°C⁄sec
Product Line	StepOnePlus™
Product Size	1 system
Reaction Speed	Fast, Standard
Reaction Volume Range	10-30 µl (Standard curve experiments: 40 µl in standard mode is validated)
Run Time	<2 hrs⁄run (Standard Mode), <40 min⁄run (Fast Mode)
Sample Ramp Rate	Fast mode: ± 2.2°C⁄sec, Standard mode: ± 1.6°C⁄sec
Sensitivity	1 copy
Temperature Accuracy	0.25°C (35 to 95°C) of display temperature
Temperature Range (Metric)	4-100°C
Temperature Uniformity	0.25°C (35 to 95°C) of setpoint/display temperature
Thermal Cycling System	Peltier-Based System
Weight	24 kg (53 lbs.)

APPENDIX C

RESULT OF DEEP SEA WATER

Samihah_Mg_Ca_151215.wmq. All Data Report 15/12/2015, 3:05:23 PM

Mg 285.213 Calibration (ppm)		28/10/2015, 11:46:22 AM		Correlation Coefficient: 0.999942		
Label	Flags	Int. (c/s)	Std Conc.	Calc Conc.	Error	%Error
Blank		72.2981	0.000000	-0.037348	-	-
Standard 1		44659.5	1.00000	0.974896	-0.025104	-2.5
Standard 2		90960.9	2.00000	2.02606	0.026057	1.3
Standard 3		180273	4.00000	4.05366	0.053659	1.3
Standard 4		355621	8.00000	8.03450	0.034505	0.4
Standard 5		439916	10.0000	9.94823	-0.051768	-0.5

Curve Type: Linear Equation: y = 44047.9 x + 1717.4

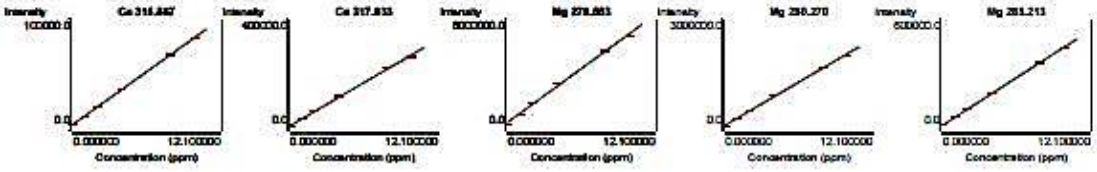

DSW 1 (100x) (Samp)		15/12/2015, 2:57:54 PM		Rack 2, Tube 1
Weight: 1		Volume: 1		Dilution: 1
Label	Replicates	Concentration		
Ca 315.887	3.58099	3.73648	3.28101	
Ca 317.933	3.60226	3.75142	3.31066	
Mg 279.553	10.4260	10.1842	9.92626	
Mg 280.270	10.7910	10.5095	10.1647	
Mg 285.213	10.9670	10.6499	10.0753	

Label	Sol'n Conc.	Units	SD	%RSD	Int. (c/s)	Calc Conc.	DF
Ca 315.887	3.53283	ppm	0.231526	6.6	29677.7	3.53283 ppm	1.00000
Ca 317.933	3.55478	ppm	0.224188	6.3	97626.1	3.55478 ppm	1.00000
Mg 279.553	10.1788	ppm	0.249887	2.5	7019508	10.1788 ppm	1.00000
Mg 280.270	10.4884	ppm	0.313665	3.0	2119159	10.4884 ppm	1.00000
Mg 285.213	10.5640	ppm	0.452004	4.3	467042	10.5640 ppm	1.00000

DSW 2 (100x) (Samp)		15/12/2015, 3:00:35 PM		Rack 2, Tube 2
Weight: 1		Volume: 1		Dilution: 1
Label	Replicates	Concentration		
Ca 315.887	4.08391	3.82201	3.67912	
Ca 317.933	4.11909	3.87152	3.72366	
Mg 279.553	11.4603x	11.0413x	10.5653	
Mg 280.270	12.0173x	11.4924x	10.8734	
Mg 285.213	12.3570x	11.7626x	11.2028x	

Label	Sol'n Conc.	Units	SD	%RSD	Int. (c/s)	Calc Conc.	DF
Ca 315.887	3.86168	ppm	0.205291	5.3	32363.1	3.86168 ppm	1.00000
Ca 317.933	3.90476	ppm	0.199802	5.1	106847	3.90476 ppm	1.00000
Mg 279.553	11.0223x	ppm	0.447828	4.1	7581298	11.0223 ppm	1.00000
Mg 280.270	11.4610x	ppm	0.572603	5.0	2312432	11.4610 ppm	1.00000
Mg 285.213	11.7741x	ppm	0.577231	4.9	520343	11.7741 ppm	1.00000

Samihah_Mg_Ca_151215.wmq. All Data Report 15/12/2015, 3:05:23 PM

DSW 3 (100x) (Samp)	**15/12/2015, 3:03:17 PM**	**Rack 2, Tube 3**
Weight: 1	**Volume: 1**	**Dilution: 1**

Label	Replicates Concentration		
Ca 315.887	4.11000	3.85073	3.56763
Ca 317.933	4.17841	3.90693	3.63554
Mg 279.553	11.7157x	11.0037x	10.4214
Mg 280.270	12.1231x	11.3946x	10.6524
Mg 285.213	12.5113x	11.6825x	10.8764

Label	Sol'n Conc.	Units	SD	%RSD	Int. (c/s)	Calc Conc.	DF
Ca 315.887	3.84279	ppm	0.271274	7.1	32208.8	3.84279 ppm	1.00000
Ca 317.933	3.90696	ppm	0.271436	6.9	106905	3.90696 ppm	1.00000
Mg 279.553	11.0469x	ppm	0.648233	5.9	7597708	11.0469 ppm	1.00000
Mg 280.270	11.3900x	ppm	0.735365	6.5	2298324	11.3900 ppm	1.00000
Mg 285.213	11.6901x	ppm	0.817500	7.0	516641	11.6901 ppm	1.00000

APPENDIX D

ACHIEVEMENTS

LIST OF PUBLICATIONS AND ACHIEVEMENTS

Journal Article

Mohd Nani, S.Z. et al., 2016. Potential Health Benefits of Deep Sea Water : A Review. *Evidence-based Complementary and Alternative Medicine*, 2016. **Sopus Index: 1.93, Q2**.

Conference Proceeding

Mohd Nani, S.Z., 2015. Proceedings 3rd International Ocean Thermal Energy Conversion (OTEC) Symposium 2015. In A. B. Jaafar, M. N. Musa, & A. M. Mahdzir, eds. *The Effects of Deep Sea Drinking Water on the Specific Adipokines of Obesity*. Kuala Lumpur: UTM Oean Thermal Energy Centre, p. 462. Available at: http://otec2015.utm.my/2015/11/30/proceedings-of-ioskl-2015/.

Mohd Nani, S.Z., ' Enhancing and Protecting the Quality of Health through the Use of Processed Clean OTEC-Waste Deep Sea Water '. Paper presented at the *2nd Program of International Platform on Ocean Energy for Young Researcher 2016*, Institure of Ocean Energy Saga University.

Magazine

Zura, S., 2015. Mineral Water From the Deep Sea: A Miracle to Health. FUTURE ENERGY: IS OTEC THE SOLUTION? *myForesight*, p.38. Available at: http://www.myforesight.my/index.php/blog/trend-energy/846-mineral-water-otec-.html.

Academic Evaluation

1. Journal Reviewer for International Journal of Tropical Disease & Health. SCIENCEDOMAIN.
2. Journal Reviewer for Journal of Advances in Microbiology. SCIENCEDOMAIN.

Research Attachment

Nine (9) months research attachment at Department of Endocrinology and Metabolism, Kanazawa University Graduate School of Medical Sciences, Kanazawa, Ishikawa 920-8641, Japan. Project: Effects of Deep Sea Water on Expression of Adipocytes Genes.